Pontifícia Universidade Católica
do Rio de Janeiro

Tonny Ssettumba

Iterative Interference Mitigation Techniques for Cell-Free Massive MIMO Systems

Tese de Doutorado

Thesis presented to the Programa de Pós–graduação em Engenharia Elétrica of PUC-Rio in partial fulfillment of the requirements for the degree of Doutor em Engenharia Elétrica.

Advisor : Prof. Rodrigo Caiado de Lamare
Co-advisor: Prof. Lukas Tobias Nepomuk Landau

Rio de Janeiro
August 2024

Pontifícia Universidade Católica
do Rio de Janeiro

Tonny Ssettumba

Iterative Interference Mitigation Techniques for Cell-Free Massive MIMO Systems

Thesis presented to the Programa de Pós–graduação em Engenharia Elétrica of PUC-Rio in partial fulfillment of the requirements for the degree of Doutor em Engenharia Elétrica. Approved by the Examination Committee.

Prof. Rodrigo Caiado de Lamare
Advisor
Departamento de Engenharia Elétrica – PUC-Rio

Prof. Lukas Tobias Nepomuk Landau
Co-advisor
Departamento de Engenharia Elétrica – PUC-Rio

Prof. Marco Antonio Grivet Mattoso Maia
Pontifícia Universidade Católica – PUC-Rio

Prof. André Robert Flores Manrique
Departamento de Engenharia Elétrica – PUC-Rio

Prof. Tadeu Nagashima Ferreira
Universidade Federal Fluminense – UFF

Prof. Paulo Ricardo Branco da Silva
Centro de Pesquisa e Desenvolvimento em Telecomunicações – CPqD

Prof. Didier Le Ruyet
Conservatoire national des arts et métiers – CNAM, France

Rio de Janeiro, August the 29th, 2024

Tonny Ssettumba

The author received the B.Sc. degree in Telecommunications Engineering and M.Sc. degree in Electronics and Communication Engineering from Makerere University, Kampala, Uganda in 2016 and the Egypt Japan University of Science and Technology, Alexandria, Egypt, in 2019, respectively.

Bibliographic data

Ssettumba, Tonny

Iterative Interference Mitigation Techniques for Cell-Free Massive MIMO Systems / Tonny Ssettumba; advisor: Rodrigo Caiado de Lamare; co-advisor: Lukas Tobias Nepomuk Landau. – Rio de janeiro: PUC-Rio, Departamento de Engenharia Elétrica, 2024.

104 f: il. color. ; 30 cm

Tese (doutorado) - Pontifícia Universidade Católica do Rio de Janeiro, Departamento de Engenharia Elétrica.

Inclui bibliografia

1. Engenharia Elétrica – Teses. 2. Processamento de Sinais, Automação e Robótica – Teses. 3. Sistemas sem células;. 4. sistemas de antenas múltiplas;. 5. detecção iterativa e decodificação;. 6. detector de cancelamento de interferência suave de erro quadrado médio mínimo;. 7. seleção de ponto de acesso.. I. de Lamare, Rodrigo C.. II. Lukas Tobias Nepomuk Landau. III. Pontifícia Universidade Católica do Rio de Janeiro. Departamento de Engenharia Elétrica. IV. Título.

CDD: 621.3

This thesis is dedicated to my parents
for their endless love, support and encouragement.

Acknowledgments

I wish to acknowledge the support accorded to me by my parents, the late Mr. Nasser Mugerwa (R.I.P) and Mrs. Esther Mugerwa Nakiyingi ever since they brought me upon earth. May God bless you for all you have done. Special consideration to my sisters Faridah, Robinah, Grace, and Juliet. I would also like to thank Ritah for her love and raising our daughter Joelina. I really appreciate the mental support accorded to me.

I would like to thank the administration of CETUC, DEE and PUC-Rio for their efforts to provide a distinctive model research university.

Special thanks go to Dr. Roberto Di Renna, who helped me during building initial models for the project, advising and helping with the correction of codes and analysis of results while conducting the research and the welcoming environment whenever I entered his office. God bless you abundantly.

Special thanks go to my main and co-advisor Prof. Rodrigo C. de Lamare and Prof. Lukas T. N. Landau, for their continuous encouragement, support, patience, discussions, valuable comments, and excellent suggestions to improve the quality of my research work.

Last but not least, I would like to show my sincere appreciation and gratitude to my colleagues especially Saeed Mashdour, Dr. Jonathan Serugunda, Dr. Zhichao Shao who helped me during the development of my models and discussing concepts during the initial and final phases of my thesis. Special thanks go to my friends, Maria Raquel da Silva, Claire Serugunda, Iam Kim, Isaac Ndawula, Herbert Kato, Dr. Edwin Mugume, Dr. Hanifah Nabuuma and Angelo who have provided me with guidance and critical help throughout my Ph.D studies.

Finally, this study was financed in part by the Coordenação de Aperfeiçoamento de Pessoal de Nível Superior - Brasil (CAPES) - Finance Code 001 and partly supported by a scholarship from the Conselho Nacional de Desenvolvimento Científico e Tecnológico (CNPq).

Abstract

Ssettumba, Tonny; de Lamare, Rodrigo C. (Advisor); Lukas Tobias Nepomuk Landau (Co-Advisor). **Iterative Interference Mitigation Techniques for Cell-Free Massive MIMO Systems** . Rio de Janeiro, 2024. 104p. PhD Dissertation – Departament of Electrical Engineering, Pontifícia Universidade Católica do Rio de Janeiro.

Cell-free massive multiple-input multiple-output (CF-mMIMO) is an advanced variant of network multiple-input multiple-output (MIMO) which considers absence of cell boundaries. Thus, the interference between cells in cellular systems is greatly minimised and the system's coverage capacity is improved due to the shorter distances between the access points (APs) and the users. It is a multi-user massive MIMO communications solution that involves an extended number of APs that can either be equipped with MIMO or single antennas to provide service to users simultaneously. The APs are controlled by a central processing unit (CPU) to ensure coordination within the network and for information processing and decoding. Possible arrangements for the CF-mMIMO architecture include, but are not limited to: centralized and decentralized schemes.

In this thesis, the uplink of a CF-mMIMO system architecture is studied for the centralized and decentralized implementations. In particular, we study the performance of interference mitigation techniques for CF-mMIMO networks using iterative detection and decoding (IDD) schemes. The performance of the system is studied assuming perfect and imperfect channel state information (CSI). Access point selection based on the effective channel gain to make the network more practical and scalable are devised. The use of low-density parity check (LDPC) codes that adopt message passing has been investigated. Furthermore, log likelihood ratio (LLR) refinement strategies have been proposed to improve decentralized processing for CF-mMIMO networks. Finally, the performance of the considered schemes is analyzed theoretically and simulations are used to assess the performance in terms of BER, number of fronthaul signaling, and computational cost.

Keywords

Cell-free systems; multiple-antenna systems; iterative detection and decoding; minimum mean square error soft interference cancellation detector; access point selection.

Resumo

Ssettumba, Tonny; de Lamare, Rodrigo C.; Lukas Tobias Nepomuk Landau. **Técnicas Iterativas de Mitigação de Interferência para Sistemas MIMO Livres de Células**. Rio de Janeiro, 2024. 104p. Tese de Doutorado – Departamento de Engenharia Elétrica, Pontifícia Universidade Católica do Rio de Janeiro.

Sistemas multi-input multi-output (MIMO) massivos livres de células são uma variante de sistemas MIMO multi-celulares que consideram a ausência de células. Desta forma, a interferência entre as células é minimizada e a capacidade de cobertura do sistema é melhorada devido à menor distância entre os pontos de acesso (APs) e os usuários. É uma solução de comunicação MIMO massiva multi-usuário que envolve um número estendido de APs que podem ser equipados com tecnologia MIMO para fornecer serviço a usuários simultaneamente. Os APs são controlados por uma unidade central de processamento (CPU) para garantir a coordenação dentro da rede e para processamento e decodificação de informação.

Possíveis arranjos para a arquitetura livre de células incluem esquemas centralizados e descentralizados. Para a configuração centralizada, os APs enviam todas as suas estimativas de canal e informações recebidas para a CPU por meio de enlaces de transporte frontais para processamento e detecção de sinais. Além disso, na arquitetura centralizada, os APs atuam como repetidores na rede. Outro nível de cooperação para sistemas MIMO massivos livre de células é o esquema descentralizado.

Nesta proposta de tese, a arquitetura dos sistema MIMO massivos livres de células no canal reverso é estudada para as implementações centralizadas e descentralizadas. Em particular, estuda-se o desempenho de técnicas de mitigação de interferência para essas redes supondo-se conhecimento perfeito de canal e usando técnicas de detecção lineares e não lineares, seleção de APs, e esquemas iterativos de detecção e decodificação com códigos LDPC para melhorar o desempenho do sistema e reduzir a carga de sinalização. Para o caso em que há falta de compartilhamento de informações sobre os canais, o uso de pilotos para obter estimativas de canais é considerado e explorado.

Palavras-chave

Sistemas sem células; sistemas de antenas múltiplas; detecção iterativa e decodificação; detector de cancelamento de interferência suave de erro quadrado médio mínimo; seleção de ponto de acesso.

Table of contents

List of figures

List of tables

1
Introduction

Cell-free massive multiple-input multiple-output (CF-mMIMO) leverages the distributed nature of multiple-input multiple-output (MIMO) to improve the quality of service as well as to result in very high throughput [1–3]. The CF-mMIMO architectures enable a user equipment (UE) to be served by a relatively large number of either single-antenna or multiple-antenna access points (APs). The large number of antenna elements and the distributed nature of the network with extra spatial degrees of freedom makes the channel between the UE and APs almost orthogonal, which reduces the level of interference and improves coverage as compared to conventional cellular systems with cell boundaries.

1.1
Motivation and Prior Works

The use of error correction and control (ECC) codes like Low-Density Parity-Check (LDPC) and Turbo codes was found to improve the performance of cellular systems, conventional MIMO, and massive MIMO [4–10]. Iterative detection and decoding (IDD) based techniques operate on the message passing principle by exchanging soft information (beliefs) in the form of log-likelihood ratios (LLRs) between the detector and the decoder. Linear block codes such as LDPC codes yield very efficient implementations and close to maximum likelihood (ML) performance when combined IDD schemes [4]. This has made them widely used in the state of the art standards and many applications in modern wireless communications systems [11–13]. The use of list-based detection techniques that are capable of eliminating error propagation that is often experienced in successive interference cancellation (SIC) and parallel interference cancellation (PIC) receivers includes strategies with multiple-feedback (MF) with SIC (MF-SIC) and multiple-branch multiple-feedback (MF) processing with SIC (MB-MF-SIC), which were reported in [9, 10].

In [14], a local partial marginalization detector based on turbo iterations was proposed for the uplink of a CF-mMIMO system architecture. The APs were assumed to locally implement soft detection and the obtained beliefs were shared over front-haul links for decoding at the central processing unit (CPU).

The proposed detector was compared with other baseline schemes such as minimum mean square error (MMSE) receive filter and MMSE with successive interference cancellation (MMSE-SIC). The work in [15] presents a joint access point selection scheme with interference cancellation (JAPSIC) for cell-free MIMO systems. The method selects APs with the strongest channel gains and cancels the contributions of interfering users. The proposed approach operates in a way that is analogous to an adaptive parallel interference cancellation (PIC) scheme in [16, 17].

Based on the literature at the time of writing and to the best of our knowledge, few works exist in the use of ECC codes such as LDPC codes that employ message passing for the CF-mMIMO cooperation architectures. Additionally, the use of list-based detection techniques such as MF-SIC have not been studied for CF-mMIMO systems. Moreover, the use of MMSE receive filters with soft interference cancellation (MMSE-Soft-IC) that apply the SIC and PIC nonlinear detectors with LPDC codes has not been studied for the CF-mMIMO setting yet its capable of achieving close to optimal performance with minimal complexity. Thus, the main contributions of this thesis are given in Section 1.2.

1.2 Contributions

In this thesis, interference mitigation techniques for centralized and decentralized CF-mMIMO antenna systems are presented. In particular, the bit error rate (BER) performance of the proposed systems using linear filters, nonlinear filters as well as soft IDD schemes for the proposed system architecture using LDPC codes is studied. To make such systems more scalable and practical, APs selection schemes that use largest-large scale fading (LLSF) coefficients are proposed. New closed-form expressions for the MMSE-Soft-IC are derived while taking into account APs selection, channel estimation and uplink transmit powers. Insights are drawn into the derived expressions as the number of iterations increase and give the expressions of the resulting receive filters. A performance comparison between the proposed list-based detector with other competing schemes such as soft MMSE, MMSE-SIC, MMSE-PIC and the list-based with MMSE-SIC is carried out. Furthermore, the performance comparison between the CF-mMIMO and co-located massive MIMO (COL-mMIMO) are compared. The system with APs selection is also compared with one that uses all the APs. Furthermore, a system that uses perfect CSI is compared with that with imperfect CSI. Additionally, the computation complexity and signaling load analyses of the centralized and decentralized CF-

mMMO implementation are performed. Furthermore, LLR refinement strategies have been proposed to improve the performance of decentralized processing for CF-mMIMO networks. Further, cluster-based IDD schemes have also been proposed and studied for CF-mMIMO networks. Finally, simulations are performed to assess the performance of the proposed schemes against existing approaches in terms of BER performance, signaling, normalized mean square error (NMSE) and computational complexity.

1.3 Notation and Outline

Throughout this thesis, the notations in table 1.1 are adopted.

Table 1.1: Notation

Small letters	Scalar, e.g., x
Bold small letters	Vector, e.g., $\mathbf{x}$
Bold capital letters	Matrix, e.g., $\mathbf{X}$
$(.)^T$	Transposition
$(.)^H$	Complex Conjugate (Hermitian) transpose
$\|.\|$	Euclidean norm of a vector
Tr(.)	Trace of a matrix
diag{...}	Creates a diagonal matrix with {...} on its diagonal entries
$[\mathbf{D}_{kl}]_{\gamma,\gamma}$	Denotes the γ-th element of matrix $\mathbf{D}_{kl}$
$\mathbf{I}_K$	Denotes an identity matrix of dimension $K \times K$
E_{tx}	Denotes the signal energy

The rest of this thesis is organised as follows:

- Chapter II presents the analysis of linear detection techniques such as those based on zero forcing (ZF) receiver filters, MMSE receive filters and receive matched filtering (RMF). A nonlinear detection scheme based on MMSE receive filters with SIC (MMSE-SIC) is also investigated. Furthermore, literature on IDD is presented and the proposed system model is introduced. Furthermore, an IDD scheme with centralized processing at the CPU for CF-mMIMO networks is proposed. The proposed model considers a CF-mMIMO system with large scale fading using the three-slope path loss model. The system is assumed to have perfect CSI of APs to user links and the small scale fading is modeled based on Rayleigh fading channel. Particularly, the BER performance of the soft MMSE, MMSE-SIC, MMSE-PIC and the list based detectors is

studied. Finally, the performance of the CF-mMIMO is compared with that one of co-located massive MIMO.

- Chapter III proposes iterative interference cancellation schemes with access points selection (APs-Sel) for CF-mMIMO systems. Closed-form expressions for centralized and decentralized linear MMSE (LMMSE) receive filters with APs-Sel are derived assuming imperfect CSI. Based on the derived expressions, insights are drawn and general expressions are devised for several cases. Firstly, MMSE-SIC receivers for the non-scalable CF-mMIMO that uses all APs are presented. Secondly, MMSE-SIC receivers assuming perfect CSI are obtained. Thirdly, for the case where there is no a priori information about the transmitted bit, a linear MMSE filter is obtained. Additionally, a new Gaussian approximation of the likelihood function is formulated by deriving new closed-form expressions for the second order statistics (mean and variance) of the detected signal parameters in presence of channel estimation errors, APs-Sel matrix and multi-user interference (MUI). Since the MMSE-SIC receiver experiences error propagation due to erroneous decisions from the previous stages, a list-based detector based on LMMSE receive filters is devised for CF-mMIMO systems that exploits interference cancellation and the constellation points to mitigate the error propagation that occurs in conventional MMSE-SIC receivers. Furthermore, low-complexity and low latency local detectors based on PIC and RMF schemes are proposed. New closed-form expressions for the local soft MMSE-PIC and RMF detectors are derived. An IDD scheme that employs LDPC codes is then developed. Moreover, LLR refinement strategies based on censoring and a linear combination of local LLRs are proposed to improve the network performance. Finally, the proposed centralized and decentralized IDD schemes are assessed against existing approaches in terms of BER, complexity, and signaling under perfect CSI and imperfect CSI and verify the superiority of the distributed IDD architecture with LLR refinements.
- Chapter IV presents two cluster-based IDD schemes for mitigating intra-cluster (ICL) and out of cluster (OCL) interference. Firstly, a soft iterative PIC receiver for network clustered CF-mMIMO networks is proposed. In particular, new closed-form expressions for MMSE-PIC receivers are derived by assuming the presence of ICL interference, channel estimation errors and additive white Gaussian noise (AWGN). The derived expressions are used to develop the resulting receivers by varying the number of iterations and assuming perfect and imperfect CSI. By determining the mean and variance of the detected signals, new closed-form

expressions for the Gaussian approximation of the likelihood function are also obtained. Simulations evaluate both clustered and full CF-mMIMO networks equipped with the proposed cluster-based MMSE-PIC and linear MMSE receivers in terms of BER and complexity. Secondly, an iterative soft IC scheme for intra-cluster (ICL) and out-of-cluster (OCL) interference in user-centric clustered CF-mMIMO networks. In particular, MMSE receive filters for the proposed IC scheme in the presence of ICL and OCL interference and noise are derived. Furthermore, a least squares estimator (LSE) to perform multiple OCL interference components estimation is devised. An IDD scheme that adopts LDPC codes and incorporates the OCL interference estimate is then presented. Simulations assess the proposed scheme against existing techniques in terms of BER performance.

- Finally, concluding remarks of this thesis are presented and future works are discussed in Chapter V.

1.4 Publication List

This work has resulted in a number of published papers as follows:

1. T. Ssettumba, R. Di Renna, L. Landau, R. C. de Lamare, **Iterative Detection and Decoding for Cell-Free Massive MIMO Using LDPC Codes**, XL Brazilian Symp. on Tel. and Signal Proc. - SBrT 2022, 25-28 September 2022, Santa Rita do Sapucaí, MG, Brazil.

2. T. Ssettumba, R. Di Renna, L. Landau, R. C. de Lamare, **A List-Based Detector for Access Point Selection in Cell-Free Massive MIMO Using LDPC Codes**, 2022 Int. Symp. on Wireless Commun. Systems (ISWCS), Hangzhou, China, 2022, pp. 1-6, doi: 10.1109/ISWCS56560.2022.9940407.

3. T. Ssettumba, S. Zhichao, L. Landau, S. P. F. Michelle, P. Branco da Silva, R. C. de Lamare, **Centralized and Decentralized IDD Schemes for Cell-Free Massive MIMO Systems: AP Selection and LLR Refinement** , in IEEE Access, vol. 12, pp. 62392-62406, 2024, doi: 10.1109/ACCESS.2024.3395585.

4. T. Ssettumba, S. Zhichao, L. Landau, S. P. F. Michelle, P. Branco da Silva, R. C. de Lamare, **LLR Refinement Strategies for Iterative Detection and Decoding Schemes in Cell-Free Massive MIMO Networks**, 2023 57th Asilomar Conf. on Signals,

Syst., and Comput., Pacific Grove, CA, USA, 2023, pp. 358-362, doi: 10.1109/IEEECONF59524.2023.10476860.

5. T. Ssettumba, Saeed Mashdour, L. Landau, P. Branco da Silva, R. C. de Lamare, **Iterative Soft Intra-Cluster Interference Cancellation for Cell-Free Massive MIMO Networks** , 2024 Int.Symp. on Wireless Commun. Syst. (ISWCS), Rio de Janeiro, Brazil, July 14-17 2024, pp. 1-6.

6. T. Ssettumba, Saeed Mashdour, L. Landau, P. Branco da Silva, R. C. de Lamare, **Iterative Interference Cancellation for Clustered Cell-Free Massive MIMO Networks**, submitted to IEEE Wireless Commun. Lett. (WCL).

2
System Models and Fundamentals of Interference Mitigation

This chapter introduces mathematical models that are used to represent single-user MIMO, multiuser MIMO, massive MIMO (mMIMO) and cell-free massive MIMO (CF-mMIMO) systems. Moreover, it gives a brief description of the basic CF-mMIMO architecture and reviews the fundamentals of interference mitigation for several MIMO systems. In particular, existing sub-optimal detection techniques such as linear ZF, linear MMSE, MMSE-SIC and RMF receivers are described. The expressions of the receive filters are derived using the adopted system models, which provides a fundamental mathematical understanding of the key concepts. Furthermore, descriptions of the PIC and list-based detectors and a brief introduction to IDD schemes is provided. Finally, an IDD scheme for CF-mMIMO systems assuming perfect CSI is proposed and its BER performance is compared with that one of co-located mMIMO systems.

2.1
Overview of MIMO Systems

This section provides an overview of MIMO systems. It starts by introducing point-to-point MIMO systems, co-located mMIMO and CF-mMIMO. Additionally, the signal model for CF-mMIMO is given. The concept of signal detection is discussed while giving examples of linear and nonlinear detection techniques applicable to CF-mMIMO systems. The concepts of list-based detection and IDD are then introduced. Numerical examples for the introduced detectors are provided along with a discussion of numerical results.

2.1.1
Point-to-Point MIMO

Point-to-point MIMO was invented at Bell Labs with the aim of increasing data rates [18].

However, the system was impractical and thus multi-user MIMO has become the most popular setting. In multiuser MIMO the base station (BS) is equipped with multiple antennas, and the users can be equipped with either single or multiple antennas. The number of antennas at the BS is assumed to be

greater than the number of users so that the system results in a mathematical model of full-rank. When multiuser MIMO systems have a large number of antennas then this configuration can make the channels nearly orthogonal, facilitating efficient signal detection [17, 19–22].

2.2 System models for the MU-MIMO Uplink

2.2.1 Co-located Massive MIMO System

In this system, the BS is located in the center and equipped with a large number of antennas. The BS broadcasts its signal to the entire network area to serve multiple user equipments (UEs) in a given cell. For a fair comparison with CF-mMIMO, the BS is equipped with a number of antenna elements equal to the number of APs in the network. The same propagation channel model is considered for the co-located mMIMO and CF-mMIMO settings.

2.2.2 Cell-Free Massive MIMO System

A CF-mMIMO system is a multiuser communications system that involves a large number of distributed antenna elements [1,3]. The system model comprises of L APs that are geographically distributed in given area, each equipped with N antenna. Additionally, there are K randomly distributed users , where $L >> K$. The APs are connected to a CPU by a backhaul connection (fronthaul links). In the uplink transmission, the users send their pilots to the APs in each coherence interval. The orthogonal frequency-division multiplexing (OFDM) sub-carrier is assumed to follow an independent and identically distributed (i.i.d) flat-fading distribution, such that the channel remains constant in the coherence bandwidth [3]. The system model is shown in Figure 2.1 but more simplified models will be presented in the subsequent chapters. The channel coefficient between the l-th access point (AP)and the k-th user is given by [13],

$$g_{l,k} = \sqrt{\beta_{l,k}} h_{l,k},$$

where $\beta_{l,k}$ is the large scale fading coefficient between the l-th AP and the k-th user, that accounts for path loss and shadowing effects. The random variable $h_{l,k}$ is the i.i.d $\mathcal{N}_{\mathbb{C}} \sim (0, 1)$ small scale fading coefficients. The large scale fading coefficients can be modeled using the three-slope pathloss model [3, 13] or the

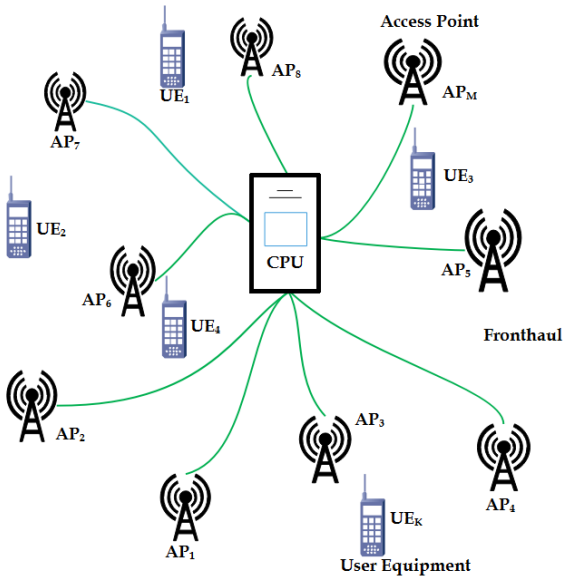

Figure 2.1: Cell-Free Massive MIMO System Model.

3GPP pathloss model [14]. The received signal is given by

$$\mathbf{y} = \mathbf{G}\mathbf{s} + \mathbf{n} \in \mathbb{C}^{NL\times 1}, \tag{2-1}$$

where $\mathbf{G} \in \mathbb{C}^{NL\times K}$ is the channel matrix, $\mathbf{s}$ is the transmitted symbol vector, and $\mathbf{n} \in \mathbb{C}^{NL\times 1}$ is the noise vector at the APs.

2.3 Detection Techniques

The signals transmitted by the users to the APs overlap and result in MUI at the receiver side. Signals suffering from interference cannot be easily demodulated at the receiver. Thus, there is need for methods to separate such signals by reducing the Euclidean distance between the transmitted signal and its estimate at the receiver.

In this thesis, the focus is on IDD techniques that utilize message passing using LDPC codes and promote the exchange of messages between a receiver that outputs soft information and the decoder. We begin our exposition by looking at linear and non-linear detection techniques that are applicable to multiple-antenna systems. Detection is necessary to equalize the channel matrix $\mathbf{G}$ as well as to estimate the transmitted symbols. Several types of detectors include the optimal detectors such maximum likelihood (ML) and maximum a-posterior (MAP) detectors, sub-optimal detectors such as linear detectors, non-linear detectors and those based on IDD schemes. To carry out linear detection, the CF-mMIMO channel is equalized with a linear receive

filter $\mathbf{W} \in \mathbb{C}^{K \times NL}$ [23,24]. It is assumed that the input symbols are taken from a discrete set, i.e., $s_k \, \epsilon \, \mathbb{A}$. For simplicity, the output of the linear equalizer is given by

$$\tilde{\mathbf{s}} = \mathbf{W}(\mathbf{G}\mathbf{s} + \mathbf{n}), \tag{2-2}$$

where $\tilde{\mathbf{s}} \in \mathbb{C}^{K \times 1}$, $\mathbf{G} \in \mathbb{C}^{NL \times K}$, $\mathbf{s} \in \mathbb{C}^{K \times 1}$, $\mathbf{n} \in \mathbb{C}^{NL \times 1}$, are the detected signal, channel matrix, transmitted symbol vector, and the noise vector, respectively. The detected symbols are mapped to the closest possible solution such as $\tilde{\mathbf{s}} \rightarrow \hat{\mathbf{s}} \in \mathbb{A}^K$. Additionally, if the noise and the signal are uncorrelated, then $\mathbb{E}\Big\{\mathbf{n}\mathbf{s}^{\mathbf{H}}\Big\} = \mathbf{0}$, $\mathbf{C_s} = \mathbb{E}\Big\{\mathbf{s}\mathbf{s}^{\mathbf{H}}\Big\}$, $\mathbf{C_n} = \mathbb{E}\Big\{\mathbf{n}\mathbf{n}^{\mathbf{H}}\Big\}$.

2.3.1 Linear Minimum Mean Square Error Receivers

The linear MMSE receive filter is obtained by solving a convex optimization problems given by [24–27]

$$\mathbf{W}_{\mathsf{MMSE}} = \mathsf{argmin}_{\mathbf{W}} \, \mathbb{E}\Big\{\|\mathbf{s} - \tilde{\mathbf{s}}\|_{\mathbf{2}}^{\mathbf{2}}\Big\}. \tag{2-3}$$

This implies that while using the MMSE receive filter, a global minimum is always guaranteed since the problem is convex. After substituting (2-2) into (2-3), the problem can be rewritten as

$$\begin{aligned} \mathbb{E}\Big\{\|\mathbf{s} - \tilde{\mathbf{s}}\|_2^2\Big\} &= \mathbb{E}\Big\{\|\Big(\mathbf{I}_K - \mathbf{W}\mathbf{G}\Big)\mathbf{s} - \mathbf{W}\mathbf{n}\|_2^2\Big\}, \\ &= \mathbb{E}\Big\{\|\Big(\mathbf{I}_K - \mathbf{W}\mathbf{G}\Big)\mathbf{s}\|_2^2\Big\} + \mathbb{E}\Big\{\|\mathbf{W}\mathbf{n}\|_2^2\Big\}, \\ &= \mathsf{tr}\Big\{\Big(\mathbf{I}_K - \mathbf{W}\mathbf{G}\Big)\mathbf{C_s}\Big(\mathbf{I}_K - \mathbf{W}\mathbf{G}\Big)^H\Big\} + \mathsf{tr}\Big\{\mathbf{W}\mathbf{C_n}\mathbf{W}^H\Big\}. \end{aligned} \tag{2-4}$$

Differentiating (2-4) with respect to $\mathbf{W}^H$ and equating the resulting terms to zero yields

$$\frac{d\mathbb{E}\Big\{\|\mathbf{s} - \tilde{\mathbf{s}}\|_{\mathbf{2}}^{\mathbf{2}}\Big\}}{d\mathbf{W}^H} = -\Big(\mathbf{I}_K - \mathbf{W}\mathbf{G}\Big)\mathbf{C_s}\mathbf{G}^H + \mathbf{W}\mathbf{C_n} = 0. \tag{2-5}$$

The optimal linear MMSE receive filter is then obtained by equating (2-5) for $\mathbf{W}$ which results in

$$\mathbf{W}_{\mathsf{MMSE}} = \mathbf{C_s}\mathbf{G}^H\Big(\mathbf{G}\mathbf{C_s}\mathbf{G}^H + \mathbf{C_n}\Big)^{-1}. \tag{2-6}$$

By applying the matrix inversion lemma in (2-6), it yields

$$\mathbf{W}_{\mathsf{MMSE}} = \left(\mathbf{C}_s^{-1} + \mathbf{G}^H \mathbf{C}_n^{-1} \mathbf{G}\right)^{-1} \mathbf{G}^H \mathbf{C}_n^{-1}. \tag{2-7}$$

In the low SNR region, when $\mathbf{C}_n^{-1}$ has very small entries the filter can be approximated as follows

$$\lim_{\mathsf{SNR}\to\infty} \mathbf{W}_{\mathsf{MMSE}} \to \mathbf{C}_{\mathbf{s}} \mathbf{G}^H \mathbf{C}_n^{-1}. \tag{2-8}$$

A more special form of this filter is obtained when the noise covariance matrix is $\mathbf{C}_{\mathbf{n}} = \sigma_{\mathbf{n}}^2 \mathbf{I}_{NL}$ and the signal covariance matrix is $\mathbf{C}_{\mathbf{s}} = \frac{E_{tx}}{K} \mathbf{I}_K$, respectively. Thus the filter can be rewritten such as

$$\mathbf{W}_{\mathsf{MMSE}} = \left(\frac{K\sigma_{\mathbf{n}}^2}{E_{tx}} \mathbf{I}_K + \mathbf{G}^H \mathbf{G}\right)^{-1} \mathbf{G}^H. \tag{2-9}$$

The main drawback of the MMSE filter is that it gives a biased estimate of the error [25, 28]. It requires a cubic cost in the number of APs and UEs due to the matrix inversion.

2.3.2 Linear Zero-Forcing Receivers

For a fair treatment of the analysis, the ZF receive filter gives an unbiased estimate of the error in the detected signal [25, 29, 30]. The expected value of the estimator conditioned on the input signal is given by

$$\mathbb{E}\Big\{\tilde{\mathbf{s}}|\mathbf{s}\Big\} = \mathbf{WGs} = \mathbf{s}, \tag{2-10}$$

This implies that the expected value of the estimator conditioned on the input signal is simply equal to identity matrix given by $\mathbf{WG} = \mathbf{I}$. This constraint for the unbiased estimate can be combined with the MMSE design criterion to formulate the ZF optimization problem such as

$$\mathbf{W}_{\mathsf{ZF}} = \mathsf{argmin}_{\mathbf{W}}\, \mathbb{E}\left\{ \|\mathbf{s} - \tilde{\mathbf{s}}\|_2^2 \right\} \; s.t \;\; \mathbf{WG} = \mathbf{I}. \tag{2-11}$$

Substituting the receive filter into the received signal in (2-11) yields

$$\mathbf{W}_{\mathsf{ZF}} = \mathsf{argmin}_{\mathbf{W}}\, \mathbb{E}\left\{ \|\mathbf{s} - \mathbf{W}(\mathbf{Gs} + \mathbf{n})\|_2^2 \right\} \; s.t \;\; \mathbf{WG} = \mathbf{I}. \tag{2-12}$$

The solution to (2-12) yields the ZF filter [25, 31] given by

$$\mathbf{W}_{\mathsf{ZF}} = \left(\mathbf{G}^H \mathbf{C}_{\mathbf{n}}^{-1} \mathbf{G}\right)^{-1} \mathbf{G}^H \mathbf{C}_{\mathbf{n}}^{-1}. \tag{2-13}$$

A special case of this filter occurs when $\mathbf{C}_{\mathbf{n}} = \sigma_n^2 \mathbf{I}$. Thus, the filter expression is modified to a form given by

$$\mathbf{W}_{\mathsf{ZF}} = \left(\mathbf{G}^H \mathbf{G}\right)^{-1} \mathbf{G}^H. \tag{2-14}$$

The drawback of this filter is that it does not take into account the noise, yet communication systems always have noise in practical scenarios. Thus, it magnifies the noise when the channel gain is small [25].

2.3.3 Receive Matched Filter

The receive matched filter (RMF) has the objective of maximizing the signal-to-noise ratio (SNR) at the receiver [25]. The SNR is given by

$$\gamma(\mathbf{W}) = \frac{|\mathbb{E}\left\{\mathbf{s}^H \tilde{\mathbf{s}}\right\}|^2}{\mathsf{Var}\left\{\mathbf{s}^H \tilde{\mathbf{s}}\right\}}. \tag{2-15}$$

With $|\mathbb{E}\left\{\mathbf{s}^H \tilde{\mathbf{s}}\right\}|^2 = |\mathsf{tr}\left\{\mathbf{W}\mathbf{G}\mathbf{C}_{\mathbf{s}}\right\}|^2$ and $\mathsf{Var}\left\{\mathbf{s}^H \tilde{\mathbf{s}}\right\} = \mathbb{E}\left\{\|\mathbf{s}\|_2^2\right\}\mathbb{E}\left\{\|\mathbf{W}\mathbf{n}\|_2^2\right\}$ the SNR can be rewritten as

$$\gamma(\mathbf{W}) = \frac{|\mathsf{tr}\left\{\mathbf{W}\mathbf{G}\mathbf{C}_s\right\}|^2}{\mathsf{tr}\left\{\mathbf{C}_s\right\}\mathsf{tr}\left\{\mathbf{W}\mathbf{C}_n\mathbf{W}^H\right\}}. \tag{2-16}$$

The filter $\mathbf{G}$ which maximizes γ corresponds to the matched filter given by

$$\mathbf{W}_{MF} = \arg\max_{\mathbf{W}} \ \gamma\left(\mathbf{W}\right). \tag{2-17}$$

By solving the optimization in (2-17), the solution to the RMF is given by

$$\mathbf{W} = \alpha \mathbf{C}_s \mathbf{G}^H \mathbf{C}_n^{-1}, \tag{2-18}$$

where α is a scalar which can be chosen arbitrarily [25].

The major drawback of the RMF is that interference remains constant regardless of the SNR of the channel. As a result, the RMF's performance for uncoded systems is always poor as compared to the MMSE and ZF receivers.

2.3.4 MMSE-Successive Interference Cancellation (SIC)

An MMSE-SIC detector is analogous to the linear MMSE detector. However, it is followed by a subtraction of the signal of the successive decoded users and processing of the remaining user data, recursively [32,33]. In general, the data symbol of each user when using any of the SIC-based receivers is given by

$$\hat{s}_k[i] = Q\bigg(\mathbf{w}_k^H \mathbf{y}_k[i]\bigg), \tag{2-19}$$

where the successively cancelled received data vector that follows from the channel with the highest norm to the lowest in the k-th stage is given by

$$\mathbf{y}_k[i] = \mathbf{y}[i] - \sum_{j=1}^{k-1} \mathbf{g}_j \hat{s}_j[i], \tag{2-20}$$

where $\mathbf{g}_j$ corresponds to the columns of the composite channel matrix $\mathbf{G}$.

Several methods for SIC detectors can be summarized as follows:

1. **SINR based ordering**
   In this SIC strategy, signals with the highest signal-to-interference-plus noise ratio (SINR) are detected first, followed by the next strongest signal. The process continues until the entire received streams is detected.

2. **SNR-based ordering**
   The operation is analogous to the SINR based approach but employs the SNR to order the received signals.

3. **Column Norm-based norm**
   This SIC scheme uses the norm of the column vectors in a channel matrix to perform the ordering and performs the cancellation.

4. **Received Signal based Ordering**
   In this method, the received signals are incorporated into deciding a detection order. This approach achieves achieves the better performance than the above three schemes. As opposed to the first three schemes in which ordering is required only once as long as the channel matrix is fixed, this method involves the highest complexity as detection ordering is required every time a signal is received at the APs.

The major challenges faced by SIC based receivers is the longer delays due to latency at each successive cancellation stage. Also, in situations where

there is an erroneous decision at any SIC stage, the receiver suffers from error propagation which compromises the system's performance. To solve these challenges, a PIC and List-based receivers are usually preferred as discussed in the next Subsections.

2.3.5 Parallel Interference Cancellation

The parallel interference cancellation (PIC) works in a way that, for each symbol, the coarse initial estimate of the interfering symbols can be used for regenerating the interference and then subtracting it from the composite received signals [34]. PIC detector has lower processing delay, and is more robust to inter-stream error propagation. The received signal at the k-th UE after PIC is given by

$$\mathbf{y}_k[i] = \mathbf{y}[i] - \sum_{j=1, j\neq k}^{K} \mathbf{g}_j \hat{s}_j[i], \tag{2-21}$$

PIC finds more applications in scenarios where the users have an equal BER performance [35].

2.3.6 List-Based Detection

The block diagram of the proposed list-based detector is shown in Figure 2.2. The design leverages multiple feedback (MF) diversity by choosing a set of constellation candidates when the previously detected symbol is considered to be unreliable [9, 13]. A shadow area constraint (SAC) is introduced in order to obtain an optimal feedback candidate. This helps to reduce the computation complexity in the search space, by avoiding it from growing exponentially. One of the positive attributes of such a selection criterion, is that there is no need for redundant processing when reliable decisions are made. Additionally, the proposed MF-SIC scheme mitigates error propagation that usually occurs when the conventional SIC-based approaches are used for detection.

The procedure for detecting $\hat{s}_k$ for the k-th user is described following a similar procedure presented in [9]. The k-th user soft estimate is obtained by $u_k = \mathbf{w}_k^H \check{\mathbf{y}}_k$ where the MMSE filter vector $\mathbf{w}_k = (\bar{\mathbf{G}}_k \bar{\mathbf{G}}_k^H + \frac{\sigma_n^2}{E_{tx}}\mathbf{I})^{-1}\mathbf{g}_k$. $\bar{\mathbf{G}}_k$ represents the matrix obtained by stacking the columns $k, k+1, ...K$ of $\mathbf{G}$ and $\check{\mathbf{y}}_k = \mathbf{y} - \sum_{t=1}^{k-1} \mathbf{g}_t \hat{s}_t$ denotes the received vector after performing cancellation of the $k-1$ previously detected symbols. The soft estimate u_k for each layer

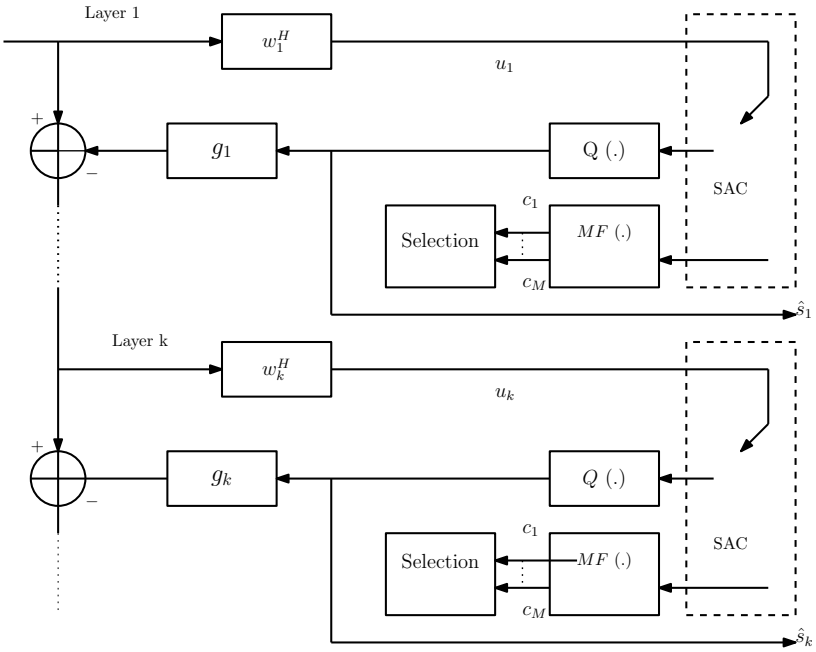

Figure 2.2: Block diagram of a the Proposed MF-SIC detector.

is examined by the SAC to determine if this decision is reliable according to

$$d_k = |u_k - \nu_f|, \tag{2-22}$$

where $\nu_f = \mathsf{arg}\min_{\nu_\mathbf{f} \in \mathcal{A}} \left\{ |u_k - \nu_f| \right\}$ denotes the closest constellation point to the k-th user soft estimate u_k. If $d_k > d_{\text{th}}$ the decision is considered to be unreliable and the selected constellation point is dropped into the shadow area of the constellation map. The parameter d_{th} is the predefined threshold Euclidean distance to guarantee reliability of the selected symbol [9]. If the soft estimate u_k is deemed to be a reliable estimate for user k, the MF-SIC algorithm performs a hard slice as in the conventional SIC approach [9, 10]. In this case, $\hat{s}_k = Q(u_k)$ is the estimated symbol, where $Q(\cdot)$ is the quantization notation which maps to the constellation symbol closest to u_k. Otherwise, the decision is deemed unreliable. In this case, a candidate set $\mathcal{L} = \{c_1, c_2, ..., c_m, ..., c_M\} \subseteq \mathcal{A}$ is generated, which consists of the M constellation points closest to u_k. The number of candidate points M is given by the QPSK symbols. As a result, there is a trade-off between performance and complexity. The algorithm selects an optimal candidate $c_{m,\text{opt}}$ from a pool of $\mathcal{L}$ candidates. As a result, the unreliable choice $Q(u_k)$ is substituted by a hard decision, and $\hat{s}_k = c_{m,\text{opt}}$ is obtained. It should be noted that the List-SIC algorithm's performance benefits are based on the assumption that $c_{m,\text{opt}}$ is correctly selected.

The following is a summary of the MF-SIC selection algorithm: To begin, the selection vectors $\boldsymbol{\phi}^1, \boldsymbol{\phi}^2, ..., \boldsymbol{\phi}^m, ...\boldsymbol{\phi}^M$ must be defined.

The size of these selection vectors is equal to the number of the constellation candidates that are used every time a decision is considered unreliable. For example, for the k-th layer, a $K \times 1$ vector $\boldsymbol{\phi}^m = \left[\hat{s}_1, ..., \hat{s}_{k-1}, c_m, \phi_{k+1}^m, ..., \phi_q^m, ..., \phi_K^m\right]^T$, which is a potential choice corresponding to c_m in the k-th user, consists of the following items: (a) The previously estimated symbols $\hat{s}_1, \hat{s}_2, ..., \hat{s}_{k-1}$. (b) The candidate symbol c_m obtained from the constellation for subtracting a decision that was considered unreliable $Q(u_k)$ of the k-th user. (c) Using (a) and (b) as the previous decisions, detection of the next user data $k+1, ..., q, ...,$ K-th is performed by the SIC approach. Mathematically, the choice ϕ^m is given by [10]

$$\phi_q^m = Q(\mathbf{w}_q^H \hat{\boldsymbol{y}}_q^m), \tag{2-23}$$

where the index q denotes a given UE between the (k+1)-th and the K-th UE,

$$\hat{\boldsymbol{y}}_q^m = \check{\boldsymbol{y}}_k - \mathbf{g}_k c_m - \sum_{p=k+1}^{q-1} \mathbf{g}_p \phi_p^m. \tag{2-24}$$

A key attribute of the proposed MF-SIC algorithm is the same MMSE filter $\mathbf{w}_k$ that is used for all the constellation candidates. Therefore, the proposed algorithm has the same computational complexity as the conventional SIC. The optimal candidate m, opt is selected according to the local ML rule given by

$$m, \text{opt} = \arg \min_{1 \le m \le M} \left\| \boldsymbol{y} - \mathbf{G}\boldsymbol{\phi}^m \right\|^2. \tag{2-25}$$

2.4 Iterative Detection and Decoding

IDD schemes combine joint detection and decoding. IDD schemes leverage message passing and the exchange of soft information in the form of LLRs to improve the performance of communication systems. The inherent benefits of IDD can be summarized as follows:

1. IDD techniques result in significant reduction in the BER.
2. IDD schemes can be implemented cheaply using linear block codes.
3. Can yield high SINRs and higher spectral efficiencies.

Several channel codes have been applied recently to improve the performance of massive MIMO systems [11–13, 23, 36–44]. In this context, LDPC

codes are simple to implement because of their linear nature and their decoding is computationally efficient.

Thus, this thesis utilizes IDD schemes based on LDPC codes to improve the performance of CF-mMIMO networks.

The block diagram in Figure 2.3 depicts how IDD is incorporated in a communication system. The K transmitted information signals from users are encoded using a channel code. The channel code converts the messages into code words of length n that are modulated to form constellation symbol points that are transmitted over the channel. The receiver has a soft detector that equalizes the received information to retrieve the originally transmitted messages. These received bits are then decoded and a hard decision is made. The IDD processing is performed through the feedback between the detector and decoder which exchange the messages in an iterative fashion using LLRs [11–13]. Examples of codes used in literature include but are not limited to convolution Codes, LDPC Codes, turbo codes, polar codes among others.

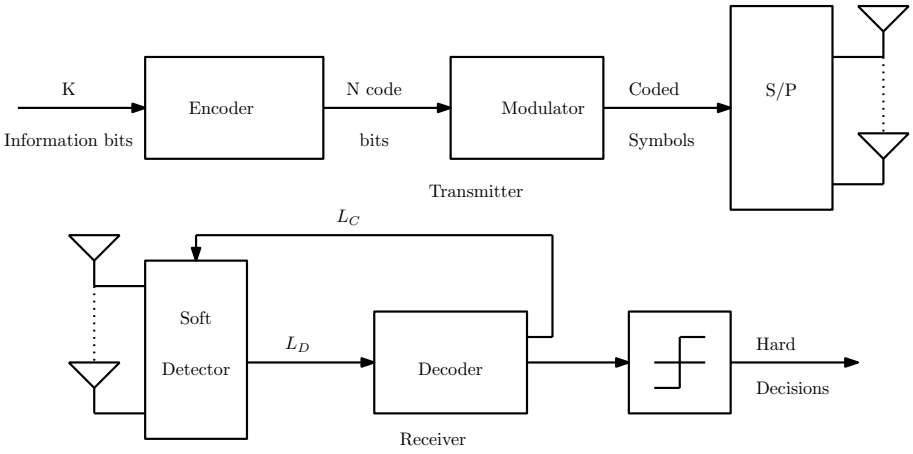

Figure 2.3: Block diagram of a communication system with IDD scheme.

In this thesis, low-complexity IDD schemes using LDPC codes are considered as it is shown in the next section and subsequent chapters of the thesis.

2.5 Iterative Detection and Decoding for Cell-Free Massive MIMO Using LDPC Codes

This section proposes an IDD scheme for a CF-mMIMO system. Users send coded data to the APs, which is jointly detected at the CPU. The symbols are exchanged iteratively in the form of LLRs between the soft detector and the LPDC decoder, increasing the coded system's performance. In particular, we present an IDD scheme for CF-mMIMO systems, which unlike the work in [14], employs message passing. Therefore, the main contributions of this section are

summarized as follows. First, a list-based soft MF-SIC detector is proposed for the CF-mMIMO architecture. This proposed approach gives lower BER values at the same computation complexity as the traditional SIC scheme. Secondly, the proposed soft receiver is compared with other detectors such as the linear MMSE, SIC, PIC and List-PIC. Thirdly, the impact of increasing the IDD iterations is examined. The BER performance of CF-mMIMO is then compared to that of co-located mMIMO systems.

2.5.1 Proposed System Model

The proposed low-complexity IDD scheme for CF-mMIMO systems is shown in Figure 2.4. Particularly, an LDPC-coded CF-mMIMO system comprising of L APs, K single antenna UEs, a joint detector at the CPU and an LDPC decoder are considered.

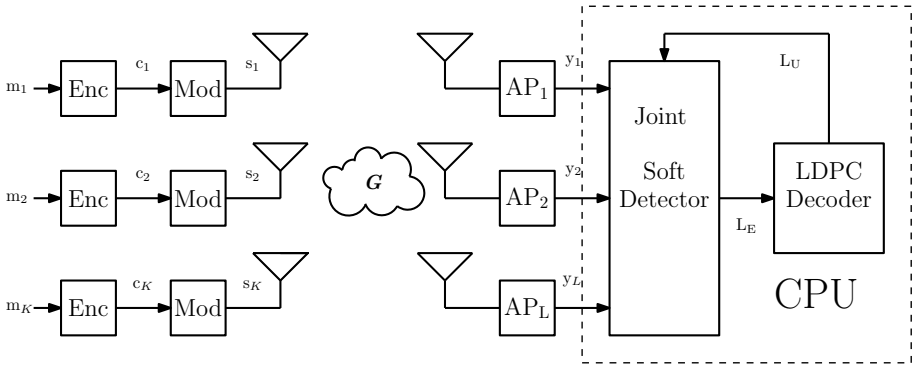

Figure 2.4: Block diagram of a CF-mMIMO system with an IDD scheme.

The data are first encoded (Enc) by an LDPC encoder having a code rate R. This encoded sequence is then modulated (Mod) to complex symbols with a complex constellation of 2^{M_c} possible signal points and average energy E_s. The coded data are then transmitted by K UEs through the channel $\mathbf{G}$ to the APs.

A centralized CF-mMIMO scenario is assumed, where the CPU does soft processing and joint detection on the received signal from the APs. Then the detector sends these soft outputs, L_E, in the form of LLRs to the LDPC decoder. The decoder adopts an iterative strategy by sending extrinsic information, L_U, to the detector. Additionally, the performance of the proposed detector is examined for the case with no iterations and the case with iterations. The channel coefficients between the l-th AP and the k-th UE are given by [3, 13]

$$g_{k,l} = \sqrt{\beta_{k,l}} h_{k,l}, \tag{2-26}$$

where $\beta_{k,l}$ is the large-scale (LS) fading coefficients as a result of path loss (PL) and shadowing. The small scale fading coefficients are given by $h_{k,l}$, that are i.i.d. Gaussian random variables with variance, $\mathbb{E}\{h_{k,l}^* h_{k,l}\} = 1$.

The LS fading coefficient is assumed to be deterministic and can be obtained using the three-slope PL model [3, 13]. More precisely, the PL exponent is 3.5 if the distance d_{kl} between the k-th UE and l-th AP is greater than d_1, equals 2 if $d_1 \geq d_{kl} > d_0$, and equals 0 if $d_{kl} \leq d_0$, for some d_0 and d_1. For $d_{kl} > d_1$, the Hata-COST231 propagation model is applied. The PL PL_{kl} in dBs between the k-th UE and l-th AP is determined using

$$\mathrm{PL}_{kl} = \begin{cases} -\Lambda - 35\log(d_{kl}), & d_{kl} > d_1 \\ -\Lambda - 15\log(d_1) - 20\log(d_{kl}), & d_0 < d_{kl} \leq d_1 \\ -\Lambda - 15\log(d_1) - 20\log(d_0), & d_{kl} \leq d_0 \end{cases}. \tag{2-27}$$

The parameter Λ is given by

$$\begin{aligned} \Lambda \triangleq & 46.3 + 33.9\log_{10}(f) - 13.82\log_{10}(h_{\mathrm{AP}}) - (1.1\log_{10}(f) - 0.7)h_{\mathrm{u}} \\ & + 1.56\log_{10}(f) - 0.8, \end{aligned} \tag{2-28}$$

where f is the carrier frequency (in MHz), h_u and h_{AP} are the antenna heights of the UE and AP, respectively. The LS coefficient $\beta_{k,l}$ models the PL and shadow fading that are given by

$$\beta_{l,k} = PL_{kl} \times 10^{\sigma_{sh}\zeta_{lk}}, \tag{2-29}$$

where $10^{\sigma_{sh}\zeta_{lk}}$ denotes the shadowing with standard deviation σ_{sh}, and $\zeta_{lk} \sim \mathcal{N}(0, 1)$. The received signal $\mathbf{y}$ at the joint soft detector is given by

$$\mathbf{y} = \mathbf{G}\mathbf{s} + \mathbf{n}, \tag{2-30}$$

where $\mathbf{G} \in C^{L \times K}$ is the channel matrix comprising of both small scale and LS fading coefficients. $\mathbf{s} = [s_1, s_2, .., s_{k-1}, s_k, s_{k+1}, ..., s_K]$, $\mathbf{n}$ is the AWGN vector that has zero mean and unit variance.

2.5.2 MMSE soft cancellation detectors

For simplicity of analysis, we consider sub-optimal detectors which consists of PIC/SIC followed by an MMSE filter. The detector first forms soft estimates of the transmitted symbols by computing the symbol mean $\bar{s}_j$

based on the available a-priori information from the decoder [6]

$$\bar{s}_j = \sum_{s \in \mathcal{A}} sP(s_j = s), \tag{2-31}$$

where $\mathcal{A}$ is the complex constellation set. By assuming statistical independence of bits within the same symbol as in [6], the a-priori probabilities are calculated from the extrinsic LLRs provided by the LDPC decoder as

$$P(s_j = s) = \prod_{l=1}^{M_c} [1 + \exp(-s^{b_l} L_c(b_{(j-1)M_c+l}))]^{-1}, \tag{2-32}$$

where $s^{b_l} \in (+1, -1)$ denotes the value of the l-th bit of symbol s, $L_c(b_i)$ denotes the extrinsic LLR of the i-th bit computed by the LDPC decoder in the previous iteration, and M_c is the modulation order. We define $L_c(b_i) = 0$ at the first iteration since the only available belief is from the channel. The variance of the j-th UE symbol is calculated as [5]

$$\sigma_j^2 = \sum_{s \in \mathcal{A}} |s - \bar{s}_j|^2 P(s_j = s). \tag{2-33}$$

For the k-th user, the soft interference from the other $K-1$ users is canceled according to PIC to obtain

$$\mathbf{y} = s_k \mathbf{g}_k + \sum_{j=1, j \neq k}^{K} (s_j - \bar{s}_j)\mathbf{g}_j + \mathbf{n}. \tag{2-34}$$

For SIC, the soft interference from the other $K-1$ users is canceled to obtain

$$\mathbf{y} = \mathbf{y} - \sum_{j=1}^{K-1} \bar{s}_j \mathbf{g}_j. \tag{2-35}$$

Using (2-34), a symbol estimate $\hat{s}_k$ of the transmitted symbol on the k-th UE is obtained by applying a linear filter $\mathbf{w}_k$ to $\mathbf{y}$ such that

$$\hat{s}_k = \mathbf{w}_k^H \mathbf{y} = (\mathbf{w}_k^H \mathbf{g}_k) s_k + \sum_{j=1,\, j \neq k}^{K} (\mathbf{w}_k^H \mathbf{g}_j)(s_j - \bar{s}_j) + \mathbf{w}_k^H \mathbf{n}, \tag{2-36}$$

where $\mathbf{w}_k$ is chosen to minimize the mean square error (MSE) between the transmitted symbol s_k and the filter output $\hat{s}_k$ and depends on the variance of the symbols used in the cancellation step. The estimated symbol while using the SIC can be obtained using a similar approach applied for the PIC. In [6]

it is shown that the corresponding linear filter is given by

$$\mathbf{w}_k = \left(\frac{\sigma_n^2}{E_s}\mathbf{I} + \mathbf{G}\boldsymbol{\Delta}_k\mathbf{G}^H\right)^{-1}\mathbf{g}_k, \tag{2-37}$$

with

$$\boldsymbol{\Delta}_k = \mathsf{diag}\left[\frac{\sigma_{s_1}^2}{E_s}, ..., \frac{\sigma_{s_{k-1}}^2}{E_s}, 1, \frac{\sigma_{s_{k+1}}^2}{E_s}, ..., \frac{\sigma_{s_K}^2}{E_s}\right], \tag{2-38}$$

where $\sigma_{s_i}^2$ is the variance of the i-th user symbol computed as

$$\sigma_{s_i}^2 = \sum_{s\in\mathcal{A}} |s - \bar{s}_i|^2 P(s_i = s). \tag{2-39}$$

2.5.3 Iterative processing

In this section, the MMSE-based detectors are presented for the IDD scheme, consisting of a joint detector and an LDPC decoder, and the iterative processing is detailed. The operation is explained based on the MMSE detector given in (2-37). Other studied detectors take the same procedure and their operation has been omitted without loss of generality. The received signal at the output of the filter, contains the desired symbol, residual co-user interference and noise. We use similar assumptions given in [5,6] to approximate the $\hat{s}_k$ as an output of an AWGN channel given by

$$\hat{s}_k = \mu_k s_k + z_k, \tag{2-40}$$

where $\mu_k = \mathbb{E}\{\hat{s}_k s_k^*\}$. The parameter z_k is a zero-mean AWGN variable. Using similar procedures as in [6], the parameter μ_k is given by

$$\mu_k = \mathbf{g}_k^H\left(\frac{\sigma_n^2}{E_s}\mathbf{I} + \mathbf{G}\boldsymbol{\Delta}_k\mathbf{G}^H\right)^{-1}\mathbf{g}_k. \tag{2-41}$$

The variance of $\hat{s}_k$ is given by

$$\lambda_k^2 = \mu_k - \mu_k^2, \tag{2-42}$$

The extrinsic LLR computed by the detector for the l-th bit $l \in \{1, 2, ..., M_c\}$ of the symbol s_k transmitted by the k-th user is [6]

$$L_D\left(b_{(k-1)M_c+l}\right) = \log \frac{\sum_{s \in A_l^{+1}} f\left(\hat{s}_k|s\right) P\left(s\right)}{\sum_{s \in A_l^{-1}} f\left(\hat{s}_k|s\right) P\left(s\right)} - Lc\left(b_{(k-1)M_c+l}\right), \tag{2-43}$$

where A_l^{+1} is the set of 2^{Mc-1} hypothesis s for which the l-th bit is $+1$. The a-priori probability $P(s)$ is given by (2-32). The approximation of the likelihood function [6] $f(\hat{s}_k|s)$ is given by

$$f\left(\hat{s}_k|s\right) \simeq \frac{1}{\pi\lambda_k^2} \exp\left(-\frac{1}{\lambda_k^2}|\hat{s}_k - \mu_k s|^2\right). \tag{2-44}$$

2.5.4 Decoder Algorithm

The soft beliefs are exchanged between the proposed detectors and the decoder in an iterative manner. The standard sum-product algorithm (SPA) suffers from performance degradation caused by the tangent function especially in the error-rate floor region [12]. Therefore, we use the box-plus SPA in this thesis because it yields less complex approximations. The decoder is made up of two stages, namely, the single parity check (SPC) stage and the repetition stage. The LLRs sent from check node $(CN)_J$ to variable node $(VN)_i$ are computed as described by

$$L_{j \longrightarrow i} = \boxplus i^{'} \in N(j) \diagdown i L_{i^{'} \longrightarrow j}. \tag{2-45}$$

As shorthand, we use $L_1 \boxplus L_2$ to denote the computation of $L(L_1 \bigoplus L_2)$. The LLRs are computed by

$$\begin{aligned} L_1 \boxplus L_2 =& \log\left(\frac{1 + e^{L_1+L_2}}{e^{L_1} + e^{L_2}}\right), \\ =& \text{sign}(L_1)\text{sign}(L_2)\min(|L_1|, |L_2|) + \log\left(1 + e^{-|L_1+L_2|}\right) \\ & - \log\left(1 + e^{-|L_1-L_2|}\right). \end{aligned} \tag{2-46}$$

The LLRs from VN_i to CN_j are given by

$$L_{i \longrightarrow j} = L_i + \sum_{j^{'} \in N(i) \backslash j} L_{j^{'} \longrightarrow i}, \tag{2-47}$$

where the parameter L_i denotes the LLR at VN_i, $j^{'} \in N(i) \backslash j$ denotes all CNs connected to VN_i except CN_j.

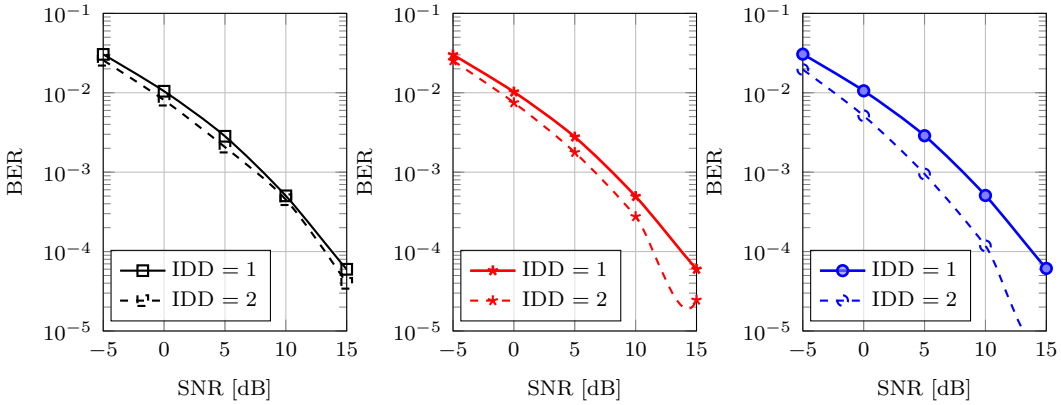

Figure 2.5: BER versus SNR for CF-mMIMO for (a) SIC, (b) List-SIC and (c) PIC with $L = 100$, $K = 40$, while varying the number of IDD iterations.

2.6 Numerical Results

In this section, the BER performance of the proposed soft detectors is presented for the CF-mMIMO and co-located mMIMO (COL-mMIMO) settings. The CF-mMIMO channel exhibits high PL values due to LS fading coefficients. Thus, the instantaneous SNR definition is given by

$$SNR = \frac{\mathrm{tr}(\sigma_s^2 \mathbf{G}\mathbf{G}^H)R}{LK\sigma_n^2}. \tag{2-48}$$

The simulation parameters are varied as follows: we consider a cell-free environment with a square of dimensions $D \times D =$, where $D = 1$ km. Distances d_0 and d_1 are 10 m and 50 m, respectively. $h_{AP} = 15$m, $h_u = 1.65$ m, $f = 1900$ MHz, $d_{th} = 0.38$, LDPC code with code word length (C_{leng}) 256 bits, $M = 128$ parity check bits and $C_{\text{leng}} - M$ message bits. The code rate $R = \frac{1}{2}$. The maximum number of inner iterations is set to 10. The signal power $\sigma_s^2 = 1$ and the simulations are run for 10^3 channel realizations. Figure 2.5 presents the BER versus the SNR as the number of IDD iterations are increased. It can be visualized that increasing IDD iterations yields lower BER. This is because more a-posterior information is exchanged between the joint detector and decoder as the iterations increase, which improves the system performance. The number of iterations do not cause any marginal effect on the linear MMSE filter without cancellation because there is no Δ_k in this filter which is needed for the IDD to improve the performance.

Figure 2.6 presents BER versus SNR while comparing the CF-mMIMO and COL-mMIMO architectures. It can be shown that the CF-mMIMO achieves low BER compared to the Col-mMIMO. This is due to the distributed

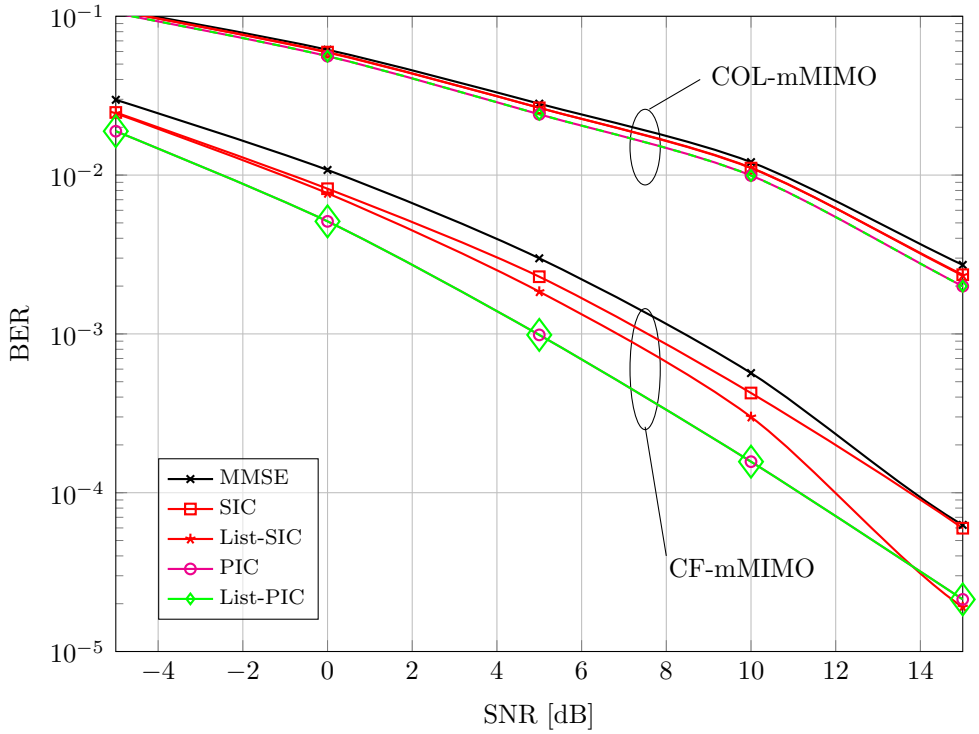

Figure 2.6: BER versus SNR for CF-mMIMO and Col-mMIMO with $L = 100$, $K = 40$, IDD = 2, single Base Station (BS) with 100 antennas.

nature of CF-mMIMO which improves the performance of the entire coverage area.

Figure 2.7 presents the BER versus the SNR for the CF-mMIMO system model for different values of L and the studied soft detectors for two (2) IDD iterations. The PIC and List-PIC achieves the lowest BER values, followed by List-SIC, SIC, MMSE, in that order. In addition, increasing L and K reduces the BER. Also, the performance benefit of conventional PIC and List-PIC is negligible.

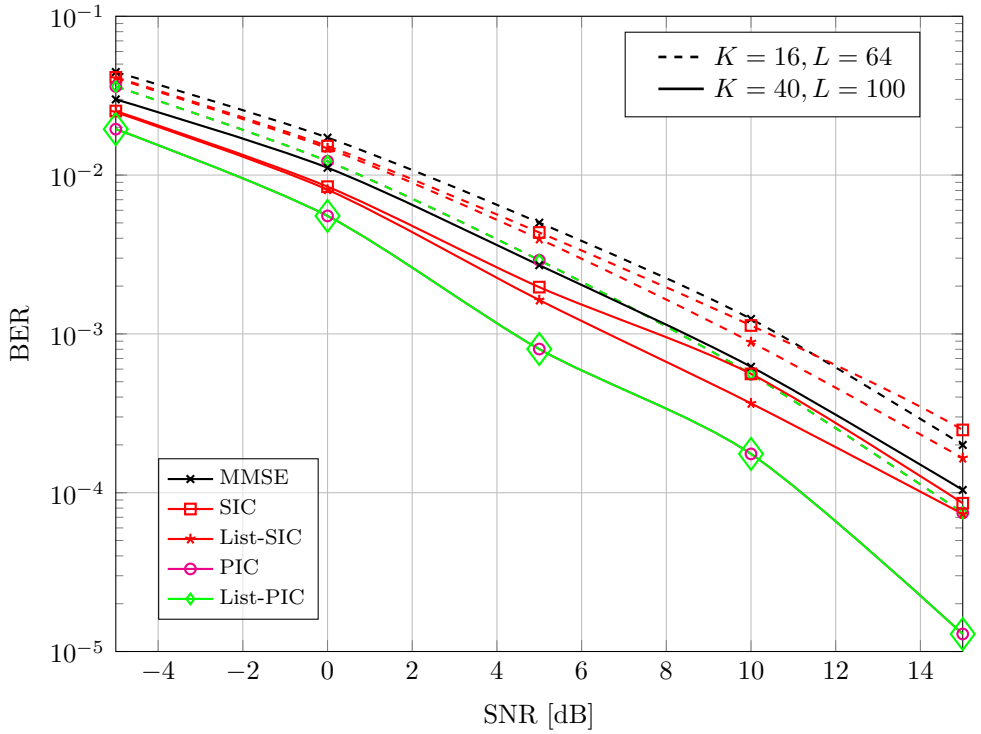

Figure 2.7: BER versus SNR for CF-mMIMO for the different detectors.

2.7 Summary

In this section, a brief background about traditional and CF mMIMO systems has been presented and analysis of the proposed receivers has been done. Specifically, an IDD scheme using LDPC codes has been studied for the CF-mMIMO networks assuming perfect CSI (PCSI). A list-based detectors for CF-mMIMO architectures and its performance has been compared with other baseline detection schemes. Furthermore, the BER performance of CF-mMIMO has been compared with co-located mMIMO. Finally, increasing IDD iterations significantly reduces the BER.

3
Centralized and Decentralized IDD Schemes with AP Selection and LLR Refinement

In this chapter, iterative interference cancellation (IC) schemes with AP selection (APs-Sel) and LLR refinement for CF-mMIMO systems are proposed. Closed-form expressions for centralized and decentralized LMMSE receive filters with APs-Sel are derived assuming imperfect CSI. Based on the derived expressions, insights are drawn and general expressions are devised for several cases, namely, MMSE-SIC filter for the non-scalable CF-mMIMO that uses all APs, an MMSE-SIC filter assuming perfect CSI, and a case with no IC and the linear MMSE filter. Furthermore, we formulate a new Gaussian approximation of the likelihood function by deriving new closed-form expressions for the second order statistics (mean and variance) of the detected signal parameters in presence of channel estimation errors, APs-Sel matrix and MUI. Since the MMSE-SIC filter experiences error propagation due to erroneous decisions from the previous stages, we develop a list-based detector based on LMMSE receive filters for CF-mMIMO systems that exploits IC and the constellation points to mitigate the error propagation that occurs in conventional MMSE-SIC receivers. An IDD scheme that employs LDPC codes is then developed. Moreover, LLR refinement strategies based on censoring and a linear combination of local LLRs are proposed to improve the network performance. We assess the proposed centralized and decentralized IDD schemes against existing approaches in terms of BER performance, complexity, and signaling under perfect CSI and imperfect CSI.

3.1
Proposed System and Signal Model

In this section, the uplink of a CF-mMIMO system with L APs and K single-antenna user equipment (UE), where each AP is equipped with N receive antennas, is considered. The system is assumed to have imperfect channel estimates. The received signal statistics and channel estimation procedures are given below.

3.1.1 Uplink Pilot Transmission and Channel Estimation

Assume that τ_p mutually orthogonal pilot sequences $\boldsymbol{\psi}_1$,..., $\boldsymbol{\psi}_{\tau_p}$ with $||\boldsymbol{\psi}_t||^2 = \tau_p$ are used to estimate the channel. Furthermore, $K > \tau_p$ is such that more than one UE can be assigned per pilot. The index of UE k that uses the same pilot is denoted as $t_k \in \{1, ..., \tau_p\}$ with $\vartheta_k \subset \{1, ..., K\}$ as the subset of UEs that use the same pilot as UE k inclusive. The complex received signal at the l-th AP after the UE transmission, [1, 45] $\mathbf{Y}_l$, with dimensions $N \times \tau_p$, is given by

$$\mathbf{Y}_l = \sum_{j=1}^{K} \sqrt{\eta_j} \mathbf{g}_{jl} \boldsymbol{\psi}_{t_j}^T + \mathbf{N}_l, \tag{3-1}$$

where η_j is the transmit power from UE j, $\mathbf{N}_l$ is the received noise signal with independent $\mathcal{N}_{\mathbb{C}} \sim (0, \sigma^2)$ entries and noise power σ^2, $\mathbf{g}_{jl} \sim \mathcal{N}_{\mathbb{C}}(0, \boldsymbol{\Omega}_{jl})$, and $\boldsymbol{\Omega}_{jl} \in \mathbb{C}^{N \times N}$ is the spatial correlation matrix that describes the channel's spatial properties between the k-th UE and the l-th AP, $\beta_{k,l} \triangleq \frac{\mathrm{tr}(\boldsymbol{\Omega}_{jl})}{N}$ is the LS fading coefficient. The first AP correlates the received signal with the associated normalized pilot signal $\boldsymbol{\psi}_{t_k}/\sqrt{\tau_p}$ to $\mathbf{y}_{t_{kl}} \triangleq \frac{1}{\sqrt{\tau_p}} \mathbf{Y}_l \boldsymbol{\psi}_{t_k}^* \in \mathbb{C}^N$ to estimate the channel $\mathbf{g}_{jl}$ given by

$$\mathbf{y}_{t_{kl}} = \sum_{j \in \vartheta_k} \sqrt{\eta_j \tau_p} \mathbf{g}_{jl} + \mathbf{n}_{t_{kl}}, \tag{3-2}$$

where $\mathbf{n}_{t_{kl}} \triangleq \frac{1}{\sqrt{\tau_p}} \mathbf{N}_l \boldsymbol{\psi}_{t_k}^* \sim \mathcal{N}_c(0, \sigma^2 \mathbf{I}_N)$ is the obtained noise sample after estimation. From [1], the MMSE estimate of $\mathbf{g}_{kl}$ is given by

$$\hat{\mathbf{g}}_{kl} = \sqrt{\eta_k \tau_p} \boldsymbol{\Omega}_{kl} \Psi_{t_{kl}}^{-1} \mathbf{y}_{t_{kl}}, \tag{3-3}$$

where $\Psi_{t_{kl}} = \mathbb{E}\left\{\mathbf{y}_{t_{kl}} \mathbf{y}_{t_{kl}}^H\right\} = \sum_{j \in \vartheta_k} \eta_j \tau_p \boldsymbol{\Omega}_{jl} + \mathbf{I}_N$ is the received signal vector correlation matrix. The channel estimate $\hat{\mathbf{g}}_{kl}$ and the estimation error $\tilde{\mathbf{g}}_{kl} = \mathbf{g}_{kl} - \hat{\mathbf{g}}_{kl}$ are independent with distributions $\hat{\mathbf{g}}_{kl} \sim \mathcal{N}_c(0, \eta_k \tau_p \boldsymbol{\Omega}_{kl} \boldsymbol{\Psi}^{-1} \boldsymbol{\Omega}_{kl})$ and $\tilde{\mathbf{g}}_{kl} \sim \mathcal{N}_c(0, \mathbf{C}_{kl})$, where the matrix $\mathbf{C}_{kl}$ is given by

$$\mathbf{C}_{kl} = \mathbb{E}\left\{\tilde{\mathbf{g}}_{kl} \tilde{\mathbf{g}}_{kl}^H\right\} = \boldsymbol{\Omega}_{kl} - \eta_k \tau_p \boldsymbol{\Omega}_{kl} \boldsymbol{\Psi}^{-1} \boldsymbol{\Omega}_{kl}. \tag{3-4}$$

It should be noted that the pilot contamination is caused by the mutual interference made by UEs using the same pilot signals in (3-2), which lowers the system's performance [1].

From (3-1), the received signal vector after stacking the channel vectors

from all the APs is given by

$$\mathbf{y} = \mathbf{G}\mathbf{s} + \mathbf{n}, \tag{3-5}$$

where the channel matrix $\mathbf{G} \in \mathbb{C}^{NL\times K}$ has both small scale and LS fading coefficients. Vector $\mathbf{s} = [s_1, .., s_K]^T$ is the transmitted symbols with $\mathbb{E}\{s_k s_k^*\} = \rho_k$, the average transmit power is given by $\boldsymbol{\rho} = [\rho_1, .., \rho_K]^T$, $\mathbf{n}$ is the AWGN sample vector with zero mean and unit variance.

In CF-mMIMO networks, there are limitations on the complexity and amount of signaling the APs and CPU must exchange. Both of these issues make system modeling and design almost impracticable. To solve this problem, we adopt a scalable CF-mMIMO setup that takes the selection of APs into account. This is accomplished using the APs-selection technique described as follows:

3.1.2 Access Point Selection Procedure

The dynamic cooperative clustering (DCC) approach described in [45] is considered when selecting the APs. Unlike existing approaches for APs-Sel, the proposed approach incorporates the APs-Sel in the receive filter expression, which facilitates its computation. By letting $\mathcal{M}_k \subset \{1, ..., L\}$ be the subset of APs in service of UE k, the matrix $\mathbf{D}_{kl}$ is defined as

$$\mathbf{D}_{kl} = \begin{cases} \mathbf{I}_N & \text{if} \quad l \in \mathcal{M}_k \\ \mathbf{0}_N & \text{if} \quad l \notin \mathcal{M}_k. \end{cases} \tag{3-6}$$

The APs that provide service to a specific UE are determined by the block diagonal matrix $\mathbf{D}_k = \text{diag}(\mathbf{D}_{k1}, .., \mathbf{D}_{kL}) \in \mathbb{C}^{NL\times NL}$. Specifically, when $\mathbf{D}_k = \mathbf{I}_{NL}$, all APs serve all the UEs. However, using all APs is not scalable and practical, and thus clustering approaches such as user-centric techniques can be adopted. Then, the set of UEs that are served by AP l is

$$\mathcal{D}_l = \left\{ k : \text{tr}(\mathbf{D}_{kl}) \geq 1, k \in \{1, .., K\} \right\}. \tag{3-7}$$

It is important to note that the DCC does not alter the received signal statistics since all APs receive the broadcast signal. An essential feature of such a selection process is limiting the number of APs that take part in signal detection. The joint AP selection criterion described in [45] determines which APs will provide service to a specific UE. In this scenario, the UE designates a master AP to coordinate uplink (UL) detection and decoding based on the

LLSF. The CPU then establishes a threshold value β_{th} for non-master APs to provide service to a certain UE. A detailed explanation of the operation of the DCC approach can be found in [45]. There is a need to demodulate the transmitted symbols at the receiver. Thus, the proposed centralized IDD receiver structure is detailed in the following section.

3.2 Proposed Centralized IDD Scheme

In this section, the proposed centralized processing architecture for coded CF-mMIMO systems is presented. The block diagram of the proposed centralized IDD scheme is depicted in Figure 3.1. The codeword sequence $\boldsymbol{c}_k$

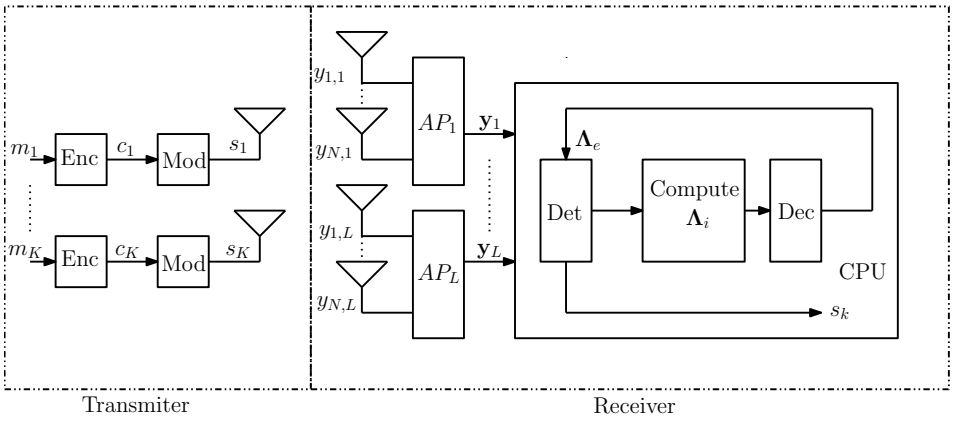

Figure 3.1: Block diagram for IDD scheme with centralized processing.

is created by first encoding the message sequence $\boldsymbol{m}_k$ for UE k by an LDPC encoder (Enc) with a code rate of R. This encoded sequence is then modulated (Mod) to form complex symbols with a complex constellation of 2^{M_c} possible signal points. The K UEs then send the modulated symbols to the APs. The APs serve as relays during data reception and transfer the information to the CPU, which has a joint detector (Det), an LLR computing module, and an LDPC decoder (Dec). Then, the detector forwards the data to a module that computes the LLRs Λ_i. These computed LLRs are then sent to the decoder. By providing extrinsic data Λ_e to the joint detector, the decoder uses an iterative technique presented in Section 3.6 that enhances the detection performance of the receiver.

3.2.1 Proposed Centralized Receiver Design

The proposed receiver configuration aims to cancel the MUI caused by the other $K-1$ UEs in the network. The receiver consists of an MMSE filter followed by a soft IC scheme, which may use either a SIC or a list-based

with SIC technique. The receiver first creates soft estimates of the transmitted symbols by computing the jth UE symbol mean $\bar{s}_j$ based on the soft beliefs from the LDPC decoder [5–7] given $\mathbb{E}\{s_j\} = \bar{s_j}$ as described by equation (2-31). The a priori probability of the extrinsic LLRs [6–8] is given by equation (2-32). The variance of the j-th UE symbol [6] can be computed using (2-33). After decomposition of (3-5) and using $\mathbf{G} = \hat{\mathbf{G}} + \tilde{\mathbf{G}}$, the received signal at the CPU is given by

$$\mathbf{y} = \hat{\mathbf{g}}_k s_k + \hat{\mathbf{G}}_{\mathrm{i}} \bar{\mathbf{s}}_{\mathrm{i}} + \sum_{m=1}^{K} \tilde{\mathbf{g}}_m s_m + \mathbf{n}, \tag{3-8}$$

where the first term on the right-hand side (RHS) is the desired signal, $\hat{\mathbf{g}}_k$ and s_k are the estimate of the channel vector. and transmitted symbol for the desired signal, respectively. The second term is the interference from the other $K-1$ users; $\bar{\mathbf{s}}_{\mathrm{i}}$ is the vector with the interfering symbols except the k-th symbol, and $\hat{\mathbf{G}}_{\mathrm{i}}$ is the matrix with channel estimates of the other $K-1$ users. The third term denotes the interference due to channel estimation errors, and the fourth is the phase-rotated noise. After the estimated MUI has been removed and APs have been selected, the received symbol estimate of the k-th UE data stream at the CPU is given by

$$\tilde{s}_k = \mathbf{w}_k^H \mathbf{D}_k \left(\mathbf{y} - \hat{\mathbf{G}}_{\mathrm{i}} \bar{\mathbf{s}}_{\mathrm{i}} \right), \tag{3-9}$$

The optimization of the receive combining filter $\mathbf{w}_k$ is achieved by minimizing the MSE between the symbol estimate and the transmitted symbol conditioned on $\hat{\mathbf{G}}$. The formulation of the optimization problem is given by

$$\mathbf{w}_k = \arg \min_{(\mathbf{w}_k)} \mathbb{E}\left\{ ||\tilde{s}_k - s_k||^2 \mid \hat{\mathbf{G}} \right\}. \tag{3-10}$$

Differentiating the objective function on the RHS of (3-10) with respect to (w.r.t.) $\mathbf{w}_k^H$, the optimal MMSE receive filter $\mathbf{w}_k$ should satisfy the following relation:

$$\mathbf{D}_k \mathbb{E}\{\mathbf{y}_R \mathbf{y}_R^H\} \mathbf{D}_k^H \mathbf{w}_k - \mathbf{D}_k \mathbb{E}\{\mathbf{y}_R s_k^*\} = 0, \tag{3-11}$$

where $\mathbf{y}_R = \mathbf{y} - \hat{\mathbf{G}}_{\mathrm{i}} \bar{\mathbf{s}}_{\mathrm{i}}$. The solution to the filter is obtained by making $\mathbf{w}_k$ the subject of (3-11) as

$$\mathbf{w}_k = \left(\mathbf{D}_k \mathbb{E}\{\mathbf{y}_R \mathbf{y}_R^H\} \mathbf{D}_k^H \right)^{-1} \mathbf{D}_k \mathbb{E}\{\mathbf{y}_R s_k^*\}. \tag{3-12}$$

By using the orthogonality principle in [46, 47] and assuming statistical independence of each term in the received signal $\mathbf{y}$, the terms $\mathbb{E}\{\mathbf{y}_R s_k^*\}$ and $\mathbb{E}\{\mathbf{y}_R \mathbf{y}_R^H\}$ are given by

$$\mathbb{E}\{\mathbf{y}_R s_k^*\} = \rho_k \hat{\mathbf{g}}_k, \tag{3-13}$$

and

$$\mathbb{E}\{\mathbf{y}_R \mathbf{y}_R^H\} = \rho_k \hat{\mathbf{g}}_k \hat{\mathbf{g}}_k^H + \hat{\mathbf{G}}_{\mathrm{i}} \Delta_{\mathrm{i}} \hat{\mathbf{G}}_{\mathrm{i}}^H + \sum_{m=1}^{K} \left(\mid s_m \mid^2 + \sigma_m^2 \right) \mathbf{C}_m + \sigma^2 \mathbf{I}_{NL}. \tag{3-14}$$

The matrix $\mathbf{\Delta}_{\mathrm{i}} = \mathsf{diag}\left[\sigma_1^2, ..., \sigma_{k-1}^2, \sigma_{k+1}^2, ..., \sigma_K^2\right]$ denotes the covariance matrix that consists of the entries computed in (2-33). By substituting (3-13) and (3-14) into (3-12), the centralized MMSE filter is given by

$$\mathbf{w}_k = \rho_k \left(\mathbf{D}_k \left(\rho_k \hat{\mathbf{g}}_k \hat{\mathbf{g}}_k^H + \hat{\mathbf{G}}_{\mathrm{i}} \mathbf{\Delta}_{\mathrm{i}} \hat{\mathbf{G}}_{\mathrm{i}}^H + \sigma^2 \mathbf{I}_{NL} + \sum_{m=1}^{K} \left(\mid s_m \mid^2 + \sigma_m^2 \right) \mathbf{C}_m \right) \mathbf{D}_k^H \right)^{-1} \mathbf{D}_k \hat{\mathbf{g}}_k. \tag{3-15}$$

A detailed derivation of (3-15) can be found in Appendix B.

3.2.2 Insights into the Centralized MMSE Filter

The major parameters that affect the performance of the derived receiver in (3-15) can be explained as follows.

- The channel estimation error, a high channel estimation error which results into imperfect CSI (ICSI). This yields poor channel coefficients which results into wrong detection decisions, thus degrading the performance. This can be reduced by using longer pilots to estimate the channel but at the expense of increasing complexity in terms of training time. On the other hand if there is no channel estimation error the performance of the network improves and this is the case with perfect channel estimates (PCSI). For the case with PCSI, the channel estimation error $\tilde{\mathbf{g}}_m$ is 0, which makes $\mathbf{C}_m = 0$. This yields $\hat{\mathbf{g}}_k = \mathbf{g}_k$. Thus, the third term in (3-15) vanishes to zero, and we obtain

$$\mathbf{w}_k = \rho_k \left(\mathbf{D}_k \left(\rho_k \mathbf{g}_k \mathbf{g}_k^H + \mathbf{G}_{\mathrm{i}} \mathbf{\Delta}_{\mathrm{i}} \mathbf{G}_{\mathrm{i}}^H + \sigma^2 \mathbf{I}_{NL} \right) \mathbf{D}_k^H \right)^{-1} \mathbf{D}_k \mathbf{g}_k. \tag{3-16}$$

- The number of APs and APs-Sel matrix $\mathbf{D}_k$. Increasing the number of

APs in the network improves the detector performance which yields lower BERs. For the case with all APs, the selection matrix $\mathbf{D}_k = \mathbf{I}_{NL}$. Thus, the filter in (3-15) is given by

$$\mathbf{w}_k = \left(\rho_k \hat{\mathbf{g}}_k \hat{\mathbf{g}}_k^H + \hat{\mathbf{G}}_{\mathrm{i}} \Delta_{\mathrm{i}} \hat{\mathbf{G}}_{\mathrm{i}}^H + \sum_{m=1}^{K} \left(\mid s_m \mid^2 + \sigma_m^2 \right) \mathbf{C}_m + \sigma^2 \mathbf{I}_{NL} \right)^{-1} \rho_k \hat{\mathbf{g}}_k. \tag{3-17}$$

Note that $\mathbf{D}_k = \mathbf{0}$, implies that $\mathbf{w}_k^H \mathbf{D}_k = \mathbf{0}$, where $\mathbf{w}_k^H$ is the receive vector. This means that only APs with $\mathbf{D}_k \neq \mathbf{0}$ will apply receive combining in the uplink detection.

- The number of IDD iterations and interference cancellation matrix $\boldsymbol{\Delta}_i$. Increasing the number of iterations improves the performance. This is because more information is exchanged between the decoder and detector with improves on the interference cancellation capability of the receiver. Mathematically, this can be explained as: In the first iteration it is considered that $\bar{\mathbf{s}}_{\mathrm{i}} = \mathbf{0}$ in (2-31). In this case, we have a linear MMSE filter and the estimated signal in (3-9) is

$$\begin{aligned} \tilde{s}_k = & \rho_k \hat{\mathbf{g}}_k^H \mathbf{D}_k^H \Bigg(\rho_k \mathbf{D}_k \hat{\mathbf{g}}_k \hat{\mathbf{g}}_k^H \mathbf{D}_k^H + \mathbf{D}_k \hat{\mathbf{G}}_{\mathrm{i}} \operatorname{diag}(\boldsymbol{\rho}_{\mathrm{i}}) \hat{\mathbf{G}}_{\mathrm{i}}^H \mathbf{D}_k^H \\ & + \mathbf{D}_k \left(\sigma^2 \mathbf{I}_{NL} + \sum_{m=1}^{K} \rho_m \mathbf{C}_m \right) \mathbf{D}_k^H \Bigg)^{-1} \mathbf{y}. \end{aligned} \tag{3-18}$$

The vector $\boldsymbol{\rho}_{\mathrm{i}}$ denotes the average transmit power vector for the other $K-1$ UEs. As the number of iterations increases, there is more a posterior information about the transmitted bit. This implies that mean of the interference symbol $\bar{\mathbf{s}}_{\mathrm{i}} \approx \mathbf{s}_{\mathrm{i}}$ in (2-31). Thus, the filter becomes a perfect interference canceler, and (3-9) yields

$$\begin{aligned} \tilde{s}_k = & \rho_k \hat{\mathbf{g}}_k^H \mathbf{D}_k^H \left(\rho_k \mathbf{D}_k \hat{\mathbf{g}}_k \hat{\mathbf{g}}_k^H \mathbf{D}_k^H + \mathbf{D}_k \left(\sigma^2 \mathbf{I}_{NL} + \sum_{m=1}^{K} \mid s_m \mid^2 \mathbf{C}_m \right) \mathbf{D}_k^H \right)^{-1} \\ & \times \left(\mathbf{y} - \mathbf{D}_k \hat{\mathbf{G}}_{\mathrm{i}} \mathbf{s}_{\mathrm{i}} \right). \end{aligned} \tag{3-19}$$

The centralized detection schemes experience high levels of complexity as the number of UEs, APs, and antennas at the APs increases. This makes the design of receivers more complicated, and the amount of required signaling between APs and the CPU increases. To alleviate the above problem, the decentralized IDD scheme is proposed as follows:

3.3 Proposed Decentralized IDD Scheme

The proposed decentralized IDD scheme is shown in Figure 3.2. The

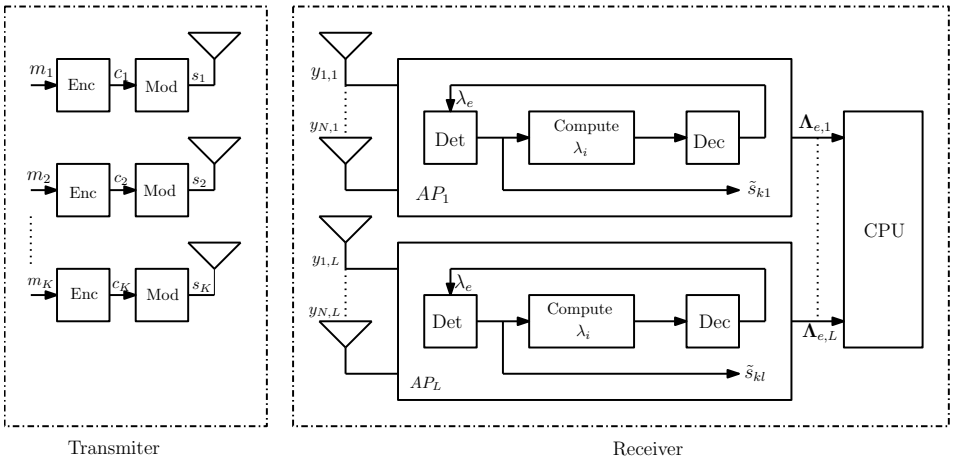

Figure 3.2: Block diagram for IDD scheme with decentralized processing.

transmitter operates in the same way as that of the centralized processor in Section 3.2. At the receiver, each AP is equipped with a local detector, an LLR computing module, and an LDPC decoder. The APs use their local channel estimates to perform IDD on the received signals. The detector sends its symbol estimates to a module that computes the local soft information λ_i in the form of LLRs. The computed LLRs are then sent to the decoder, which performs iterative processing by exchanging extrinsic information λ_e with the local detector. In the decentralized operation, the APs act as compute-and-forward relays by sending their soft beliefs to the CPU for further processing. The challenge at the CPU is to design an intelligent way of processing these LLRs. We devised three techniques for processing these LLRs. The first scheme (standard LLR processing) is based on individual decisions from each AP, and an average BER is then computed based on these decisions from each AP. The second scheme considers censoring the LLRs (LLR censoring) and decoding each UE data at the AP, where it achieves the largest mean absolute value of LLRs. The third scheme is based on the linear combination of the LLRs (LLR Ref). A detailed explanation, operation, and analysis of the proposed LLR processing schemes are given in Section 3.6.

3.3.1 Proposed Decentralized Receiver Design

The channel statistics, estimation, and received signals follow the model introduced in Section 3.1.1. The received signal at the l-th AP is given by

$$\mathbf{y}_l = \sum_{i=1}^{K} \mathbf{g}_{il} s_i + \mathbf{n}_l \in \mathbb{C}^{N\times 1}, \tag{3-20}$$

which can further be decomposed as

$$\mathbf{y}_l = \hat{\mathbf{g}}_{kl} s_k + \hat{\mathbf{G}}_{\mathrm{i}l} \mathbf{s}_{\mathrm{i}} + \sum_{m=1}^{K} \tilde{\mathbf{g}}_{ml} s_m + \mathbf{n}_l, \tag{3-21}$$

where the first term on the RHS is the desired signal, the second term is the interference from the other $K-1$ users, the third term denotes the interference due to channel estimation errors, and the fourth term is the phase-rotated noise. The received local symbol estimate of the k-th UE data stream at the l-th AP after removing the MUI is given by

$$\tilde{s}_{kl} = \mathbf{w}_{kl}^H \mathbf{D}_{kl} \left(\mathbf{y}_l - \hat{\mathbf{G}}_{\mathrm{i}l} \bar{\mathbf{s}}_{\mathrm{i}} \right), \tag{3-22}$$

where the notation $\mathbf{D}_{kl}$ implies that the l-th AP is among the selected APs. Here, the optimization of the received combining filter $\mathbf{w}_{kl}$ is obtained by minimizing the error between the estimated detected symbol and the transmitted symbol. The optimization problem is formulated as

$$\mathbf{w}_{kl} = \arg \min_{(\mathbf{w}_{kl})} \mathbb{E}\left\{ ||\tilde{s}_{kl} - s_k||^2 \mid \hat{\mathbf{G}}_l \right\}. \tag{3-23}$$

The derivation is similar to the centralized approach, and, for completeness, it is described in detail in Appendix C. The optimal receive filter $\mathbf{w}_{kl}$ should satisfy the following relation:

$$\mathbf{D}_{kl} \mathbb{E}\{\mathbf{y}_{Rl} \mathbf{y}_{Rl}^H\} \mathbf{D}_{kl}^H \mathbf{w}_{kl} - \mathbf{D}_{kl} \mathbb{E}\{\mathbf{y}_{Rl} s_k^*\} = 0. \tag{3-24}$$

Thus, the solution to the receive filter is given by

$$\mathbf{w}_{kl} = \left(\mathbf{D}_{kl} \mathbb{E}\{\mathbf{y}_{Rl} \mathbf{y}_{Rl}^H\} \mathbf{D}_{kl}^H \right)^{-1} \mathbf{D}_{kl} \mathbb{E}\{\mathbf{y}_{Rl} s_k^*\}. \tag{3-25}$$

The terms $\mathbb{E}\{\mathbf{y}_{Rl} s_k^*\}$ and $\mathbb{E}\{\mathbf{y}_{Rl} \mathbf{y}_{Rl}^H\}$ are respectively, given by

$$\mathbb{E}\{\mathbf{y}_{Rl} s_k^*\} = \rho_k \hat{\mathbf{g}}_{kl}, \tag{3-26}$$

$$\mathbb{E}\{\mathbf{y}_{Rl}\mathbf{y}_{Rl}^H\} = \rho_k\hat{\mathbf{g}}_{kl}\hat{\mathbf{g}}_{kl}^H + \hat{\mathbf{G}}_{\mathrm{i}l}\Delta_{\mathrm{i}l}\hat{\mathbf{G}}_{\mathrm{i}l}^H + \sum_{m=1}^{K}\left(\mid s_m \mid^2 + \sigma_m^2\right)\mathbf{C}_{ml} + \sigma^2\mathbf{I}_N, \quad (3\text{-}27)$$

where $\Delta_{\mathrm{i}l}$ denotes the covariance matrix that consists of the entries computed in (2-33), locally computed at the l-th AP. By substituting (3-26) and (3-27) into (3-25), the solution of the local receive filter $\mathbf{w}_{kl}^H$ is given by

$$\mathbf{w}_{kl} = \rho_k\left(\mathbf{D}_{kl}\left(\rho_k\hat{\mathbf{g}}_{kl}\hat{\mathbf{g}}_{kl}^H + \hat{\mathbf{G}}_{\mathrm{i}l}\Delta_{\mathrm{i}l}\hat{\mathbf{G}}_{\mathrm{i}l}^H + \sigma^2\mathbf{I}_N + \sum_{m=1}^{K}\left(\mid s_m \mid^2 + \sigma_m^2\right)\mathbf{C}_{ml}\right)\mathbf{D}_{kl}^H\right)^{-1}$$
$$\times\, \mathbf{D}_{kl}\hat{\mathbf{g}}_{kl}. \quad (3\text{-}28)$$

3.3.2 Insights into the Decentralized MMSE Filter

In what follows, we draw insights into the derived local MMSE filter expression to study the impact of the major parameters and scenarios that affect the receiver's performance for the cases with a selected AP, PCSI, and different number of iterations. When the local AP is selected with all its antennas, the selection matrix $\mathbf{D}_{kl} = \mathbf{I}_N$. The local filter in (3-28) is

$$\mathbf{w}_{kl} = \rho_k\left(\rho_k\hat{\mathbf{g}}_{kl}\hat{\mathbf{g}}_{kl}^H + \hat{\mathbf{G}}_{\mathrm{i}l}\Delta_{\mathrm{i}l}\hat{\mathbf{G}}_{\mathrm{i}l}^H + \left(\sum_{m=1}^{K}\left(\mid s_m \mid^2 + \sigma_m^2\right)\mathbf{C}_{ml} + \sigma^2\mathbf{I}_N\right)\right)^{-1}\hat{\mathbf{g}}_{kl}. \quad (3\text{-}29)$$

Assuming PCSI, the fourth term in (3-28) vanishes to zero, and we obtain the filter given by

$$\mathbf{w}_{kl} = \rho_k\left(\rho_k\mathbf{D}_{kl}\mathbf{g}_{kl}\mathbf{g}_{kl}^H\mathbf{D}_{kl}^H + \mathbf{D}_{kl}\mathbf{G}_{\mathrm{i}l}\Delta_{\mathrm{i}l}\mathbf{G}_{\mathrm{i}l}^H\mathbf{D}_{kl}^H + \sigma^2\mathbf{D}_{kl}\mathbf{I}_N\tilde{\mathbf{D}}_{kl}^H\right)^{-1}\mathbf{g}_{kl}\mathbf{D}_{kl}. \quad (3\text{-}30)$$

In the first iteration, $\bar{\mathbf{s}}_{\mathrm{i}} = \mathbf{0}$ in (2-31), which yields the linear MMSE filter and the estimated signal in (3-22) given by

$$\tilde{s}_{kl} = \rho_k\hat{\mathbf{g}}_{kl}^H\mathbf{D}_{kl}^H$$
$$\times\left(\mathbf{D}_{kl}\left(\rho_k\hat{\mathbf{g}}_{kl}\hat{\mathbf{g}}_{kl}^H + \hat{\mathbf{G}}_{\mathrm{i}l}\mathrm{diag}\left(\boldsymbol{\rho}\right)\hat{\mathbf{G}}_{\mathrm{i}l}^H + \sum_{m=1}^{K}\left(\mid \bar{s}_m \mid^2 + \sigma_m^2\right)\mathbf{C}_{ml} + \sigma^2\mathbf{I}_N\right)\mathbf{D}_{kl}^H\right)^{-1}\mathbf{y}_l, \quad (3\text{-}31)$$

where the parameter $\boldsymbol{\rho}$ denotes the average transmit power vector for the other $K-1$ UEs. The mean symbol $\bar{\mathbf{s}}_{\mathrm{i}} \approx \mathbf{s}_{\mathrm{i}}$ in (2-31) increases as the number of iterations increases. Thus, the filter becomes a perfect interference canceler.

(3-22) yields

$$\tilde{s}_{kl} = \rho_k \hat{\mathbf{g}}_{kl}^H \mathbf{D}_{kl}^H \left(\mathbf{D}_{kl} \left(\rho_k \hat{\mathbf{g}}_{kl} \hat{\mathbf{g}}_{kl}^H + \sum_{m=1}^{K} \mid s_m \mid^2 \mathbf{C}_{ml} + \sigma^2 \mathbf{I}_N \right) \mathbf{D}_{kl}^H \right)^{-1} \times \left(\mathbf{y}_l - \mathbf{D}_{kl} \hat{\mathbf{G}}_{il} \mathbf{s}_{\mathrm{i}} \right). \tag{3-32}$$

The derived MMSE-SIC filters in (3-15) and (3-28) experience error propagation at each sequential step. In what follows, we describe the proposed list-based detector that is capable of suppressing the error propagation that occurs at each cancellation step.

3.4 Proposed List-based detector

In this section, a list-based detection scheme is proposed and detailed [13, 48, 49] as presented in Subsection 2.3.6.

The latency and complexity for the above SIC-based receivers is quite high and gets worse as the number of UE and antennas in the network increases, which is inevitable in CF-mMIMO networks [50]. To handle the issue of latency, we propose the use of PIC based receiver. Also, the RMF is known for its low complexity since it does not require any matrix inversions. Therefore, we present the analysis of the proposed local low latency and complexity receivers in the following section.

3.5 Low Latency and Low Complexity Local receivers

This section presents low latency and low complexity soft iterative detectors for a coded CF-mMIMO based on PIC and RMF, respectively. Particularly, new closed-form expressions for the local MMSE-PIC detector are derived considering the interference from channel estimation and APs-Sel. Assuming the absence of prior information on the transmitted code bit at the first iteration, a local linear MMSE detector expression is deducted from the MMSE-PIC expression. Furthermore, the MMSE-PIC detector is compared with the linear MMSE and RMF detectors.

3.5.1 Iterative Local Receiver Design

The proposed low-complexity and low-latency local receivers are examined in this section.

The estimate of the detected signal of the k-th UE at the $l-$th selected AP is given by

$$\tilde{s}_{kl} = \mathbf{w}_{kl}^{H}\mathbf{D}_{kl}\mathbf{y}_{l}, \tag{3-33}$$

where $\mathbf{w}_{kl}^{H}$ denotes the receive local filter.

3.5.2 Receive Matched Filter

For the RMF, the weighting vector for the k-th UE stream is given by [48]

$$\mathbf{w}_{kl,\mathrm{RMF}} = \mathbf{D}_{kl}\hat{\mathbf{g}}_{kl}. \tag{3-34}$$

By substituting (3-34) into (3-33), the detected signal at the output of a RMF for the k-th UE is given by

$$\begin{aligned}\tilde{s}_{kl} = &\sum_{\gamma=1}^{N} \mid \hat{g}_{kl,\gamma} \mid^{2} \left[\mathbf{D}_{kl}\right]_{\gamma,\gamma} s_k + \sum_{\gamma=1}^{N}\sum_{i=1,i\neq k}^{K} \hat{g}_{kl,\gamma}^{*}\hat{g}_{il,\gamma}\left[\mathbf{D}_{kl}\right]_{\gamma,\gamma} s_i \\ &+ \sum_{\gamma=1}^{N} \hat{g}_{kl,\gamma}^{*}\left[\mathbf{D}_{kl}\right]_{\gamma,\gamma} n_{l,\gamma} + \sum_{\gamma=1}^{N}\sum_{m=1}^{K} \hat{g}_{kl,\gamma}^{*}\tilde{g}_{ml,\gamma}\left[\mathbf{D}_{kl}\right]_{\gamma,\gamma} s_m,\end{aligned} \tag{3-35}$$

The detection estimate in (3-35) can be further simplified to yield

$$\begin{aligned}\tilde{s}_{kl} = N\theta s_k + \sum_{\gamma=1}^{N}\sum_{i=1,i\neq k}^{K} \hat{g}_{kl,\gamma}^{*}\hat{g}_{il,\gamma}\left[\mathbf{D}_{kl}\right]_{\gamma,\gamma} s_i + \sum_{\gamma=1}^{N}\sum_{m=1}^{K} \hat{g}_{kl,\gamma}^{*}\tilde{g}_{ml,\gamma}\left[\mathbf{D}_{kl}\right]_{\gamma,\gamma} s_m \\ + \sum_{\gamma=1}^{N} \hat{g}_{kl,\gamma}^{*}\left[\mathbf{D}_{kl}\right]_{\gamma,\gamma} n_{l,\gamma}.\end{aligned} \tag{3-36}$$

The parameter θ is given by $\theta = \frac{1}{N}\sum_{\gamma=1}^{N} \mid \hat{g}_{kl,\gamma} \mid^{2} \left[\mathbf{D}_{kl}\right]_{\gamma,\gamma} = \sum_{\gamma=1}^{N}\left(\nu_{kl,\gamma}^{2} + \psi_{kl,\gamma}^{2}\right)\left[\mathbf{D}_{kl}\right]_{\gamma,\gamma}$, where $\nu_{kl,\gamma} = \frac{1}{\sqrt{N}}\Re\{\hat{g}_{kl,\gamma}\}$ and $\psi_{kl,\gamma} = \frac{1}{\sqrt{N}}\Im\{\hat{g}_{kl,\gamma}\}$. We assume that $\nu_{kl,\gamma}$ and $\psi_{kl,\gamma}$ are Gaussian random variables (RVs) with zero mean and variance $\sigma_{\nu}^{2} = \frac{1}{2N}$. Then, for a selected AP θ is a Chi-Squared RV with $2N$ degrees of freedom whose mean and variance are given by $\mathbb{E}\{\theta\} = 2N\sigma_{\nu}^{2} = 1$ and $\mathrm{Var}\{\theta\} = 4N\sigma_{\nu}^{2} = \frac{1}{N}$, respectively [50]. The second order moment of θ is mathematically expressed as

$$\mathbb{E}\left\{\theta^{2}\right\} = \mathbb{E}\{\theta\} + \mathrm{Var}\{\theta\} = 1 + \frac{1}{N}. \tag{3-37}$$

From (3-37), we can deduct that as the number of antennas $N \gg 1$ at each AP, $\theta^{2} \approx \mathbb{E}\{\theta^{2}\} \approx 1$. The MUI and the channel estimate error of the RMF are denoted by the second and third terms of (3-36). Interference remains constant

regardless of the SNR of the channel. As a result, the RMF's performance for uncoded systems is never good. We propose to enhance its performance with soft RMF and LLR refining techniques. We also propose a low-latency local iterative interference cancellation strategy based on soft MMSE-PIC, detailed in the next subsection.

3.5.3 MMSE with Parallel Interference Cancellation

The local detected symbol estimate of the k-th UE at the l-th AP is obtained by applying an MMSE-PIC filter after subtracting the expectation of the soft mean values computed in (2-31). This is given by

$$\begin{aligned}\tilde{s}_{kl} =&\mathbf{w}_{kl,\mathrm{PIC}}^{H}\mathbf{D}_{kl}\hat{\mathbf{g}}_{kl}s_k + \mathbf{w}_{kl,\mathrm{PIC}}^{H}\mathbf{D}_{kl}\sum_{i=1,i\neq k}^{K}\hat{\mathbf{g}}_{il}\left(s_i-\bar{s}_i\right) + \mathbf{w}_{kl,\mathrm{PIC}}^{H}\mathbf{D}_{kl}\mathbf{n}_l \\ &+ \mathbf{w}_{kl,\mathrm{PIC}}^{H}\mathbf{D}_{kl}\sum_{m=1}^{K}\tilde{\mathbf{g}}_{ml}s_m. \end{aligned} \tag{3-38}$$

The receive filter $\mathbf{w}_{kl,\mathrm{PIC}}^{H}$ is chosen to minimize the error between the symbol estimate and the transmitted symbol. The optimization problem to obtain the optimal value of $\mathbf{w}_{kl,\mathrm{PIC}}^{H}$ is formulated as

$$\mathbf{w}_{kl,\mathrm{PIC}}^{H} = \mathsf{arg}\min_{\left(\mathbf{w}_{kl,\mathrm{PIC}}^{H}\right)}\mathbb{E}\left\{||\tilde{s}_{kl}-s_k||^2 \mid \hat{\mathbf{G}}_l\right\}. \tag{3-39}$$

The objective on the RHS of (3-39) is obtained by assuming statistical independence between each term of $\mathbf{y}_l$ and ignoring terms that do not depend on $\mathbf{w}_{kl,\mathrm{PIC}}^{H}$. After some mathematical and algebraic manipulations, the objective should satisfy the following relation

$$\begin{aligned}\mathbb{E}\left\{||\tilde{s}_{kl}-s_k||^2 \mid \hat{\mathbf{G}}_l\right\} = \mathbf{w}_{kl,\mathrm{PIC}}^{H}\mathbf{D}_{kl}\Bigg(\rho_k\hat{\mathbf{g}}_{kl}\hat{\mathbf{g}}_{kl}^{H} + \sum_{i=1,i\neq k}^{K}\hat{\mathbf{g}}_{il}\mathbb{E}\left\{\mid s_i-\bar{s}_i\mid^2\right\}\hat{\mathbf{g}}_{il}^{H} \\ + \sum_{m=1}^{K}\left(\mid s_m\mid^2+\sigma_m^2\right)\mathbf{C}_{ml} + \sigma^2\mathbf{I}_N\Bigg)\mathbf{D}_{kl}^{H}\mathbf{w}_{kl,\mathrm{PIC}} - \rho_k\mathbf{w}_{kl,\mathrm{PIC}}^{H}\mathbf{D}_{kl}\hat{\mathbf{g}}_{kl},\end{aligned} \tag{3-40}$$

where $\mathbb{E}\left\{\tilde{\mathbf{g}}_{ml}\tilde{\mathbf{g}}_{ml}^{H}\right\} = \mathbf{C}_{ml}$, $\mathbb{E}\left\{\mathbf{n}_l\mathbf{n}_l^{H}\right\} = \sigma^2\mathbf{I}_N$, $\mathbb{E}\left\{s_k s_k^{H}\right\} = \rho_k$, $\mathbb{E}\left\{s_m s_m^{*}\right\} = |s_m|^2+\sigma_m^2$. The term $\mathbb{E}\left\{\mid s_i-\bar{s}_i\mid^2\right\}$ denotes the covariance and its values are computed locally at each AP according to (2-33). By differentiating (3-40) with respect to (w.r.t) $\mathbf{w}_{kl,\mathrm{PIC}}^{H}$ and equating to zero , the optimal local MMSE-PIC

filter is given by

$$\mathbf{w}_{kl,\mathrm{PIC}} = \rho_k \Bigg[\mathbf{D}_{kl} \Bigg(\rho_k \hat{\mathbf{g}}_{kl} \hat{\mathbf{g}}_{kl}^H + \sum_{i=1, i \neq k}^{K} \hat{\mathbf{g}}_{il} \mathbb{E} \left\{ \mid s_i - \bar{s}_i \mid^2 \right\} \hat{\mathbf{g}}_{il}^H + \sum_{m=1}^{K} \left(\mid s_m \mid^2 + \sigma_m^2 \right) \mathbf{C}_{ml} + \sigma^2 \mathbf{I}_N \Bigg) \mathbf{D}_{kl}^H \Bigg]^{-1} \mathbf{D}_{kl} \hat{\mathbf{g}}_{kl}. \tag{3-41}$$

At the first iteration, there is no prior information about the transmitted code bit. In this case, $\bar{s}_i = 0$ in (3-41). This yields the local linear MMSE filter given by

$$\mathbf{w}_{kl,\mathrm{MMSE}} = \rho_k \Bigg[\mathbf{D}_{kl} \Bigg(\rho_k \hat{\mathbf{g}}_{kl} \hat{\mathbf{g}}_{kl}^H + \sum_{i=1, i \neq k}^{K} \hat{\mathbf{g}}_{il} \hat{\mathbf{g}}_{il}^H \rho_i + \sum_{m=1}^{K} \left(\mid s_m \mid^2 + \sigma_m^2 \right) \mathbf{C}_{ml} + \sigma^2 \mathbf{I}_N \Bigg) \mathbf{D}_{kl}^H \Bigg]^{-1} \mathbf{D}_{kl} \hat{\mathbf{g}}_{kl}, \tag{3-42}$$

where $\rho_i = \mathbb{E} \{ \mid s_i \mid^2 \}$.

The derived centralized and decentralized filters suffer from interference due to the other $K-1$ users, channel estimation errors, and AWGN noise. This makes the derived filters non-Gaussian because the output of a Gaussian filter should be Gaussian for a Gaussian input. In the next section, we approximate the filters to be Gaussian by computing the mean and variances, present the LLR processing schemes, perform signaling and computational complexity analysis, and explain the considered decoding algorithm.

3.6 Iterative Processing and Refinement

This section presents the iterative processing of the IDD schemes for the studied MMSE-based detectors, which employ a detector and an LDPC decoder, and the proposed LLR refinement techniques. The received signal at the output of the receive filter contains the desired symbol, MUI, and noise. The parameter u_k in Figure 2.2 is assumed to be an output of an AWGN channel [9–11, 14, 51] given by

$$u_k = \omega_k s_k + z_k, \tag{3-43}$$

where $\mathbb{E}\{s_k^* u_k\} = \rho_k \mathbf{w}_k^H \tilde{\mathbf{D}}_k \hat{\mathbf{g}}_k$ and $\mathbb{E}\{s_k^* u_{kl}\} = \rho_k \mathbf{w}_{kl}^H \tilde{\mathbf{D}}_{kl} \hat{\mathbf{g}}_{kl}$ are for the centralized and decentralized schemes, respectively. The parameter z_k is a zero-mean AWGN variable. Using similar procedures as in [12, 49, 52], the variance

κ^2 of z_k is computed by $\kappa^2 = \mathbb{E}\{\mid u_k - \omega_k s_k \mid^2\}$:

$$\kappa^2 = \mathbf{w}_k^H \mathbf{D}_k \left(\hat{\mathbf{G}}_{\mathrm{i}} \Delta_{\mathrm{i}} \hat{\mathbf{G}}_{\mathrm{i}}^H + \sum_{m=1}^{K} \rho_m \mathbf{C}_m + \sigma^2 \mathbf{I}_{NL} \right) \mathbf{D}_k^H \mathbf{w}_k, \tag{3-44}$$

and

$$\kappa_l^2 = \mathbf{w}_{kl}^H \mathbf{D}_{kl} \left(\hat{\mathbf{G}}_{\mathrm{i}l} \Delta_{\mathrm{i}} \hat{\mathbf{G}}_{\mathrm{i}l}^H + \sum_{m=1}^{K} \rho_m \mathbf{C}_{ml} + \sigma^2 \mathbf{I}_N \right) \mathbf{D}_{kl}^H \mathbf{w}_{kl}, \tag{3-45}$$

are for the centralized and decentralized schemes, respectively. Detailed derivations of (3-44) and (3-45) are presented in Appendices D and E for centralized and decentralized processing schemes, respectively. For the case of low complexity and latency receivers, consider the relation given by

$$\tilde{s}_{kl} = \mu_{kl} s_k + \varsigma_{kl}. \tag{3-46}$$

By comparing (3-46) with (3-36) and (3-38), $\mu_{kl,\mathrm{RMF}} = N\theta$ and $\mu_{kl,\mathrm{PIC}} = \mathbf{w}_{kl,\mathrm{PIC}}^H \mathbf{D}_{kl} \hat{\mathbf{g}}_{kl}$. The noise terms ς_{kl} are

$$\begin{aligned} \varsigma_{kl,\mathrm{RMF}} =& \sum_{\gamma=1}^{N} \sum_{i=1, i\neq k}^{K} \hat{g}_{kl,\gamma}^* \hat{g}_{il,\gamma} \left[\mathbf{D}_{kl}\right]_{\gamma,\gamma} s_i + \sum_{\gamma=1}^{N} \sum_{m=1}^{K} \hat{g}_{kl,\gamma}^* \tilde{g}_{ml,\gamma} \left[\mathbf{D}_{kl}\right]_{\gamma,\gamma} s_m \\ &+ \sum_{\gamma=1}^{N} \hat{g}_{kl,\gamma}^* \left[\mathbf{D}_{kl}\right]_{\gamma,\gamma} n_{l,\gamma}, \end{aligned} \tag{3-47}$$

and

$$\varsigma_{kl,\mathrm{PIC}} = \mathbf{w}_{kl,\mathrm{PIC}}^H \mathbf{D}_{kl} \sum_{i=1, i\neq k}^{K} \hat{\mathbf{g}}_{il} \left(s_i - \bar{s}_i\right) + \mathbf{w}_{kl,\mathrm{PIC}}^H \mathbf{D}_{kl} \sum_{m=1}^{K} \tilde{\mathbf{g}}_{ml} s_m + \mathbf{w}_{kl,\mathrm{PIC}}^H \mathbf{D}_{kl} \mathbf{n}_l. \tag{3-48}$$

The variance $\sigma_h^2 = \mathbb{E}\{\mid \tilde{s}_{kl} - \mu_{kl} s_k \mid^2\} = \mathbb{E}\{\varsigma_{kl} \varsigma_{kl}^*\}$ of ς_{kl} can be obtained using similar steps used in [5, 6] and is expressed as

$$\sigma_{\mathrm{RMF}}^2 = N \left(E_s \left(K - 1\right) + \sum_{m=1}^{K} \left(\mid s_m \mid^2 + \sigma_m^2 \right) \mathrm{tr}\left\{\mathbf{C}_{ml}\right\} + \sigma^2 \right), \tag{3-49}$$

and

$$\begin{aligned} \sigma_{\mathrm{PIC}}^2 =& \mathbf{w}_{kl,\mathrm{PIC}}^H \mathbf{D}_{kl} \left(\sum_{i=1, i\neq k}^{K} \hat{\mathbf{g}}_{il} \mathbb{E}\left\{ \mid s_i - \bar{s}_i \mid^2 \right\} \hat{\mathbf{g}}_{il}^H + \sum_{m=1}^{K} \left(\mid s_m \mid^2 + \sigma_m^2 \right) \mathbf{C}_{ml} + \sigma^2 \mathbf{I}_N \right) \\ &\times \mathbf{D}_{kl}^H \mathbf{w}_{kl,\mathrm{PIC}}. \end{aligned} \tag{3-50}$$

Where (3-44) is based on the assumption that $\mathbf{D}_{kl} = \mathbf{I}_N$.

The extrinsic LLR computed by the detector for the l-th bit $l \in \{1, 2, ..., M_c\}$ of the symbol s_k [4–6, 53] is given by

$$\begin{aligned}\Lambda_e\left(b_{(k-1)M_c+l}\right) =& \frac{\log P\left(b_{(k-1)M_c+l}=+1|u_k\right)}{\log P\left(b_{(k-1)M_c+l}=-1|u_k\right)} - \frac{\log P\left(b_{(k-1)M_{c+1}}=+1\right)}{\log P\left(b_{(k-1)M_{c+1}}=-1\right)} \\ &= \log \frac{\sum_{s\in A_l^{+1}} f\left(u_k|s\right) P\left(s\right)}{\sum_{s\in A_l^{-1}} f\left(u_k|s\right) P\left(s\right)} - \Lambda_i\left(b_{(k-1)M_c+l}\right), \end{aligned} \tag{3-51}$$

where the last equality of (4-51) follows from Bayesian rule. The parameter A_l^{+1} is the set of 2^{Mc-1} hypotheses for which the l-th bit is $+1$. The a-priori probability $P(s)$ is given by (2-32). The approximation of the likelihood function [7, 53] $f(u_k|s)$ is given by

$$f\left(u_k|s\right) \simeq \frac{1}{\pi\kappa^2} \exp\left(-\frac{1}{\kappa^2}|u_k - \omega_k s|^2\right). \tag{3-52}$$

After local processing, the CPU has to perform final decisions by using the LLRs from the different APs. This is accomplished by proposing three LLR processing strategies presented as follows:

3.6.1 Standard LLR Processing

In this strategy, each AP computes the BER based on decisions from its LLRs. After obtaining the BER from each AP, an average BER is calculated for the entire network. However, such an approach yields poor results, as some APs have very unreliable LLRs for particular UEs. We then discuss two proposed strategies to improve the performance of local detectors.

3.6.2 LLR Censoring

In this subsection, we present an LLR censoring technique that helps to reduce the redundant processing of LLRs at the CPU. First, the independent streams of LLRs are sent from the APs to the CPU with dimensions KC_{leng}. At each AP, we compute the mean absolute value of the LLRs, which is given by

$$\mu_{\Lambda_{kl,e}} = \frac{1}{C_{\text{leng}}} \sum_{c=1}^{C_{\text{leng}}} |\Lambda_{l,e}|. \tag{3-53}$$

Based on $\mu_{\Lambda_{kl,e}}$, the UE is decoded at the AP when this parameter is highest and the other LLRs are discarded. This is done for all APs, and a new matrix

$\boldsymbol{\Lambda}_{\boldsymbol{k,e}}^{\text{new}}$ with the censored LLRs is formed and used in performing final decoding. The LLR censoring strategy is summarized in Algorithm 1.

Algorithm 1 Algorithm for Censoring Local LLRs

$\boldsymbol{\Lambda}_e \in \mathbb{C}^{KC_{\text{leng}}L}$, $\boldsymbol{\Lambda}_{\boldsymbol{k,e}}^{\text{new}} = \mathbf{0}_{KC_{\text{leng}}}$
for l=1 to L **do**
  for k=1 to K **do**
    if $\mu_{\Lambda_{kl,e}} \geq \max\left(\mu_{\boldsymbol{\Lambda}_{k,e}}\right)$ **then**
      $\boldsymbol{\Lambda}_{\boldsymbol{k,e}}^{\text{new}} = \boldsymbol{\Lambda}_{kl,e}$
    else
      Continue
    end if
    $k \leftarrow k+1$
  end for
  $l \leftarrow l+1$
end for
Output $\boldsymbol{\Lambda}_{\boldsymbol{k,e}}^{\text{new}}$

3.6.3 LLR Refinement

We propose an LLR refinement strategy that computes the linear summation of the multiple streams of LLRs obtained from the locally computed joint IDD detectors. Mathematically, the refined combination of LLRs at the CPU is given by

$$\Lambda_{\text{avg,e}}\left(b_{(k-1)M_c+l}\right) = \sum_{l=1}^{L} \Lambda_{l,e}\left(b_{(k-1)M_c+l}\right). \tag{3-54}$$

The idea of combining multiple streams of LLRs creates some diversity benefits from the LLRs and yields some performance improvement in the network. Another key advantage of decentralized processing is that each AP has accurate channel estimates; thus, it is better to perform the detection locally than at the CPU. The mean of the refined LLRs is given by

$$\mathbb{E}[\Lambda_{\text{avg,e}}\left(b_{(k-1)M_c+l}\right)] = \sum_{l=1}^{L} \mathbb{E}[\Lambda_{l,e}\left(b_{(k-1)M_c+l}\right)], \tag{3-55}$$

$$= \mu_{\Lambda_{\text{avg,e}}}, \tag{3-56}$$

where $\mathbb{E}[\Lambda_{l,e}\left(b_{(k-1)M_c+l}\right)] \to 0$ since

$$\mathbb{E}[\Lambda_{l,e}\left(b_{(k-1)M_c+l}\right)] = \log \int \Lambda_{l,e}\left(b_{(k-1)M_c+l}\right) p_{\Lambda_{l,e}|H_0} d\Lambda_{l,e},$$

$$= \log \int \frac{p_{\Lambda_{l,e}|H_1}}{p_{\Lambda_{l,e}|H_0}} p_{\Lambda_{l,e}|H_0} d\Lambda_{l,e} = 0,$$

where $p_{\Lambda_{l,e}|H_1}$ is the conditional probability density function (pdf) of the LLR of stream l given bit 1 and $p_{\Lambda_{l,e}|H_0}$ is the conditional pdf of the LLR given bit 0. The variance of the refined LLRs is given by

$$\begin{aligned}\sigma^2_{\Lambda_{\text{avg,e}}} &= \mathbb{E}[\Big(\Lambda_{\text{avg,e}}\left(b_{(k-1)M_c+l}\right) - \mu_{\Lambda_{\text{avg,e}}}\Big)^2] \\ &= \frac{1}{L}\sum_{l=1}^{L}\Big((\Lambda_{\text{avg,e}}\left(b_{(k-1)M_c+l}\right)^2 - \sum_{n=1}^{L}\Lambda_{n,e}\left(b_{(k-1)M_c+l}\right)\Big).\end{aligned} \tag{3-57}$$

This suggests that the refinement benefits come from enhancing the quality of the LLRs through their variance reduction, which shifts the LLRs with small values away from the origin.

3.6.4 Computational Complexity

The worst-case with all APs to assess the computational complexity of obtaining the studied detection schemes is considered. A key observation from the derived expressions is that decentralized detection reduces the complexity at the CPU in terms of computations since each AP locally detects its signal based on the available channel estimates, i.e., local detection only requires $N \times N$ matrix inversions. On the other hand, $NL \times NL$ matrix inversions are required for the centralized processing scenario since all the combined signal is detected as a whole at the CPU, which increases the complexity of the detectors. However, the CPU is designed to have high processing power to handle such complexity [1]. A detailed complexity analysis for the considered detectors can be found in Table A.1. It can be observed that the computational complexity of the decentralized and centralized detectors is of the order $\mathcal{O}(N^2LK)$ and $\mathcal{O}(N^2L^2K)$, respectively. Where $\mathcal{O}(\cdot)$ is the big O notation.

3.6.5 Signaling Analysis

In CF-mMIMO, the APs detect the signals locally or delegate the task fully or partially to the CPU. However, there should be a trade off between the required front-haul signaling amount and detection performance [45]. Both the centralized and the decentralized processing require $(\tau_c - \tau_p)\,N$ scalars for the uplink received data and $\tau_p N$ complex scalars for the pilot sequences. Additionally, the centralized processing requires the $\frac{KLN^2}{2}$-dimensional spatial correlation matrix $\mathbf{\Omega}_{kl}$. For decentralized processing, the CPU does not require any statistical parameters for the spatial correlation matrix since the local channel estimates exist at the APs. However, the CPU should know the

Table 3.1: Computational complexity per detector.

Detector	**Multiplications**
Decentralized-MMSE	$2N^2LK+2K^2NL+8KNL+4KL2^{M_c}+2M_cKL2^{M_c}+KL$
Centralized-MMSE	$2N^2L^2K+8KNL+2K^2NL+4K2^{M_c}+2M_cK2^{M_c}+K$
Decentralized-SIC	$4N^2LK+2K^2NL+8KNL+9KL2^{M_c}+4M_cKL2^{M_c}+KL$
Centralized-SIC	$2(NLK)^2+2(NL)^2K+K^2NL+5NLK+K+9K2^{M_c}+4M_cK2^{M_c}$
Decentralized-List	$4N^2LK+5K^2NL+12KNL+9KL2^{M_c}+4M_cKL2^{M_c}+2KL$
Centralized-List	$2(NLK)^2+2(NL)^2K+3K^2NL+9NLK+K+9K2^{M_c}+4M_cK2^{M_c}$
Decentralized-RMF	$2K^2L+4KNL+4KLM_c2^{M_c}+4KL2^{M_c}$
Decentralized-MMSE-PIC	$4N^2LK+3K^2NL+8KNL+9KL2^{M_c}+4M_cKL2^{M_c}+KL$

$KC_{\text{leng}}L$-dimensional matrix of the LLRs in (3-54) to compute the average, where C_{leng} is the code word length. Thus, the signaling is summarized in Table A.2 and is analogous to the one in [45], with additional knowledge of the dimension of the LLR matrix for the final decoding of the LLRs received from local processors.

Table 3.2: Number of complex sequences to share via front haul connections, from APs to CPU.

Processing Scenario	**Each Coherence block**	**Statistical Parameters**
Centralized	τ_cNL [45]	$KLN^2/2$ [45]
Decentralized	$(\tau_c-\tau_p)\,KL$ [45]	–

3.6.6 Decoding Algorithm

The proposed detectors use the box-plus SPA decoder discussed in chapter two. The decoder comprises of two steps namely: Single parity check (SPC) stage and the repetition stage. The LLRs sent from check node $(\text{CN})_J$ to variable node $(\text{VN})_i$ are computed as

$$\Lambda_{j\longrightarrow i}=\boxplus_{i'\in N(j)\setminus i}\Lambda_{i'\longrightarrow j}, \tag{3-58}$$

where $\boxplus$ denotes the pairwise "box-plus" operator given by

$$\begin{aligned}\Lambda_1 \boxplus \Lambda_2 =& \log\left(\frac{1+e^{\Lambda_1+\Lambda_2}}{e^{\Lambda_1}+e^{\Lambda_2}}\right), \\ =& \text{sign}(\Lambda_1)\text{sign}(\Lambda_2)\min(|\Lambda_1|,|\Lambda_2|) + \log\left(1+e^{-|\Lambda_1+\Lambda_2|}\right) \\ & - \log\left(1+e^{-|\Lambda_1-\Lambda_2|}\right).\end{aligned} \tag{3-59}$$

The LLR from VN_i to CN_j is given by

$$\Lambda_{i\longrightarrow j} = \Lambda_i + \sum_{j^{'}\in N(i)\backslash j} \Lambda_{j^{'}\longrightarrow i}, \tag{3-60}$$

where the parameter Λ_i denotes the LLR at VN_i, $j^{'} \in N(i)\backslash j$ means that all CNs connected to VN_i except CN_j.

3.7 Simulation Results

In this section, the bit error rate (BER) performance of the proposed soft detectors is presented for the CF-mMIMO settings. The CF-mMIMO channel exhibits high PL values due to LS fading coefficients. Thus, the instantaneous SNR is expressed by

$$SNR = \frac{\sum_{l=1}^{L}(\mathbf{G}_l \text{ diag}(\boldsymbol{\rho})\mathbf{G}_l^H)}{\sigma_n^2 NLK}. \tag{3-61}$$

The simulation parameters are varied according to Table 4.2, unless stated otherwise.

Network setup, assumptions and remarks: We consider a cell-free environment with a square of dimensions $D \times D$. The spatial correlation matrices $\boldsymbol{\Omega}_{jl}$ are assumed to be locally available at the APs, and their entries are generated using the Gaussian local scattering model [45] with an angular standard deviation defined in Table 4.2. The modulation scheme used is QPSK. The LS fading coefficients are obtained according to the 3rd Generation Partnership Project (3GPP) Urban Microcell model in [45] given by

$$\beta_{k,l}\,[\text{dB}] = -30.5 - 36.7\log_{10}\left(\frac{d_{kl}}{1m}\right) + \Upsilon_{kl}, \tag{3-62}$$

where d_{kl} is the distance between the k-th UE and l-th AP, $\Upsilon_{kl} \sim \mathcal{N}(0, 4^2)$ is the shadow fading. We believe that the considered propagation channel model is sufficiently general to allow simple changes and assessments of line of sight (LoS), path loss, and shadowing distributions for evaluating CF-mMIMO

Table 3.3: Simulation Parameters.

Parameter	**Value**
Codeword length (C_{leng})	256
Parity Check bits (M)	128
Message bits	$C_{\text{leng}} - M$
Code rate R	$\frac{1}{2}$
Threshold Euclidean distance (d_{th})	0.38
τ_u, τ_p, τ_c	$190, 10, 200$
η_k	100 mW
Threshold for non-master AP (β_{th})	-20 dB
Maximum decoder iterations	10
Signal power ρ	1 W
Maximum decoder iterations	10
Square length of CF-mMIMO Network D	1 km
Angular standard deviation	15°
Noise power	-96 dBm
Bandwidth	20 MHz
Number of channel realizations	10000

networks, as recommended in the literature for micro cell scenarios [45]. The simulation results are based on single antenna UEs for simplicity of analysis, the test of ideas, and to allow a shorter simulation time. However, this can be extended to multiple antenna UEs to fully address the most practical systems. Note should also be taken that the considered scenarios and network settings in terms of code word length, number of APs, and antennas provide reasonably acceptable performances in terms of BER. However, improvements in the BER can be obtained by using longer channel codes and increasing the number of APs and antennas in the network at the expense of increased complexity.

In Table 3.4, we provide numerical values for the number of multiplications that should be done per iteration for each detector for different numbers of UEs K, APs L and APs antennas N. It can be seen that the linear MMSE-based receivers have low complexity values as compared to the SIC and list-based receivers. Also, it is noteworthy that decentralized receivers have lower complexity values as compared to centralized receivers. Nevertheless, the proposed list-based receivers achieve costs that are slightly higher than those of

the SIC-based receivers. However, using list-based detection improves performance, as shown in the numerical results. Figure 4.3 presents the BER versus

Table 3.4: Cost in number of multiplications for the detectors.

Detector	**Cost for** $K = 8$**,** $L = 16$**,** $N = 4$	**Cost for** $K = 8$**,** $L = 32$**,** $N = 4$
Decentralized-MMSE	1.70×10^3	3.40×10^4
Centralized-MMSE	7.81×10^4	2.87×10^5
Decentralized-SIC	2.57×10^4	5.15×10^4
Centralized-SIC	5.97×10^5	2.37×10^6
Decentralized-List	3.84×10^4	7.68×10^4
Centralized-List	6.08×10^5	2.39×10^6

the SNR for the cases (a) before LLR refinement (w/o-LLR-Ref) and (b) after LLR refinement (w-LLR-Ref) for the studied detectors. It can be noticed that there is a significant reduction in the BER for the case with LLR refinement as compared to the scenario without LLR refinement. This performance improvement is attributed to the linear combination of the multiple streams of LLRs from the different APs, which improves their reliability by shifting the LLRs with small values away from the origin. Secondly, some benefits arise due to the diversity of LLRs, which improves the system performance, whereas in the w/o-LLR-Ref case, the hard decisions are made based on the individual APs LLRs, and later an average BER is obtained. This naive approach leads to performance degradation as some APs have very unreliable estimates and hence poor LLRs. Thus, hard decisions made on LLRs from such APs compromise the entire network performance. Additionally, the figure compares the case with perfect CSI (PCSI) and imperfect CSI (ICSI). It can be observed that the detection based on the PCSI achieves lower BERs as compared to the case with the ICSI. This is because the channel estimation error and pilot contamination degrade the network performance, resulting in high BERs. Another key observation is that the proposed list-based detector achieves lower BER values than the SIC detector. This is because the conventional SIC experiences error propagation that occurs due to erroneous decisions in the previous cancellation stages. To overcome this issue and improve performance, list-based detection provides multi-feedback (MF) diversity that helps to correct this error propagation as the number of iterations increases. Note also that the linear MMSE receiver has the worst performance among the studied detectors since it does not have the Δ_{i} matrix used for interference cancellation.

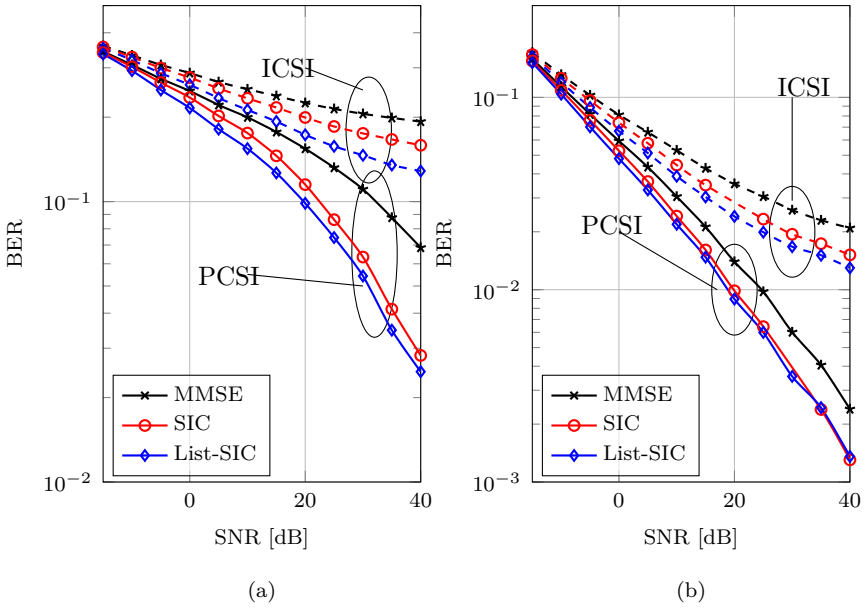

Figure 3.3: BER versus SNR while comparing detectors for decentralized processing for $L = 4$, $N = 4$, $K = 4$: (a) Before LLR Refinement and (b) After LLR Refinement.

A comparison of the centralized and decentralized processing schemes in terms of BER versus SNR is presented in Figure 3.4. The results show that the case with centralized processing achieves lower BER values than the case with decentralized processing. This is because centralized processing takes the joint detection of all the received signals into account. Also, the case w/o-LLR-Ref achieves the worst performance since each AP performs its hard decisions locally based on the available LLRs and an average BER is obtained for the entire network, which yields a huge performance gap and degradation. The case w-LLR-Ref outperforms the standard processing scheme since it takes advantage of LLR combining. This yields more reliable LLRs around the mean, which improves performance. This performance improvement is significant for CF-mMIMO architectures as it can yield less complex solutions in uplink detection schemes, i.e., for the decentralized processing, there is a substantial reduction in the computation complexity and the fronthaul signaling load in the network, as shown in Tables A.1 and A.2, respectively.

Figure 3.5 shows the BER versus SNR for the decentralized processing cases using w-LLR-Ref and LLR-Censoring. It is clear that the case using LLR refinement has a lower BER than the one using LLR censoring. The UE can only be decoded at the AP, achieving the highest mean absolute value when LLR censoring is used. In contrast, LLR refinement enhances performance by performing a linear combination of the LLRs from all APs. Nonetheless, censoring LLRs prevents the redundant processing of the LLRs. The only difficulty that might arise is a slight increase in the hardware complexity of the

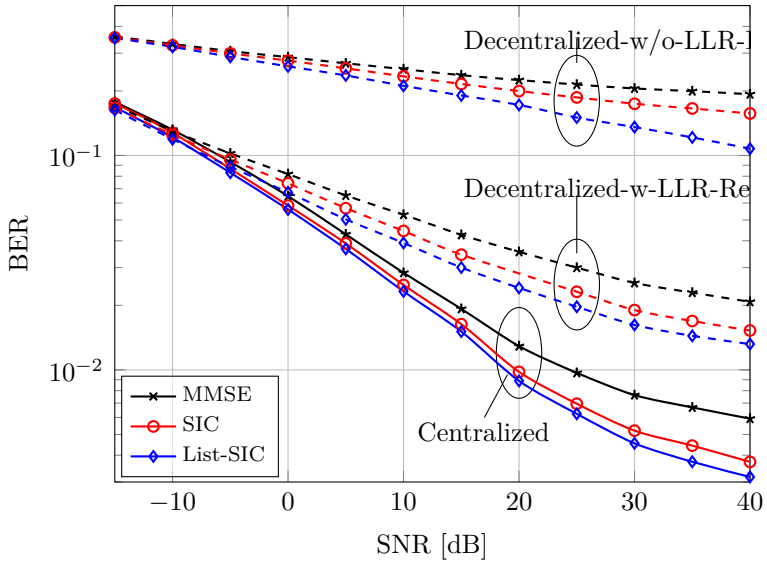

Figure 3.4: BER versus SNR for All APs comparing decentralized and centralized processing for the case with imperfect CSI with $L = 4$, $K = 4$, $N = 4$, IDD $= 2$.

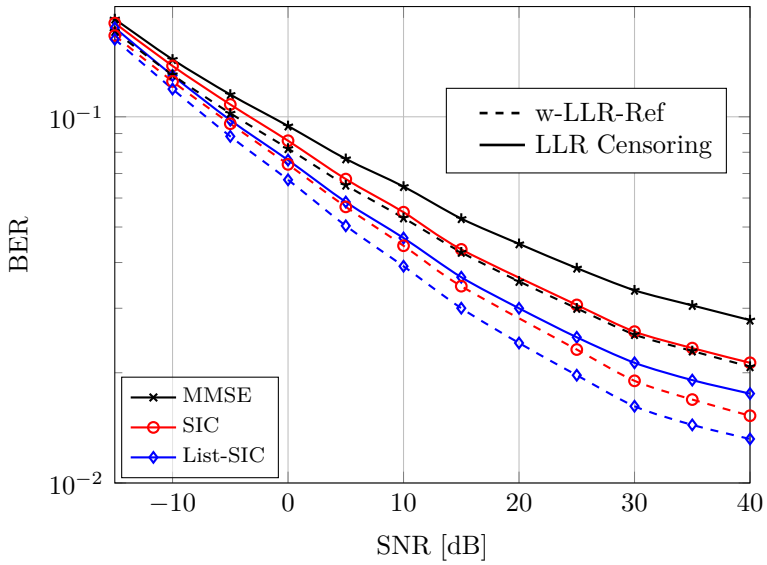

Figure 3.5: BER versus SNR for All APs comparing LLR Censoring and LLR Refinement for decentralized processing for the case with imperfect CSI with $L = 4$, $K = 4$, $N = 4$, IDD $= 2$.

receiver design since the CPU must constantly scan all the APs to identify the one that offers the largest absolute value of LLRs to a specific UE. However, the CPU is usually designed with strong computing power, so it can handle such complexity. One could interpret the proposed LLR censoring and refinement as analogous to the selection combining and maximal ratio combining used in diversity analysis. However, the former leverages the distributed computation of LLRs from each AP, and therefore it should not be confused with the latter schemes.

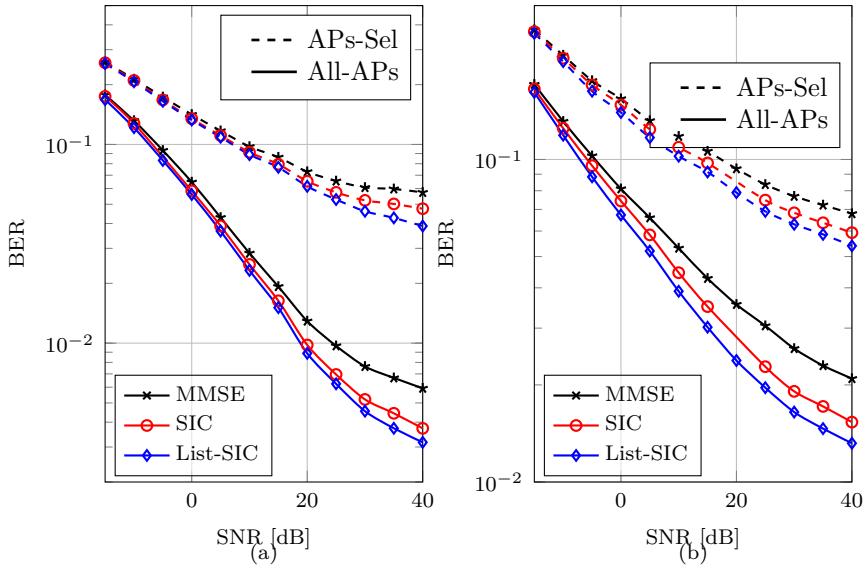

Figure 3.6: BER versus SNR for a case that uses All APs and a case that uses APs-Sel for $L = 4$, $N = 4$, $K = 4$: (a) Centralized Processing and (b) Decentralized Processing

.

Figure 3.6 plots the BER versus SNR for the case that the detectors use all APs (All-APs) and the case that uses AP selection (APs-Sel) with (a) centralized and (b) decentralized processing schemes. It can be observed that for both processing levels, the system that uses All-APs achieves lower BER values as compared to the one that selects the APs. This is because selecting APs reduces the number of antennas in the network, distorting the performance. However, APs-Sel reduces the signaling load, making the network more scalable and practical. Moreover, the distributed location, the delay spread of the APs, and the associated signal propagation latency will limit the APs involved in cell-free MIMO systems. Therefore, APs-Sel techniques are key to reducing fronthaul signaling, computational costs, and latency.

The BER versus SNR of the detectors while varying the number of outer iterations for the detectors is presented in Figure 3.7. From the curves, it can be noticed that increasing the number of iterations reduces the BER. Specifically, for both centralized and decentralized (a) SIC and (b) List-SIC, there is a significant performance improvement when the number of iterations is increased from 1 to 2 iterations for both detectors. However, after the third iteration, the performance benefits are marginal.

Figure 3.8 (a) plots the computational complexity versus the number of UEs K while considering the studied detectors for centralized and decentralized processing. It can be observed that the linear MMSE detectors have the lowest computation complexity for both cases. The list-based detectors have slightly higher computation complexity than the SIC-based detectors. It is worth mentioning that the differences in computational complexity between

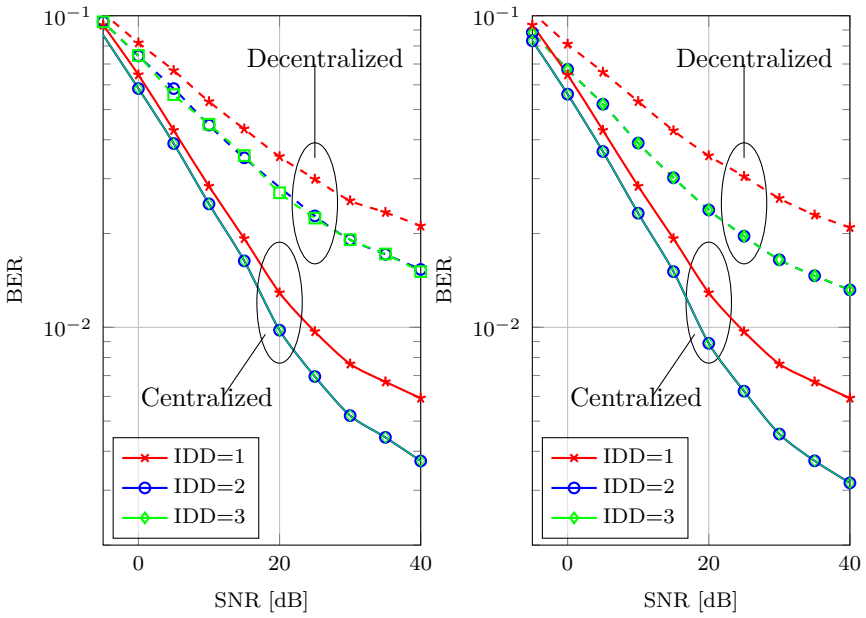

Figure 3.7: BER versus SNR while varying number of IDD iterations for $L = 4$, $N = 4$, $K = 4$: (a) SIC and (b) List-SIC.

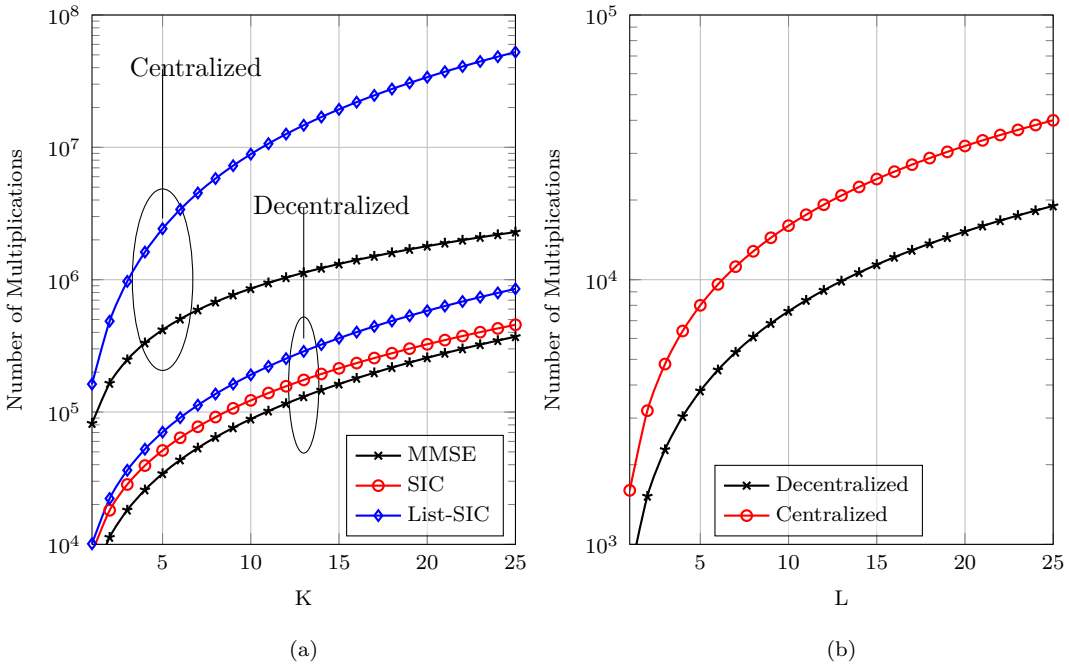

Figure 3.8: Number of multiplications versus number of UE K and number of APs L (a) Computational complexity for $L = 50$, $M_c = 2$, $N = 4$ and (b) Signaling load for $K = 4$, $N = 8$.

SIC and List-SIC are marginal, whereas centralized detectors have a higher computation cost than decentralized detectors. The signaling load is given by the number of complex scalars that must be exchanged in the network, which is shown in Figure 3.8 (b) for the centralized and decentralized CF-mMIMO setups. From the curves, it can be noticed that decentralized processing requires less signaling between the APs and CPU than the centralized setup. The decentralized processing requires knowledge of the $KC_{\text{leng}}L$-dimensional matrix of the LLRs from all APs to perform the final processing. Nevertheless, decentralized schemes greatly reduce the required signaling in the network and can achieve close performance to that of centralized processing while using LLR refinement.

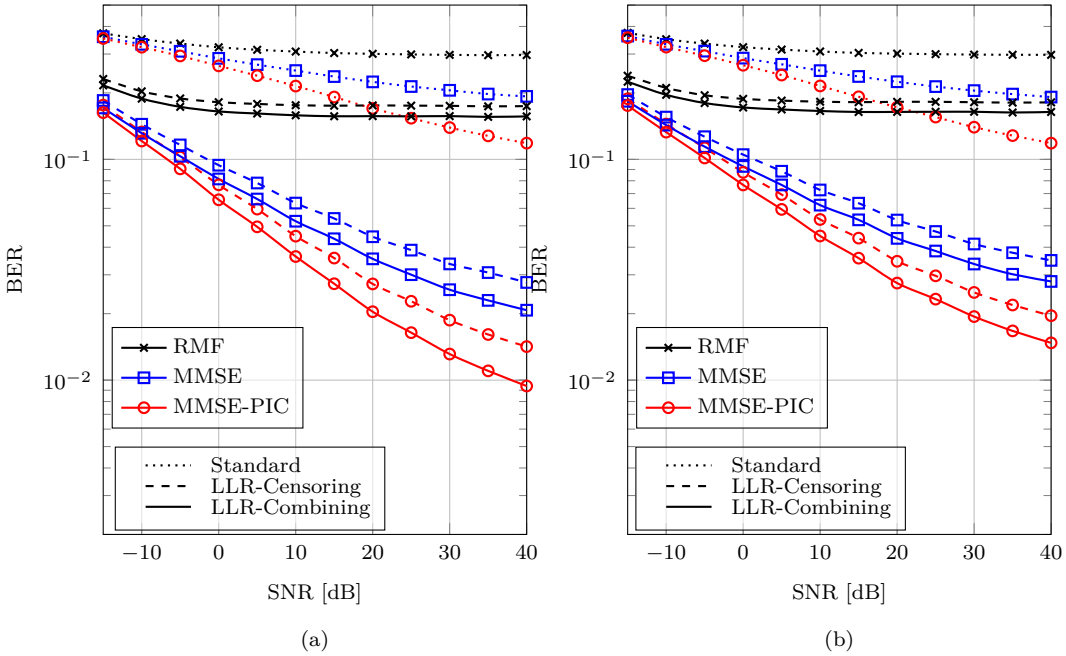

Figure 3.9: BER versus SNR while comparing the studied detectors and LLR refinement strategies for $L = 4$, $N = 4$, $K = 4$: (a) all APs (Full-Network), IDD = 2 (b) LP-wAPS (Scalable), IDD = 2.

The BER versus SNR characteristic for the three LLR processing schemes is presented in Figures 3.9 (a) and 3.9 (b) for all APs and scalable networks, respectively, while comparing the detectors. The MMSE-PIC detector achieves the lowest BER, followed by the MMSE and lastly the RMF. The LLR combining and censoring schemes achieve the best performance, while individual decoding at each AP achieves the worst performance. This is because the LLR refinements improve the network's performance. The superior performance of the PIC-based detector is attributed to its ability to cancel MUI in a robust manner. On the other hand, RMF has poor performance but does not require any matrix inversions, which reduces the complexity. Furthermore, LLR censoring helps to mitigate redundant processing at the CPU. However, because

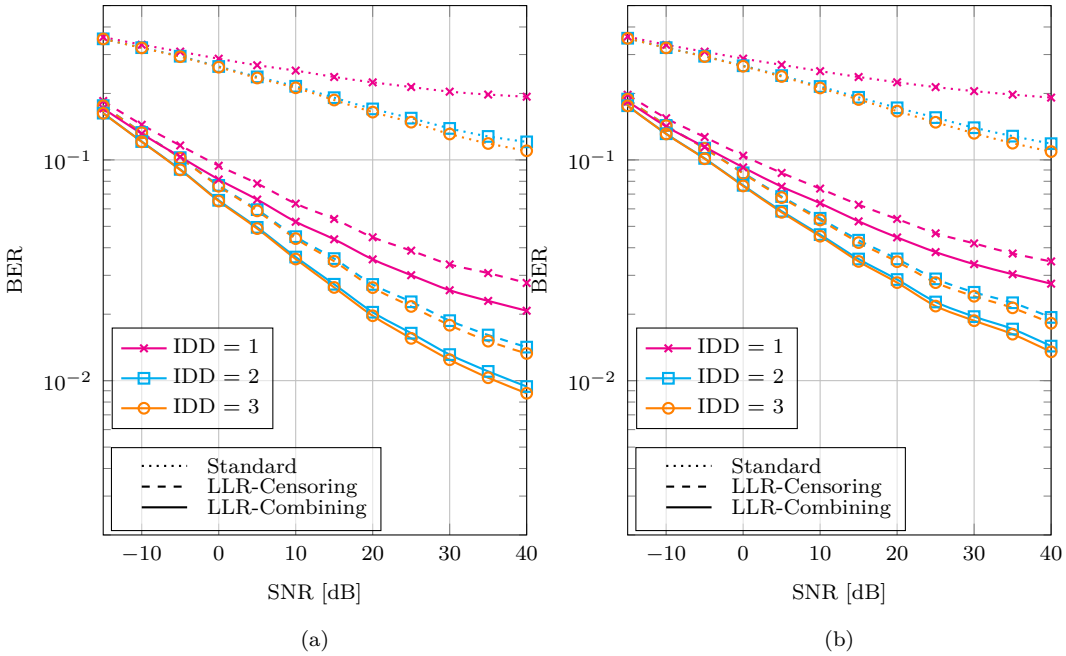

Figure 3.10: BER versus SNR while variying number of IDD Iterations for PIC with different LLR refinement strategies for $L = 4$, $N = 4$, $K = 4$: (c) Full-Network (d) Scalable-Network.

the CPU must constantly search through all APs to identify the one with the most reliable LLRs for a specific UE, which increases the hardware complexity of the receiver. The superior performance of LLR combining is due to its ability to achieve LLR diversity and shift LLRs with poor beliefs away from the origin. Figures 3.10 (c) and 3.10 (d) are, respectively, for all APs and scalable networks with the MMSE-PIC detector. Varying iterations from one to two provide a significant reduction in BER for LLR processing schemes but a marginal reduction after the second iteration. The exchange of soft beliefs between decoders and detectors improves performance as more prior information is useful in the cancellation step.

3.8 Summary

In this chapter, an IDD scheme using LDPC codes has been devised with APs selection for centralized and decentralized CF-mMIMO architectures. In particular, we have proposed low-complexity interference mitigation techniques including a list-based detector that uses MMSE receive filter to improve the performance. New closed-form expressions for the MMSE-soft-IC detectors have been derived for both the centralized and decentralized implementations, taking the channel estimation errors and APs selection into account. The performance of the proposed list-based detector is compared with other baseline detectors, such as the soft linear MMSE, MMSE-SIC, and the results show that the list-based detector yields low BER values compared to the other detectors. Additionally, Low-complexity and low-latency local receive filters based on RMF and MMSE-PIC have been studied for the decentralized CF-mMIMO network. Furthermore LLR refinement strategies based on combining and censoring LLRs have been proposed. The results have shown that LLR refinement strategies obtained lower BER values than standard processing. The proposed scalable APs-Sel APs-Sel scheme based on LLSF coefficients can reduce the signaling load between APs and the CPU, resulting in a trade-off between performance, signaling load and network feasibility.

4
Iterative Soft Intra-Cluster and Out-of-Cluster Interference Cancellation

In this chapter, cluster-based IDD schemes for network and user-centric CF-mMIMO networks are proposed. This is motivated by the fact that cluster-based transmit and receive processing strategies are scalable, requiring much lower signaling loads to convey CSI to the APs and CPUs, and reduced computational complexity to compute transmit and receive filters [45]. In fact, IDD schemes used with both linear and non-linear receivers have been found to provide performances that are close to the optimal receivers [9–12, 48, 49].

We first develop an IDD scheme for network clustered CF-mMIMO network that can mitigate intra-cluster (ICL) interference in the presence of both ICL and out-of-cluster (OCL) interference in CF-mMIMO networks. New closed-form expressions for cluster-based MMSE-PIC receivers by considering channel estimation errors, interference, and AWGN for full and clustered CF-mMIMO networks are derived. Moreover, we devise closed-form expressions for the Gaussian approximation of the likelihood function by computing the mean and variance of the detected signals. Simulations evaluate both clustered and full CF-mMIMO networks equipped with the proposed cluster-based MMSE-PIC and linear MMSE receivers in terms of BER and complexity.

We then propose an iterative soft interference cancellation scheme for ICL and OCL interference in user-centric clustered CF-mMIMO networks. In particular, we develop MMSE receive filters for the proposed interference cancellation scheme in the presence of ICL and OCL interference and noise. We also devise a least squares estimator (LSE) to perform multiple OCL interference estimation. An IDD scheme that adopts LDPC codes and incorporates the OCL interference estimate is then presented. Simulations assess the proposed scheme against existing techniques in terms of BER performance.

4.1
Proposed System Model and Statistical Analysis

The proposed full and network cluster-based IDD schemes and receiver designs are presented in this section.

4.1.1 Proposed IDD Scheme for full CF-mMIMO networks

The block diagram of the proposed IDD scheme for full CF-mMIMO networks is shown in Figure 4.1. The transmitter comprises of K UEs, an LDPC encoder (Enc) and a modulator (Mod). The receiver is equipped with L APs each with N antennas, and a CPU which comprises of a detector, an LLR computing module and an LDPC decoder. The detector computes a symbol estimate $\tilde{x}_k$ and sends it to a module which computes the intrinsic LLRs. These obtained LLRs are then sent to the decoder which computes the extrinsic LLRs Λ_e that are sent as feedback to the detector in an iterative fashion. This feedback between the decoder and detector improves the performance as the number of iterations increases as it shall be seen in the results.

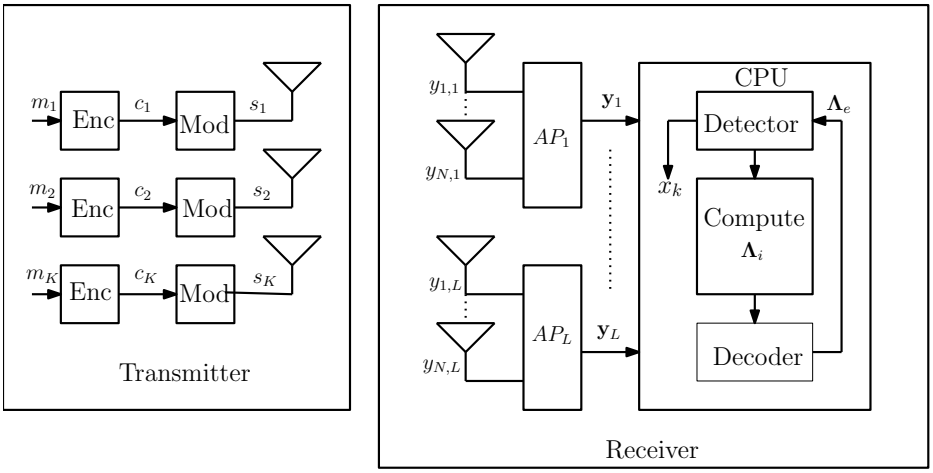

Figure 4.1: Block diagram for the IDD scheme of the full CF-mMIMO.

The received signal at the CPU for the full CF-mMIMO network setting is given by

$$\mathbf{y} = \mathbf{G}\mathbf{s} + \mathbf{n}, \tag{4-1}$$

where $\mathbf{s} \in \mathbb{C}^{K\times 1}$ and $\mathbf{n} \in \mathbb{C}^{NL\times 1}$ are the transmitted symbol vector and the AWGN noise vector with zero mean and unit variance, respectively. The channel matrix $\mathbf{G} \in \mathbb{C}^{NL\times K}$ comprises of both the small scale fading (SSF) and large scale fading (LSF) coefficients and its entries between the l-th AP and the k-th UE are given by [54]

$$g_{kl} = \sqrt{\beta_{kl}} h_{kl}, \tag{4-2}$$

where β_{kl} is the LSF coefficients as a result of path loss (PL) and shadowing. The SSF coefficients are given by h_{kl} that are assumed to be i.i.d. Gaussian random variables with variance $\mathbb{E}\{|h_{kl}|^2\} = 1$.

4.1.1.1 Proposed Receiver Design for full CF-mMIMO

After PIC and channel estimation, the received signal at the CPU for the k-th UE can be decomposed as

$$\mathbf{y} = (\hat{\mathbf{g}}_k + \tilde{\mathbf{g}}_k) + \sum_{i=1, i\neq k}^{K} (s_i - \bar{s}_i)\,(\hat{\mathbf{g}}_i + \tilde{\mathbf{g}}_i) + \mathbf{n}, \tag{4-3}$$

where the first term on the RHS of (4-3) is the desired signal, the second term is the residue interference from the other $K-1$ UEs and the third term is an AWGN noive vector with zero mean and unit variance. The parameters $\hat{\mathbf{g}}_k \in \mathbb{C}^{NL\times 1}$, $\tilde{\mathbf{g}}_k \in \mathbb{C}^{NL\times 1}$, $\hat{\mathbf{g}}_i \in \mathbb{C}^{NL\times 1}$, and $\tilde{\mathbf{g}}_i \in \mathbb{C}^{NL\times 1}$ are the estimated channels and channel estimation errors for the k-th UE and interfering UEs, respectively. The estimated symbol x_k for the k-th UE is given by

$$x_k = \mathbf{w}_k^H \mathbf{y}, \tag{4-4}$$

where $\mathbf{w}_k^H \in \mathbb{C}^{1\times NL}$is the receive weighting vector for the k-th UE that is chosen so that the error between the transmitted signal and the estimated symbol is minimized.

The optimization problem to obtain $\mathbf{w}_k$ is formulated as follows

$$\mathbf{w}_k = \arg\min_{(\mathbf{w}_k)} \mathbb{E}\left\{ ||x_k - s_k||^2 \right\}. \tag{4-5}$$

The objective function on the RHS of (4-5) is obtained after assuming that $\mathbb{E}\{s_k s_k^*\} = 1$ and can be written as

$$\begin{aligned} F =& \mathbf{w}_k^H \Bigg((\hat{\mathbf{g}}_k + \tilde{\mathbf{g}}_k)(\hat{\mathbf{g}}_k + \tilde{\mathbf{g}}_k)^H + \sum_{i=1, i\neq k}^{K} (\hat{\mathbf{g}}_i + \tilde{\mathbf{g}}_i)\,\mathbb{E}\left\{ |\, s_i - \bar{s}_i \,|^2 \right\} (\hat{\mathbf{g}}_i + \tilde{\mathbf{g}}_i)^H \\ & \times + \mathbb{E}\left\{ \mathbf{n}\mathbf{n}^H \right\} \Bigg) \mathbf{w}_k - \mathbf{w}_k^H (\hat{\mathbf{g}}_k + \tilde{\mathbf{g}}_k). \end{aligned} \tag{4-6}$$

The optimal receive vector is obtained by differentiating (4-6) w.r.t $\mathbf{w}_k^H$ and equating to zero which yields

$$\begin{aligned} \mathbf{w}_k = & \left((\hat{\mathbf{g}}_k + \tilde{\mathbf{g}}_k)(\hat{\mathbf{g}}_k + \tilde{\mathbf{g}}_k)^H + \sum_{i=1, i\neq k}^{K} \sigma_i^2 (\hat{\mathbf{g}}_i + \tilde{\mathbf{g}}_i)(\hat{\mathbf{g}}_i + \tilde{\mathbf{g}}_i)^H + \sigma_n^2 \mathbf{I}_{NL} \right)^{-1} \\ & \times (\hat{\mathbf{g}}_k + \tilde{\mathbf{g}}_k), \end{aligned} \tag{4-7}$$

where $\sigma_i^2 = \mathbb{E}\{|\, s_i - \bar{s}_i \,|^2\}$ given by (2-33), $\sigma_n^2 \mathbf{I}_{NL} = \mathbb{E}\left\{ \mathbf{n}\mathbf{n}^H \right\}$.

4.1.1.2 Insights into the receiver

For the case when there is no a-priori information about the transmitted symbol, $\bar{s}_i = 0$, the receiver in (4-7) yields an MMSE filter given by

$$\mathbf{w}_k = \left(\left(\hat{\mathbf{g}}_k + \tilde{\mathbf{g}}_k\right) \left(\hat{\mathbf{g}}_k + \tilde{\mathbf{g}}_k\right)^H + \sum_{i=1, i\neq k}^{K} \left(\hat{\mathbf{g}}_i + \tilde{\mathbf{g}}_i\right) \left(\hat{\mathbf{g}}_i + \tilde{\mathbf{g}}_i\right)^H + \sigma_n^2 \mathbf{I}_{NL} \right)^{-1} \left(\hat{\mathbf{g}}_k + \tilde{\mathbf{g}}_k\right), \tag{4-8}$$

where $\mathbb{E}\{s_i s_i^*\} = 1$. As the number of iterations increases, $s_i \approx \bar{s}_i$. The receiver in (4-7) becomes a perfect interference canceler which yields a maximum ratio combiner (MRC) given by

$$\mathbf{w}_k = \left(\left(\hat{\mathbf{g}}_k + \tilde{\mathbf{g}}_k\right) \left(\hat{\mathbf{g}}_k + \tilde{\mathbf{g}}_k\right)^H + \sigma_n^2 \mathbf{I}_{NL} \right)^{-1} \left(\hat{\mathbf{g}}_k + \tilde{\mathbf{g}}_k\right). \tag{4-9}$$

4.1.2 Proposed IDD Scheme for Network Clustered CF-mMIMO networks

The uplink of a cluster-based CFm-MIMO network with M clusters is considered. Each cluster has $\mathcal{L}$ APs, each equipped with N antennas and $\mathcal{K}$ UEs. The code word sequence in each cluster is formed by first encoding the message sequence for a particular UE by an LDPC encoder with a code rate of R. The encoded sequence is modulated to form a complex constellation of 2^{M_c} possible signal points. Then, the UEs send their encoded and modulated data to the APs which act as forwarding relays to transfer the information to the CPU, which has a joint detector that can either be a soft MMSE or MMSE-PIC receiver, an LLR computing module and an LDPC decoder. The detector and decoder exchange the information iteratively in a way that is analogous to that of the full CF-mMIMO receiver.

The NL-dimensional received signal vector at the CPU is given by

$$\mathbf{y}_i = \mathbf{G}_{ii}\mathbf{s}_i + \sum_{j=1, j\neq i}^{M} \mathbf{G}_{ij}\mathbf{s}_j + \mathbf{n}_i, \tag{4-10}$$

where $\mathbf{G}_{ii} \in \mathbb{C}^{N\mathcal{L}\times\mathcal{K}}$, $\mathbf{s}_i \in \mathbb{C}^{\mathcal{K}\times 1}$, $\mathbf{G}_{ij} \in \mathbb{C}^{N\mathcal{L}\times\mathcal{K}}$, and $\mathbf{s}_j \in \mathbb{C}^{\mathcal{K}\times 1}$ are the sub matrices in the i-th cluster, transmitted symbol vector in the i-th cluster, sub matrices in the j-th cluster due to the i-th cluster, and the transmitted symbol vector in the j-th cluster, respectively. The AWGN vector with zero mean and unit variance is denoted by $\mathbf{n}_i \in \mathbb{C}^{N\mathcal{L}\times 1}$.

4.1.2.1 Proposed Intra-Cluster Soft Interference Cancellation

The proposed receiver configuration aims to cancel the MUI or the ICL interference that is caused by the other $K-1$ UEs in the desired cluster without removing the OCL interference from the neighboring clusters.

The received signal for the i-th cluster is given by

$$\mathbf{y}_i = \mathbf{g}_{k,ii}s_{k,i} + \sum_{q=1,q\neq k}^{\mathcal{K}} \mathbf{g}_{q,ii}\left(s_{q,i} - \bar{s}_{q,i}\right) + \sum_{j=1,j\neq i}^{M} \mathbf{G}_{ij}\mathbf{s}_j + \mathbf{n}_i, \tag{4-11}$$

where the first term on RHS denotes the desired signal of the k-th UE in the i-th cluster, the second term is ICL interference from the other $K-1$ UEs in the i-th cluster, OCL from the other neighboring clusters. The parameter $\bar{s}_{q,i}$ is the symbol mean in the i-th cluster and can be computed using (2-31), $\mathbf{g}_{k,ii} \in \mathbb{C}^{N\mathcal{L}\times 1}$ and $\mathbf{g}_{q,ii} \in \mathbb{C}^{N\mathcal{L}\times 1}$, respectively. The estimated symbol at the i-th cluster after parallel ICL interference suppression is given by

$$\tilde{x}_{k,i} = \mathbf{w}_{ki}^H\mathbf{g}_{k,ii}s_{k,i} + \mathbf{w}_{ki}^H \sum_{q=1,q\neq k}^{\mathcal{K}} \mathbf{g}_{q,ii}\left(s_{q,i} - \bar{s}_{q,i}\right) + \mathbf{w}_{ki}^H \sum_{j=1,j\neq i}^{M} \mathbf{G}_{ij}\mathbf{s}_j + \mathbf{w}_{ki}^H\mathbf{n}_i. \tag{4-12}$$

The design of the optimal filter $\mathbf{w}_{ki}^H \in \mathbb{C}^{1\times N\mathcal{L}}$ aims to reduce the Euclidean distance between the transmitted symbol s_{ki} and the estimated symbol $\tilde{x}_{k,i}$. The optimization problem is formulated as

$$\mathbf{w}_{ki} = \arg\min_{(\mathbf{w}_{ki})} \mathbb{E}\left\{||\tilde{x}_{k,i} - s_{k,i}||^2\right\}. \tag{4-13}$$

The objective function on the RHS of (4-13) is given by (4-14) and it is obtained after assuming that $\mathbb{E}\left\{s_{k,i}s_{k,i}^*\right\} = 1$ and $\sigma_n^2\mathbf{I}_{N\mathcal{L}} = \mathbb{E}\left\{\mathbf{n}_i\mathbf{n}_i^H\right\}$.

$$\begin{aligned} F_1 =& \mathbf{w}_{ki}^H\Bigg(\mathbf{g}_{k,ii}\mathbf{g}_{k,ii}^H + \sigma_n^2\mathbf{I}_{N\mathcal{L}} + \sum_{q=1,q\neq k}^{\mathcal{K}} \mathbf{g}_{q,ii}\mathbb{E}\left\{|\ s_{qi} - \bar{s}_{qi}\ |^2\right\}\mathbf{g}_{q,ii}^H \\ &+ \sum_{j=1,j\neq i}^{M} \mathbf{G}_{ij}\mathbf{C}_j\mathbf{G}_{ij}^H\Bigg)\mathbf{w}_{ki} - \mathbf{w}_{ki}^H\mathbf{g}_{k,ii}. \end{aligned} \tag{4-14}$$

Differentiating (4-14) w.r.t $\mathbf{w}_{ki}^H$ and equating to zero, the optimal receive

filter $\mathbf{w}_{ki}$ is given by

$$\mathbf{w}_{ki} = \left(\mathbf{g}_{k,ii}\mathbf{g}_{k,ii}^H + \sum_{q=1,q\neq k}^{\mathcal{K}} \mathbf{g}_{q,ii}\mathbb{E}\left\{ \mid s_{qi} - \bar{s}_{qi} \mid^2 \right\} \mathbf{g}_{q,ii}^H + \sum_{j=1,j\neq i}^{M} \mathbf{G}_{ij}\mathbf{C}_j\mathbf{G}_{ij}^H + \sigma_n^2\mathbf{I}_{N\mathcal{L}} \right)^{-1} \mathbf{g}_{k,ii}. \tag{4-15}$$

4.1.2.2 Insights into the derived filter

At the first iteration, the parameter $\bar{s}_{qi} = 0$ and the filter in (4-15) yields an MMSE filter given by

$$\mathbf{w}_{ki} = \left(\mathbf{g}_{k,ii}\mathbf{g}_{k,ii}^H + \sum_{q=1,q\neq k}^{\mathcal{K}} \mathbf{g}_{q,ii}\mathbf{g}_{q,ii}^H + \sum_{j=1,j\neq i}^{M} \mathbf{G}_{ij}\mathbf{C}_j\mathbf{G}_{ij}^H + \sigma_n^2\mathbf{I}_{N\mathcal{L}} \right)^{-1} \mathbf{g}_{k,ii}. \tag{4-16}$$

As the number of iterations increase, a posterior information is exchanged between the decoder and detector, thus $\bar{s}_{qi} \approx s_{qi}$. In this case, we have a maximal ratio combining with the addition of OCL interference

$$\mathbf{w}_{ki} = \left(\mathbf{g}_{k,ii}\mathbf{g}_{k,ii}^H + \sum_{j=1,j\neq i}^{M} \mathbf{G}_{ij}\mathbf{C}_j\mathbf{G}_{ij}^H + \sigma_n^2\mathbf{I}_{N\mathcal{L}} \right)^{-1} \mathbf{g}_{k,ii}. \tag{4-17}$$

For the case with imperfect channel state information (ICSI), $\mathbf{g}_{k,ii} = \hat{\mathbf{g}}_{k,ii} + \tilde{\mathbf{g}}_{k,ii}$, $\mathbf{g}_{q,ii} = \hat{\mathbf{g}}_{q,ii} + \tilde{\mathbf{g}}_{q,ii}$, $\mathbf{G}_{ij} = \hat{\mathbf{G}}_{ij} + \tilde{\mathbf{G}}_{ij}$. where, $\hat{\mathbf{g}}_{k,ii}$, $\tilde{\mathbf{g}}_{k,ii}$, are the estimated channels, channel estimation errors for the desired UE in the i-th cluster, $\hat{\mathbf{g}}_{q,ii}$, $\tilde{\mathbf{g}}_{q,ii}$, are estimated channels, channel estimation errors for the interference UEs in the i-th cluster and $\hat{\mathbf{G}}_{ij}$, $\tilde{\mathbf{G}}_{ij}$ are estimated channels, channel estimation errors for the channel sub-matrices in the j-th cluster due to APs in in the i-th cluster, respectively. The resulting filter with ICSI is given by

$$\begin{aligned} \mathbf{w}_{ki} = & \Bigg(\left(\hat{\mathbf{g}}_{k,ii} + \tilde{\mathbf{g}}_{k,ii}\right)\left(\hat{\mathbf{g}}_{k,ii} + \tilde{\mathbf{g}}_{k,ii}\right)^H + \sigma_n^2\mathbf{I}_{N\mathcal{L}} + \sum_{q=1,q\neq k}^{\mathcal{K}} \left(\hat{\mathbf{g}}_{q,ii} + \tilde{\mathbf{g}}_{q,ii}\right) \\ & \times \mathbb{E}\left\{ \mid s_{qi} - \bar{s}_{qi} \mid^2 \right\} \left(\hat{\mathbf{g}}_{q,ii} + \tilde{\mathbf{g}}_{q,ii}\right)^H + \sum_{j\neq i}^{M} \left(\hat{\mathbf{G}}_{ij} + \tilde{\mathbf{G}}_{ij}\right) \mathbf{C}_j \left(\hat{\mathbf{G}}_{ij} + \tilde{\mathbf{G}}_{ij}\right)^H \Bigg)^{-1} \\ & \times \left(\hat{\mathbf{g}}_{k,ii} + \tilde{\mathbf{g}}_{k,ii}\right). \end{aligned} \tag{4-18}$$

4.1.3 Gaussian Approximation of the Receive Filter

The received signal at the output of the receive filter, contains the desired symbol, residual co-user interference and noise. We use similar assumptions given in [9–11, 14, 51] to approximate the $\hat{s}_k$ as an AWGN channel given by

$$\tilde{x}_{k,i} = \mu_{k,\mathrm{e}} s_{k,i} + z_{k,\mathrm{e}}, \tag{4-19}$$

where $\mathrm{e} \in (\text{CL-CF}, \text{Full-CF})$ denote the clustered and full CF mMIMO networks, respectively. By comparing (4-19) with (4-4) and (4-12) , $\mu_{k,\text{CL-CF}} = \mathbf{w}_{ki}^H \mathbf{g}_{k,ii}$ and $\mu_{k,\text{Full-CF}} = \mathbf{w}_k^H \mathbf{g}_k$ for clustered CF and Full-CF mMIMO networks, respectively. The parameter $z_{k,\mathrm{e}}$ is a zero-mean AWGN variable given by

$$z_{k,\text{CL-CF}} = \mathbf{w}_{ki}^H \sum_{q=1,q\neq k}^{\mathcal{K}} \mathbf{g}_{q,ii} \left(s_{q,i} - \bar{s}_{q,i}\right) + \mathbf{w}_{ki}^H \sum_{j=1,j\neq i}^{M} \mathbf{G}_{ij} \mathbf{s}_j + \mathbf{w}_{ki}^H \mathbf{n}_j, \tag{4-20}$$

and

$$z_{k,\text{Full-CF}} = \mathbf{w}_k^H \sum_{i=1,i\neq k}^{K} \left(s_i - \bar{s}_i\right) \left(\hat{\mathbf{g}}_i + \tilde{\mathbf{g}}_i\right) + \mathbf{w}_k^H \mathbf{n}. \tag{4-21}$$

The variance $\sigma_{z,\mathrm{e}}^2 = \mathbb{E}\{z_{k,\mathrm{e}} z_{k,\mathrm{e}}^*\}$ of $z_{k,\mathrm{e}}$ is given by

$$\sigma_{z,\text{CL-CF}}^2 = \mathbf{w}_{ki}^H \left(\sum_{q=1,q\neq k}^{\mathcal{K}} \mathbf{g}_{q,ii} \mathbb{E}\left\{ \left| s_{q,i} - \bar{s}_{q,i} \right|^2 \right\} \mathbf{g}_{q,ii}^H + \sum_{j=1,j\neq i}^{M} \mathbf{G}_{ij} \mathbb{E}\left\{ \mathbf{s}_j \mathbf{s}_j^H \right\} \mathbf{G}_{ij}^H + \sigma_{n,i}^2 \mathbf{I}_{N\mathcal{L}} \right) \mathbf{w}_{ki}. \tag{4-22}$$

$$\sigma_{z,\text{Full-CF}}^2 = \mathbf{w}_{ki}^H \left(\sum_{i=1,i\neq k}^{K} \sigma_i^2 \left(\hat{\mathbf{g}}_i + \tilde{\mathbf{g}}_i\right) \left(\hat{\mathbf{g}}_i + \tilde{\mathbf{g}}_i\right)^H + \sigma_n^2 \mathbf{I}_{NL} \right) \mathbf{w}_{ki}. \tag{4-23}$$

4.2 Iterative Detection and Decoding

The extrinsic LLRs computed by the soft MMSE-PIC receiver for the l-th bit $l \in \{1, 2, ..., M_c\}$ of symbol s_k transmitted by the k-th UE [9–11, 51]

are given by

$$\Lambda_e\left(b_{(k-1)M_c+l}\right) = \frac{\log P\left(b_{(k-1)M_c+l}=+1|\tilde{x}_k\right)}{\log P\left(b_{(k-1)M_c+l}=-1|\tilde{x}_k\right)} - \frac{\log P\left(b_{(k-1)M_{c+1}}=+1\right)}{\log P\left(b_{(k-1)M_{c+1}}=-1\right)} \tag{4-24}$$

$$= \log \frac{\sum_{s\in\mathcal{A}_l^{+1}} F\left(\tilde{x}_k|s\right) P\left(s\right)}{\sum_{s\in\mathcal{A}_l^{-1}} F\left(\tilde{x}_k|s\right) P\left(s\right)} - \Lambda_i\left(b_{(k-1)M_c+l}\right),$$

where Bayes's rule is applied to obtained the last equality of (4-51).The 2^{Mc-1} hypothesis set for which the l-th bit is $+1$ is denoted by the parameter $\mathcal{A}_l^{+1}$. The a-priori probability $P(s)$ is obtained from (2-32). The likelihood function $F(\tilde{x}_k|s)$ is approximated as [9–11, 51]

$$F\left(\tilde{x}_k|s\right) \simeq \frac{1}{\pi\sigma_{z,\mathrm{e}}^2}\exp\left(-\frac{1}{\sigma_{z,\mathrm{e}}^2}|\tilde{x}_k - \mu_{k,\mathrm{e}}s|^2\right). \tag{4-25}$$

4.2.1 Decoding Algorithm

The box-plus SPA decoder is used as discussed in Chapter 2 Subsection 2.5.4. The decoder comprises of two steps namely: Single parity check (SPC) stage and the repetition stage. The LLRs sent from check node $(\mathrm{CN})_J$ to variable node $(\mathrm{VN})_i$ are computed as

$$\Lambda_{j\longrightarrow i} = \boxplus_{i'\in N(j)\diagdown i}\Lambda_{i'\longrightarrow j}, \tag{4-26}$$

where $\boxplus$ denotes the pairwise "box-plus" operator given by

$$\begin{aligned}\Lambda_1 \boxplus \Lambda_2 =& \log\left(\frac{1+e^{\Lambda_1+\Lambda_2}}{e^{\Lambda_1}+e^{\Lambda_2}}\right), \\ =& \mathrm{sign}(\Lambda_1)\mathrm{sign}(\Lambda_2)\min(|\Lambda_1|,|\Lambda_2|) + \log\left(1+e^{-|\Lambda_1+\Lambda_2|}\right) \\ & - \log\left(1+e^{-|\Lambda_1-\Lambda_2|}\right).\end{aligned} \tag{4-27}$$

The LLR from VN_i to CN_j is given by

$$\Lambda_{i\longrightarrow j} = \Lambda_i + \sum_{j'\in N(i)\backslash j}\Lambda_{j'\longrightarrow i}, \tag{4-28}$$

where the parameter Λ_i denotes the LLR at VN_i, $j' \in N(i)\backslash j$ means that all CNs connected to VN_i except CN_j.

4.2.2 Computational Complexity

The number flops for the receivers of the full CF-mMIMO and clustered CF-mMIMO networks are presented in Table A.1. It can be observed the full CF-mMIMO receivers achieve the highest number of flops as compared to that of the clustered CF-mMIMO with orders of $\mathcal{O}\left(\frac{(NL)^3K}{3}\right)$ and $\mathcal{O}\left(\frac{(N\mathcal{L})^3\mathcal{K}}{3}\right)$, respectively, where $\mathcal{O}(\cdot)$ is the Big O notation.

Table 4.1: Number of flops per detector.

Receiver	**Number of flops**
PIC-Full-CF	$\frac{(NL)^3K}{3} + (NL)^2K + 4NLK^2 + 6NLK + 4KM_c2^{M_c} + 9K2^{M_c}$
Linear MMSE-Full CF	$\frac{(NL)^3K}{3} + (NL)^2K + 2NLK^2 + 6NLK + 4KM_c2^{M_c} + 9K2^{M_c}$
PIC-WITH-OCL	$\frac{(N\mathcal{L})^3\mathcal{K}}{3} + 2(N\mathcal{L})^2\mathcal{K}M + 2MN\mathcal{L}\mathcal{K}^2 + 9N\mathcal{L}\mathcal{K} + 4\mathcal{K}M_c2^{M_c} + 9\mathcal{K}2^{M_c} - M(N\mathcal{L})^2\mathcal{K} - MN\mathcal{L}\mathcal{K}$
Linear MMSE-WITH-OCL	$\frac{(N\mathcal{L})^3\mathcal{K}}{3} + 2(N\mathcal{L})^2\mathcal{K}M + 3MN\mathcal{L}\mathcal{K}^2 + 9N\mathcal{L}\mathcal{K} + 4\mathcal{K}M_c2^{M_c} + 9\mathcal{K}2^{M_c} - M(N\mathcal{L})^2\mathcal{K} - MN\mathcal{L}\mathcal{K} - N\mathcal{L}\mathcal{K}^2$

4.3 Simulation Results

In this section, the BER performance of the proposed receivers is presented for the full CF-mMIMO and clustered CF-mMIMO networks. The CF-mMIMO channel exhibits high PL values due to LS fading coefficients. Thus, the instantaneous SNR definition takes into account the channel coefficients and it is given by

$$SNR = \frac{\mathrm{tr}(\sigma_s^2\mathbf{G}\mathbf{G}^H)R}{NLK\sigma_n^2}. \tag{4-29}$$

The simulation parameters are varied as follows: We consider a cell-free environment with a square of dimensions $D \times D$ =, where $D = 0.4$ km. Distances d_0 and d_1 are 10 m and 50 m, respectively. $h_{AP} = 15$m, $h_u = 1.5$ m, $f = 1900$ MHz, LDPC code with code word length 32 bits, $M = 16$ parity check bits and $N - M$ message bits. The code rate $R = \frac{1}{2}$. The maximum number of inner iterations is set to 10. The signal power $\sigma_s^2 = 1$ and the simulations are run for 10^4 channel realizations for fair statistical inference. The modulation scheme used is quadrature phase shift keying (QPSK). We consider $\mathbf{G}$ as the perfect CSI. Then the estimated channel and channel estimation error are

modeled as $\hat{\mathbf{G}} = \sqrt{\gamma}\mathbf{G}$ and $\tilde{\mathbf{G}} = \sqrt{\alpha}\mathbf{G}$. thus, the imperfect CSI channel is modeled as $\mathbf{G}_I = \hat{\mathbf{G}} + \tilde{\mathbf{G}}$, where the parameters γ and α should satisfy the relations $\alpha + \gamma = 1$, $\gamma >> \alpha$. In the simulations, $\gamma = 0.95$ and $\alpha = 0.05$. For the full CF-mMIMO network, there are L randomly located APs with K uniformly distributed UEs for simplicity of the analysis. For the clustered CF-mMIMO network, we consider M non-overlapping clusters each equipped with L randomly distributed APs and K uniformly distributed UEs with uniform power allocation.

The three-slope PL model is used to obtain the LS fading coefficients, which are assumed to be deterministic [54]. More specifically, the PL exponent is 3.5 if the distance d_{kl} between the k-th UE and the l-th AP is more than d_1, equals 2 if the distance is $d_1 \geq d_{kl} > d_0$, and equals 0 if the distance is $d_{kl} \leq d_0$. If $d_{kl} > d_1$, the Hata-COST231 propagation model is used. The PL PL_{kl} in dBs between the k-th UE and l-th AP can be given such as

$$\mathrm{PL}_{kl} = \begin{cases} -\Theta - 35\log d_{kl}, \ d_{kl} > d_1 \\ -\Theta - 15\log d_1 - 20\log d_{kl}, \ d_0 < d_{kl} \leq d_1 \\ -\Theta - 15\log(d_1) - 20\log d_0, \ \text{if} d_{kl} \leq d_0 \end{cases} . \tag{4-30}$$

The parameter Θ is given by $\Theta \triangleq 46.3 + 33.9\log_{10}(f) - 13.82\log_{10}(h_{\mathrm{AP}}) - (1.1\log_{10}(f) - 0.7)h_{\mathrm{u}} + (1.56\log_{10}(f) - 0.8)$, where f is the carrier frequency (in MHz), h_u and h_{AP} are the antenna heights of the UE and AP, respectively. The shadow fading and PL are modelled by the LS coefficient β_{kl} that is given by $\beta_{kl} = \mathrm{PL}_{kl} \times 10^{\sigma_{sh}\zeta_{lk}}$. Where $10^{\sigma_{sh}\zeta_{lk}}$ denotes the shadowing with standard deviation σ_{sh}, and $\zeta_{lk} \sim \mathcal{N}(0, 1)$.

Figure 4.6 presents the BER versus SNR as the number of iterations increases for the full CF-mMIMO network. From this figure, it can be observed that there is a significant performance improvement as the number of iterations increase from the first to second iteration. After the second iterations, there is moderate performance gains and after the third iteration the gains are marginal. This improvement in the performance is due to reliable LLRs in the cancellation step as the number of iterations increases, which yields to reductions in the BER. Figure 4.3 (a) and 4.3 (b) present the BER versus the SNR for the linear MMSE and PIC-MMSE receivers for full and cluster-based CF-mMIMO networks with and without OCL for different UE and AP settings. The details of the receivers compared are summarized as follows:

- Baseline MMSE: no statistics of the OCL in the covariance matrix of the receiver but with OCL in the received signal.
- Linear MMSE-With-OCL: OCL statistics in the covariance matrix and

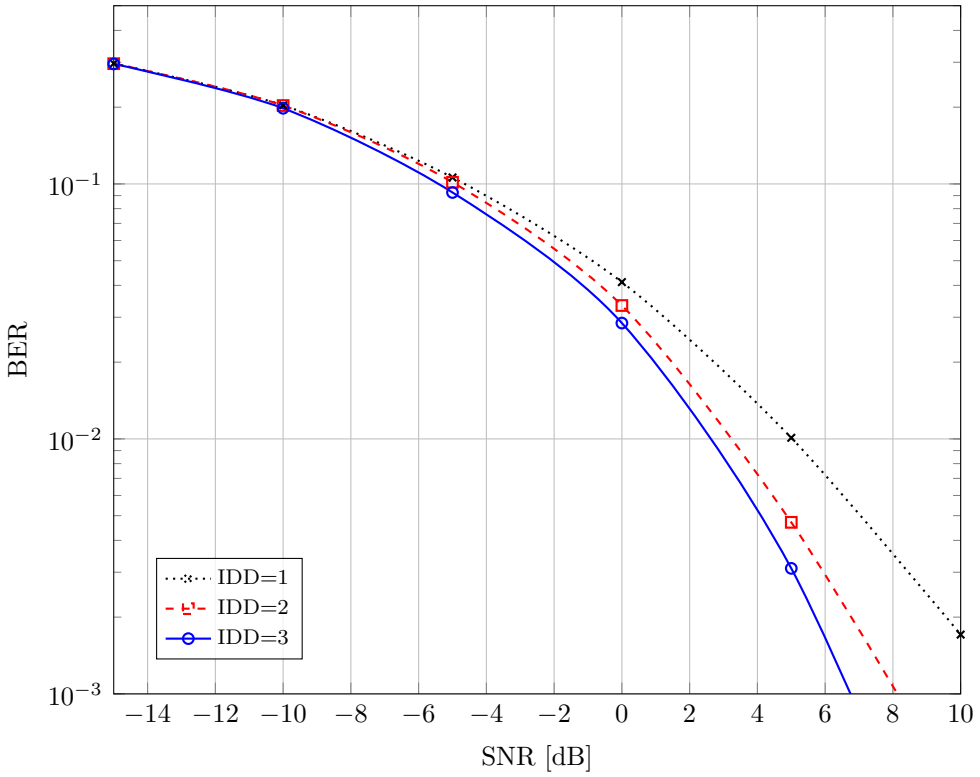

Figure 4.2: BER versus SNR while varying number of IDD iterations for $L = 16$, $N = 1$, $K = 8$, for the full-CF-mMIMO Network.

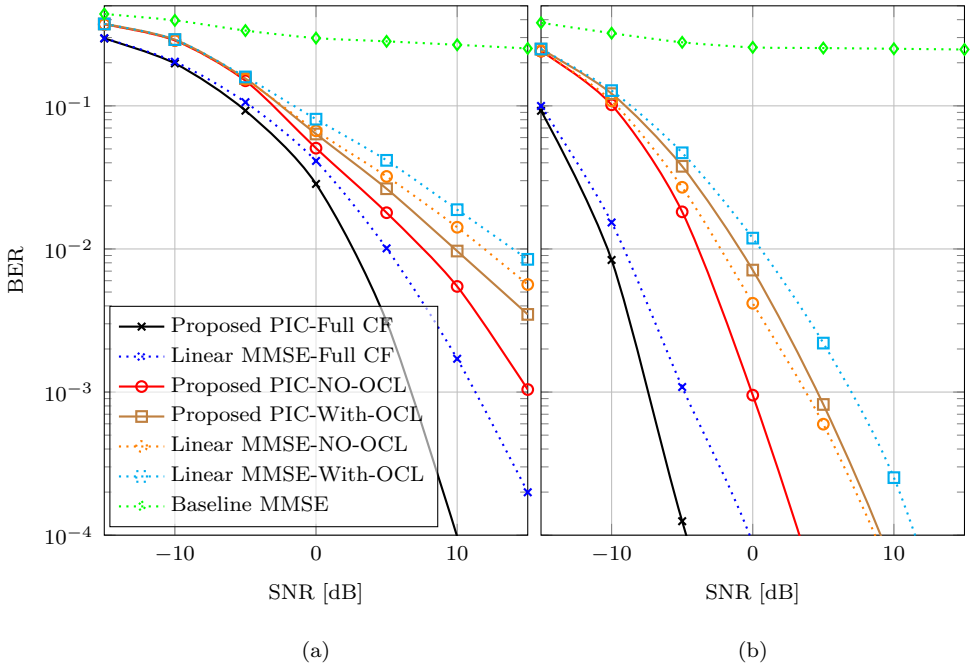

Figure 4.3: BER versus SNR for Linear and Non-Linear receivers for (a) $L = 4$, $N = 1$, $K = 2$ in each cluster and $L = 16$, $N = 1$, $K = 8$, for the full-CF-mMIMO Network and (b) $L = 16$, $N = 1$, $K = 4$ in each cluster and $L = 64$, $N = 1$, $K = 16$, for the full-CF-mMIMO Network.

in the received signal.

- Linear MMSE-Without-OCL: no OCL in both the received signal and covariance matrix of the receiver.
- Linear MMSE-Full-CF: uses all APs and UEs in the network.
- Proposed PIC-Full CF: uses all APs and UEs in the network.
- Proposed PIC-No-OCL: no OCL in both the received signal and covariance matrix of the receiver.
- Proposed PIC-With-OCL: OCL statistics in both the received signal and covariance matrix of the receiver.

.

From both figures, it can be observed that the PIC-based receivers achieve the lowest BER values because of their capability of canceling OCL interference for both clustered and full-CF networks. The linear MMSE receiver without OCL (Linear MMSE-no-OCL) yields lower BER than the MMSE with OCL (Linear MMSE-With-OCL). The same performance is analogous to the PIC-MMSE-based receiver without OCL (PIC-NO-OCL) and PIC-With-OCL. This performance degradation is due to OCL interference from the other clusters which yields very poor beliefs and thus high BER values. Furthermore, note should be taken that the baseline MMSE without statistics of the OCL in the covariance matrix achieves the worst performance in the studied receivers. Thus, it is always important to include the effects of OCL in the receiver computation to avoid such a performance degradation. It is also noteworthy that the performance of figure 4.3 (b) is better than that of 4.3 (a) since the former employs more APs in the network as compared to the later. This performance improvement is also due to the higher diversity order and reduction in the large scale fading as the number of APs in the network increases due to the channel hardening property and orthogonality of the channels. Finally, the Full-CF network receivers achieve the lowest BER values than the clustered network due to use of more APs in the network.

4.4 Iterative Interference Cancellation with Interference Estimation

In this section, OCL interference estimation is performed and it is used in the proposed user-centric CF-mMIMO architecture IDD scheme as discussed in the following subsection.

4.4.1 Proposed System Model, Channel and Interference Estimation

The uplink of a user-centric clustered CF-mMIMO system [55] is considered as shown in Figure 4.4. Figure 4.4 (a) shows the desired (dotted) links within a given cluster as well as OCL (dashed) links to each cluster. The proposed IDD scheme is presented in Figure 4.4 (b), where the transmitter comprises of K single antenna user equipment (UEs), encoders which employ LDPC codes and quadrature phase-shift keying (QPSK) modulators. The system suffers from M OCL interfering sources that are assumed to be identical to the UEs in terms of operation. The receiver consists of L APs each equipped with N antennas, and a central processing unit (CPU) which comprises of a detector, a log-likelihood ratio (LLR) computing module (LLR Mod) and an LDPC decoder. The detector computes a symbol estimate $\tilde{r}_d$ and sends it to the LLR Mod which computes the intrinsic LLRs Λ_i. The obtained LLRs are then sent to the decoder which computes extrinsic LLRs Λ_e. The exchange of LLRs between the detector and the decoder is done in an iterative fashion to improve performance.

4.4.2 Channel Estimation for the Serving Users

To estimate the channels, K mutually orthogonal $\tau_p \geq K$ length pilot signals are assumed to be assigned to UE k denoted by ϕ_k, with $\|\phi_k\|^2 = 1$. The received signal during the pilot phase at AP l is given by [56]

$$\mathbf{Y}_l = \sqrt{p\tau_p}\mathbf{H}_l\mathbf{\Phi}^H + \mathbf{G}_l\mathbf{S}^H + \mathbf{N}_l \tag{4-31}$$

where p, $\mathbf{H}_l \in \mathbb{C}^{N\times K}$, $\mathbf{\Phi} \in \mathbb{C}^{\tau_p\times K}$, $\mathbf{G}_l \in \mathbb{C}^{N\times M}$,$\mathbf{S} \in \mathbb{C}^{\tau_p\times M}$, and $\mathbf{N}_l \in \mathbb{C}^{N\times\tau_p}$ is the transmit power of each UE, the channel matrix between UEs and l-th AP, the channel matrix between the OCL interference and the l-th AP, the transmitted signal matrix of OCL interference, and the receiver noise at the l-th AP, respectively. The LSE is then applied to compute the channel estimate given by

$$\hat{\mathbf{H}}_l = \frac{1}{\sqrt{p\tau_p}}\mathbf{Y}_l\mathbf{\Phi} \tag{4-32}$$

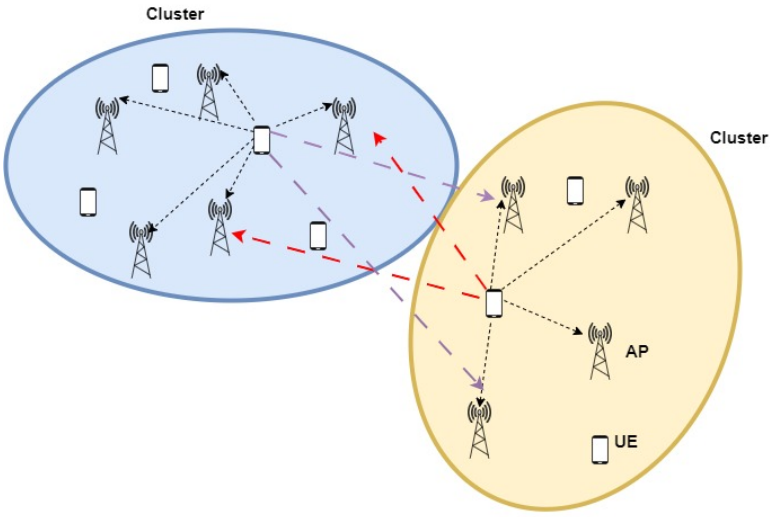

(a)

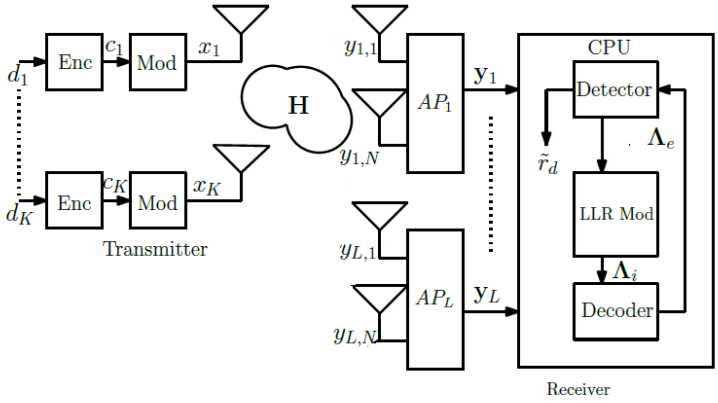

(b)

Figure 4.4: (a) Schematic of the clustered cell-free systems. (b) Proposed IDD scheme with users and APs in a cluster.

4.4.3 Interference Estimation

Unlike prior work on estimation of out-of-system channels [56], we consider the estimation of OCL interference in user-centric clustered CF-mMIMO networks. To estimate the OCL interference, the received signal at each AP is first pre-processed to reduce the impact of the channel components of the serving UEs from them, i.e $\{\mathbf{H}_l, l = 1, ..., L\}$. This preprocessed signal is called the residual signal [56] given by

$$\mathbf{Z}_l = \mathbf{Y}_l - \sqrt{p\tau_p}\hat{\mathbf{H}}_l\mathbf{\Phi}^H. \tag{4-33}$$

After some mathematical manipulations and following similar steps as in [56], (4-33) can be written as

$$\mathbf{Z}_l = \left(\mathbf{G}_l \mathbf{S}^H + \mathbf{N}_l\right) \mathbf{P}^{\perp}, \tag{4-34}$$

where $\mathbf{P}^{\perp} = \left(\mathbf{I} - \mathbf{\Phi}\mathbf{\Phi}^H\right)$ is the projection onto the orthogonal complement of the pilot matrix $\mathbf{\Phi}$.

4.4.3.1 Remarks

Note that the projection matrix is non invertible, and thus the OCL interfering signals can not be estimated completely. Therefore, only its components spanned by $\mathbf{P}^{\perp}$ can be estimated [56]. Thus, to make meaningful the estimates of $\mathbf{S}$ from $\mathbf{Z}_l$, the condition $\tau_p > K$ should be verified. Otherwise, the residual matrices at all the APs will be zero [56]. From these two remarks, the projection matrix P can be decomposed as

$$\mathbf{P}^{\perp} = \mathbf{\Psi}\mathbf{\Psi}^H, \tag{4-35}$$

where $\mathbf{\Psi} \in \mathbb{C}^{\tau_p \times (\tau_p - K)}$ is a tall matrix that satisfies the orthogonality property $\mathbf{\Psi}^H\mathbf{\Psi} = \mathbf{I}$, which yields the economy-size singular value decomposition (SVD) of $\mathbf{P}$. The projected signal component is then given by

$$\bar{\mathbf{S}} = \mathbf{\Psi}^H \mathbf{S} \tag{4-36}$$

. In order to estimate $\hat{\bar{\mathbf{S}}}$ of $\bar{\mathbf{S}}$, the residual signal is first despread by projecting it on $\mathbf{\Psi}$ as follows

$$\begin{aligned} \mathbf{Z}_l\mathbf{\Psi} &= \left(\mathbf{G}_l \mathbf{S}^H + \mathbf{N}_l\right) \mathbf{\Psi}, \\ &= \mathbf{G}_l \bar{\mathbf{S}}^H + \mathbf{N}_l^{'}, \end{aligned} \tag{4-37}$$

where $\mathbf{N}_l^{'} = \mathbf{N}_l\mathbf{\Psi}$. Having obtained the processed signal at each AP, the channel and signal estimates $\hat{\bar{\mathbf{S}}}$ of the OCL interference can be obtained by adopting the centralized processing scheme proposed in [56]. In this scheme, the processed signals from all APs are collected at the CPU and the following least squares problem is formulated:

$$\min_{\mathbf{G},\ \bar{\mathbf{S}}} ||\mathbf{Z}\mathbf{\Psi} - \mathbf{G}\bar{\mathbf{S}}^H||_F, \tag{4-38}$$

where $\mathbf{Z} = \left[\, \mathbf{Z}_1^T, ..., \mathbf{Z}_L^T \right]$, $\mathbf{G} = \left[\, \mathbf{G}_1^T, ..., \mathbf{G}_L^T \right]$, $\|\cdot\|_F$ denotes the Frobenius norm of the argument. The solution to the problem is obtained by taking the best rank-1 approximation of $\mathbf{Z\Psi}$ using the SVD. The estimated values of the matrices $\mathbf{G}$ and $\mathbf{S}$ are the left and right singular matrices of $\mathbf{Z\Psi}$ scaled by the largest singular value [56], which requires $O(KNL)$.

4.4.4 Uplink Data Transmission

The received signal at the l-th AP after estimating the channels of the serving UEs and OCL interference sources is given by

$$\mathbf{y}_l = \mathbf{H}_l\mathbf{x} + \mathbf{G}_l\mathbf{s} + \mathbf{n}_l, \tag{4-39}$$

where $\mathbf{H}_l \in \mathbb{C}^{N\times K}$, $\mathbf{x} \in \mathbb{C}^{K\times 1}$, $\mathbf{G}_l \in \mathbb{C}^{N\times M}$, $\mathbf{s} \in \mathbb{C}^{M\times 1}$, $\mathbf{n}_l \in \mathbb{C}^{N\times 1}$, is the channel matrix of the UEs in the system, the transmitted signals of the UEs in the system, the channel matrix of the OCL interference, the transmitted symbol for the OCL interference and AWGN vector with zero mean and unit variance, respectively.

4.4.5 Proposed Iterative Receiver Design

The proposed soft receiver aims to cancel the ICL and OCL interference sources. The demodulator comprises an MMSE filter followed by a SIC, PIC or list-based interference canceller. The receiver first computes the jth UE symbol mean $\bar{s}_j$ to obtain soft estimates [5]. The symbol mean is defined as $\mathbb{E}\{s_j\} = \bar{s_j}$ and it is given by equation (2-31) The a priori probability of the extrinsic LLRs [5] is given by equation (2-32). The symbol variances can be computed from (2-33).

After channel estimation and interference estimation, the received signal in (4-39) can be re-written as

$$\mathbf{y}_l = \begin{bmatrix} \hat{\mathbf{H}}_l & \hat{\mathbf{G}}_l \end{bmatrix} \begin{bmatrix} \mathbf{x} \\ \mathbf{s} \end{bmatrix} + \mathbf{n}_l. \tag{4-40}$$

Let us define $\mathbf{A}_l = \begin{bmatrix} \hat{\mathbf{H}}_l & \hat{\mathbf{G}}_l \end{bmatrix} \in \mathbb{C}^{N\times(K+M)}$ and $\mathbf{r} = \begin{bmatrix} \mathbf{x} \\ \bar{\mathbf{s}} \end{bmatrix} \in \mathbb{C}^{(K+M)\times 1}$, which allows the received signal at the l-th AP be described by

$$\mathbf{y}_l = \mathbf{A}_l\mathbf{r} + \mathbf{n}_l. \tag{4-41}$$

For centralized processing, the received signal at the CPU is given by

$$\mathbf{y} = \mathbf{A}\mathbf{r} + \mathbf{n}, \tag{4-42}$$

where $\mathbf{A} = \left[\mathbf{A}_1^T, ..., \mathbf{A}_L^T \right]$ is the matrix consisting of all the channels from the serving UEs and the OCL interfering signals. The received signal in (4-42) can be decomposed as

$$\mathbf{y} = \mathbf{a}_{\mathrm{d}} r_{\mathrm{d}} + \sum_{i=1, i\neq \mathrm{d}}^{K+M} \mathbf{a}_{\mathrm{i}} r_{\mathrm{i}} + \mathbf{n}, \tag{4-43}$$

where $\mathbf{a}_d$ and r_d, are the channel vector and transmitted symbol of the desired signal, the second term denotes the interference signal from the other $K-1$ UEs and the OCL interference and the third term denotes the noise. The detected signal for the desired UE after PIC is given by

$$\tilde{r}_d = \mathbf{w}_d^H \left(\mathbf{a}_{\mathrm{d}} r_{\mathrm{d}} + \sum_{i=1, i\neq \mathrm{d}}^{K+M} \mathbf{a}_{\mathrm{i}} \left(r_{\mathrm{i}} - \bar{r}_{\mathrm{i}} \right) + \mathbf{n} \right), \tag{4-44}$$

where $\mathbf{w}_d$ is the receive combining vector. The design of an efficient receive filter $\mathbf{w}_d$ aims at minimizing the error between the desired user signal r_d and the estimated signal $\tilde{r}_d$. The optimization problem to minimize the mean square error (MSE) between $\tilde{r}_d$ and r_d is formulated as

$$\mathrm{MSE} = \mathbb{E}\left\{ \left| r_{\mathrm{d}} - \tilde{r}_{\mathrm{d}} \right|^2 \right\}. \tag{4-45}$$

By substituting (4-44) into (4-45), yields the MSE given by

$$\begin{aligned} \mathrm{MSE} = & -\mathbf{w}_{\mathrm{d}}^H \rho_{\mathrm{d}} \mathbf{a}_{\mathrm{d}} \\ & + \mathbf{w}_{\mathrm{d}}^H \left[\rho_{\mathrm{d}} \mathbf{a}_{\mathrm{d}} \mathbf{a}_{\mathrm{d}}^H + \sum_{i=1, i\neq \mathrm{d}}^{K+1} \mathbf{a}_{\mathrm{i}} \mathbb{E}\left\{ \left| r_{\mathrm{i}} - \tilde{r}_{\mathrm{i}} \right|^2 \right\} \mathbf{a}_{\mathrm{i}}^H + \sigma_n^2 \mathbf{I}_{NL} \right] \mathbf{w}_{\mathrm{d}}. \end{aligned} \tag{4-46}$$

By differentiating (4-46) with respect to (w.r.t) $\mathbf{w}_{\mathrm{d}}^H$ and equating to zero, the optimal MMSE-PIC receive filter is given by

$$\begin{aligned} \mathbf{w}_{\mathrm{d}} = & \rho_{\mathrm{d}} \left[\rho_{\mathrm{d}} \mathbf{a}_{\mathrm{d}} \mathbf{a}_{\mathrm{d}}^H + \sum_{i=1, i\neq \mathrm{d}}^{K+M} \mathbf{a}_{\mathrm{i}} \mathbb{E}\left\{ \left| r_{\mathrm{i}} - \tilde{r}_{\mathrm{i}} \right|^2 \right\} \mathbf{a}_{\mathrm{i}}^H + \sigma_n^2 \mathbf{I}_{NL} \right]^{-1} \\ & \times \mathbf{a}_{\mathrm{d}}. \end{aligned} \tag{4-47}$$

The main factors affecting the performance of the receiver are the number of OCL interference sources, the parameter $\mathbb{E}\left\{ \left| r_{\mathrm{i}} - \tilde{r}_{\mathrm{i}} \right|^2 \right\}$ which consists of entries computed in (2-33), the number of UEs K, as well as the number of APs L.

The impact of these parameters on the performance are discussed in detail in the simulations section. Receivers for SIC and list-based receivers modify the PIC as in [46]. A Gaussian approximation of the receiver output is needed and detailed next.

4.5 Proposed Iterative Detection and Decoding

The received signal at the output of the filter in (4-44), contains the desired symbol, ICL and OCL interference as well as the noise. We use similar assumptions given in [46–48] to approximate the $\tilde{r}_d$ as a Gaussian output given by

$$\tilde{r}_d = \mu_{\mathrm{d}} r_d + z_{\mathrm{d}}, \tag{4-48}$$

By comparing (4-48) with (4-44) $\mu_{\mathrm{d}} = \mathbf{w}_d^H \mathbf{a}_d$. The parameter z_{d} is a zero-mean AWGN variable given by

$$z_{\mathrm{d}} = \mathbf{w}_d^H \left(\sum_{i=1, i\neq \mathrm{d}}^{K+M} \mathbf{a}_{\mathrm{i}} \left(r_{\mathrm{i}} - \bar{r}_{\mathrm{i}} \right) + \mathbf{n} \right). \tag{4-49}$$

The variance $\sigma_z^2 = \mathbb{E}\{z_{\mathrm{d}} z_{\mathrm{d}}^*\}$ of z_{d} is given by

$$\sigma_z^2 = \mathbf{w}_{\mathrm{d}}^H \left[\sum_{i=1, i\neq \mathrm{d}}^{K+M} \mathbf{a}_{\mathrm{i}} \mathbb{E}\left\{ \left| r_{\mathrm{i}} - \tilde{r}_{\mathrm{i}} \right|^2 \right\} \mathbf{a}_{\mathrm{i}}^H + \sigma_n^2 \mathbf{I}_{NL} \right] \mathbf{w}_{\mathrm{d}}. \tag{4-50}$$

The extrinsic LLR computed by the soft MMSE receiver for the l-th bit $l \in \{1, 2, ..., M_c\}$ of symbol r_d [48] is given by

$$\begin{aligned} &\Lambda_e \left(b_{(d-1)M_c+l} \right) = \\ &\frac{\log P\left(b_{(d-1)M_c+l} = +1 | \tilde{r}_d \right)}{\log P\left(b_{(d-1)M_c+l} = -1 | \tilde{r}_d \right)} - \frac{\log P\left(b_{(d-1)M_{c+1}} = +1 \right)}{\log P\left(b_{(d-1)M_{c+1}} = -1 \right)} \\ &= \log \frac{\sum_{s \in \mathcal{A}_l^{+1}} F\left(\tilde{r}_d | s \right) P\left(s \right)}{\sum_{s \in \mathcal{A}_l^{-1}} F\left(\tilde{r}_d | s \right) P\left(s \right)} - \Lambda_i \left(b_{(d-1)M_c+l} \right), \end{aligned} \tag{4-51}$$

where Bayes's rule is applied to obtain the last equality of (4-51).The 2^{Mc-1} hypothesis set for which the l-th bit is $+1$ is denoted by the parameter $\mathcal{A}_l^{+1}$. The a priori probability $P(s)$ is obtained from (2-32). The likelihood function $F(\tilde{r}_d|s)$ is approximated as [48]

$$F\left(\tilde{r}_d | s \right) \simeq \frac{1}{\pi \sigma_z^2} \exp\left(-\frac{1}{\sigma_z^2} |\tilde{r}_d - \mu_d s|^2 \right). \tag{4-52}$$

The decoder used is the box-plus SPA in this work is discussed in chapter II.

4.6 Simulation Results

The performance of the proposed approaches is assessed in this section. The instantaneous SNR used in the simulations is defined by

$$SNR = \frac{\sum_{l=1}^{L}(\mathbf{H}_l \, \mathrm{diag}\,(\boldsymbol{\rho})\, \mathbf{H}_l^H)}{\sigma_n^2 NLK}. \tag{4-53}$$

The simulation parameters are in Table 4.2.

Table 4.2: Simulation Parameters.

Parameter	**Value**
Codeword length (C_{leng})	512
Parity Check bits ($C_{\text{leng}} - M$)	256
Message bits (M)	128
Code rate R	$\frac{1}{2}$
Threshold Euclidean distance (d_{th})	0.38
τ_u, τ_p, τ_c	$190, 10, 200$
Maximum decoder iterations	10
Signal power ρ	1 W
Maximum decoder iterations	10
Number of channel realizations	10000

Network setup: We consider a cell-free cluster with square of dimensions of $D \times D$ where $D = 1$ km. The channels between OCL interference sources and APs are generated randomly by assuming them to follow block fading. The QPSK modulation is used and the LS fading coefficients are obtained according to the 3rd Generation Partnership Project (3GPP) Urban Microcell model in [45] given by

$$\beta_{k,l}\,[\mathrm{dB}] = -30.5 - 36.7 \log_{10}\left(\frac{d_{kl}}{1m}\right) + \Upsilon_{kl}, \tag{4-54}$$

where d_{kl} is the distance between the k-th UE and l-th AP, $\Upsilon_{kl} \sim \mathcal{N}\,(0, 4^2)$ is the shadow fading [45].

Fig. 4.5 presents the normalized mean square error (NMSE) for the interference estimation and channel estimation. It can be observed that for

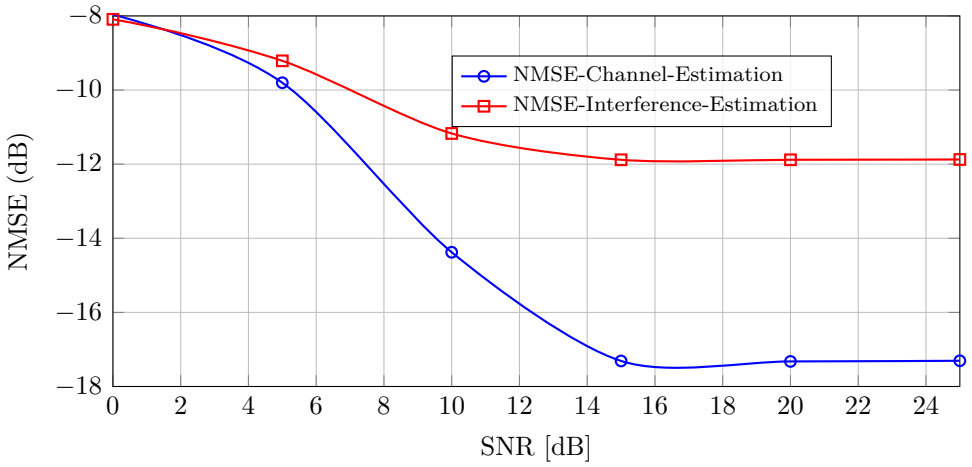

Figure 4.5: NMSE versus SNR $L = 32$, $N = 4$, $K = 8$, OCLIs $= 4$ for OCL interference estimation and channel estimation.

both cases the NMSE reduces as we approach higher SNR values up to the error floor region. For the case with channel estimation this can be further reduced by using longer pilots to provide more accurate estimation. The interference estimation is based on a sub optimal approach and more improvements in performance can be obtained by using advanced estimators. Accurate estimation of the interference channels is useful in the IDD cancellation step as it improves the accuracy and efficiency of the receiver.

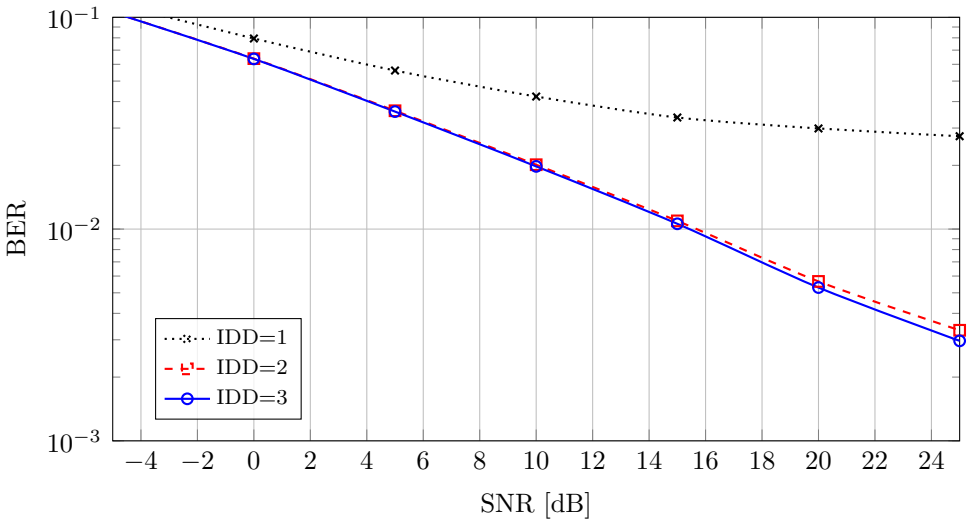

Figure 4.6: BER versus SNR $L = 32$, $N = 4$, $K = 8$, OCLIs $= 4$ for the system with ICL and OCL interference and varying number of PIC IDD iterations.

The BER performance versus SNR for a varying number of IDD iterations for the system that suffers from both ICL and OCL interference is shown in Fig. 4.6. Note that as the number of iterations is increased from the first to the second iteration, there is a significant reduction in BER. After the second iteration to the third iteration, there is a marginal reduction in BER at high SNR regime. This improvement is attributed to the fact that as the number of

IDD iterations is increased, extra a posterior information is exchanged between the decoder and the detector which improves the quality of the soft beliefs used at the interference cancellation scheme.

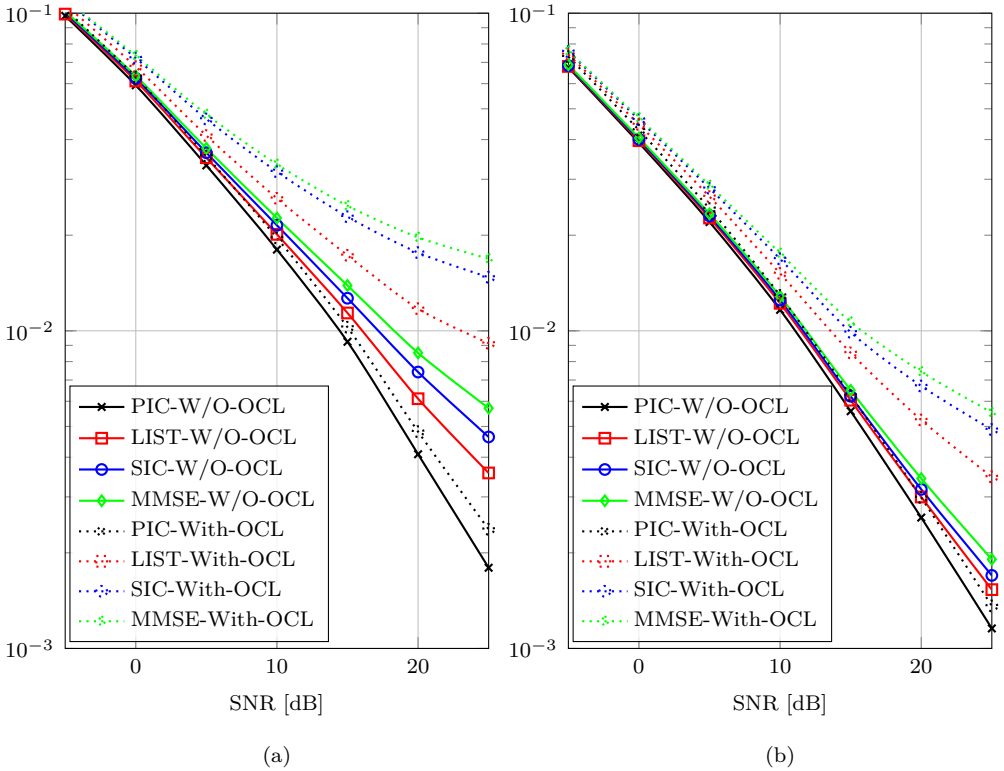

Figure 4.7: BER versus SNR for (a) $L = 32$, $N = 4$, $K = 8$, $M = 4$ and (b) $L = 32$, $N = 4$, $K = 8$, $M = 2$ for the system with ICL and OCL interference.

Fig. 4.7 presents the BER versus SNR for the system with OCL and ICL interference. It can be observed that the system which suffers from only ICL interference achieves lower BER values than that which experiences both OCL and ICL interference. Moreover, PIC receivers achieve the lowest BER values as compared to the other studied receivers. This is because of PICs ability in cancelling multiple streams of interference. Moreover, the List-based receiver performs better than the conventional SIC receivers because of its ability in removing the error propagation that is prevalent at each stage of SIC. Linear MMSE-based receivers achieve the worst performance because of their inability of cancelling interference but with performances that are still acceptable. Fig. 4.7 (a) and 4.7 (b) compare the impact of the reducing the number of OCL interference sources from 4 to 2. It is shown that the curves in Fig. 4.7 (b) achieve lower BER than those in Fig. 4.7 (a) for all the receivers with OCL interference. This is because increasing the OCL interference sources yields more unreliable channel estimates which compromises the entire network performance.

4.7 Summary

In this chapter, IDD schemes for network and user-centric clustered CF-mMIMO networks have been proposed. For the case of network clustering, new closed-form expressions for the linear MMSE receiver and the soft PIC-MMSE cluster-based receivers have been derived assuming ICSI, the presence of ICI signals and AWGN. Insights into the derived filters are drawn by assuming PCSI, and varying the number of IDD iterations to yield the resulting receivers. Moreover, the proposed cluster-based MMSE-PIC receivers are compared in terms of BER and computational complexity. The numerical results show that the full-CF-mMIMO network achieves lower BER values than the clustered one. However, clustering reduces both the computation complexity of the MMSE receive filters as well as reducing the amount of required signaling.

In the case where user-centric clustering is assumed, we have investigated soft interference cancellation schemes for user-centric clustered CF-mMIMO networks in the presence of ICL and OCL interference. We developed MMSE receive filters for the proposed interference cancellation schemes and devised a LSE to perform OCL interference estimation. An IDD scheme that adopts LDPC codes and incorporates the OCL interference estimate was presented. The results showed that the proposed algorithms outperform competing techniques and approach the performance of the system without OCL interference.

5
Conclusions and Future Work

In this chapter, the conclusions of the main contributions of this thesis are drawn and future works that could be based on the concepts and algorithms developed in this thesis are discussed.

5.1
Concluding Remarks

In this thesis, an IDD scheme using LDPC codes has been devised for centralized and decentralized CF-mMIMO architectures. In particular, low-complexity interference mitigation techniques that use MMSE-based detectors to improve the performance have been proposed. Moreover, list-based detectors that can mitigate error propagation at the interference cancellation stage have been proposed along with PIC based detectors. The main conclusions of this thesis are summarized in what follows.

List-based detectors have been proposed for the CF-mMIMO architecture. Specifically, an IDD scheme using LDPC codes has been studied for CF-mMIMO systems and it has been shown that increasing IDD iterations significantly reduces the BER. The performance of the CF-mMIMO architecture has been compared with standard mMIMO systems with co-located antennas. The results have shown that CF-mMIMO systems achieve better performance than mMIMO systems with co-located antennas. Additionally, the performance of the proposed MF-SIC/PIC schemes has been compared with other detectors. The proposed MF-PIC achieves lower BER values than those of the SIC and linear schemes.

An IDD scheme for decentralized and centralized CF-mMIMO architectures has also been proposed. New closed-form expressions for the MMSE-soft-IC detectors have been derived for both the centralized and decentralized implementations, taking into account the channel estimation errors. Insights have been drawn into the derived expressions as the number of iterations increase, and provide the resulting detectors with reasoning for their performance in the considered scenarios. Low-complexity and low-latency local receive filters based on RMF and MMSE-PIC have been also been studied for the CF-mMIMO network. The performance of a system that uses all APs and the system with

AP selection has been evaluated and it has been shown that the system that uses all APs achieves lower BER values as compared to the one with AP selection. Thus, there is a trade-off between scalability and BER performance while using AP selection. The major advantage gained with AP selection is the reduction in the signaling between the APs and the CPU, which makes the network more scalable and practical. Moreover, novel LLR refinement techniques based of LLR censoring and combination to improve the performance of the decentralized CF-mMIMO architecture have been proposed. The results have shown that the centralized architecture achieves lower BER than the decentralized setup. This is because the centralized one uses a joint sum of all the channels and thus, with the many nodes and antennas, the channels become nearly orthogonal, which minimises the interference as compared to the decentralized scenario. However, one advantage of the decentralized processing as compared to the centralized one is the reduction in signaling at the CPU. The main advantages of the decentralized processing over the centralized processing is reduction in computation complexity for each detector and reduction in signaling in the network.

An IDD scheme for network clustered CF-mMIMO networks has also been proposed to mitigate ICL and OCL interference. New closed-form expressions for the linear MMSE receiver and the soft PIC-MMSE cluster-based receivers have been derived assuming imperfect CSI, the presence of ICL and OCL signals and AWGN. Insights into the derived filters have been drawn by assuming perfect CSI, and varying the number of IDD iterations. Moreover, the proposed cluster-based MMSE-PIC receivers are compared in terms of BER and computational complexity. Furthermore, soft interference cancellation schemes for user-centric clustered CF-mMIMO networks in the presence of ICL and OCL interference have been proposed. MMSE receive filters for the proposed interference cancellation schemes have been developed and an LSE to perform OCL interference estimation has been devised. An IDD scheme that adopts LDPC codes and incorporates the OCL interference estimate was then developed. The results have shown that the proposed approaches outperform competing techniques and approach the performance of the system without OCL interference.

5.2 Future Work

In general, all the schemes and architectures presented in this thesis are based on single antenna users, as detailed in Chapters 2, 3 and 4. These can be extended to more general scenarios and configurations where multiple antenna

users are taken into consideration. Furthermore, the simulations have been based on the use of LDPC codes. Alternative coding schemes such as polar codes can also be adopted to replace the LDPC codes used in this thesis. Other possible suggestions for future works based on this thesis are summarized as follows.

A study on energy-efficient interference cancellation techniques for CF-mMIMO networks equipped with low-resolution signal processing using one-bit quantization in the analog-to-digital converters (ADCs) and IDD schemes could be carried out. Moreover, an investigation of the network throughput along with an analysis of the sum rate and the spectral efficiency of the proposed IDD schemes might be promising. In addition, further research could be pursued with the aim of studying and developing machine learning models and algorithms, which are capable of providing more robustness to IDD schemes against imperfect CSI in CF-mMIMO networks.

Bibliography

[1] BJÖRNSON, E.; SANGUINETTI, L., **Making cell-free massive MIMO competitive with MMSE processing and centralized implementation**, IEEE Trans. Wireless Commun., vol. 19, no. 1, pp. 77–90, 2019.

[2] YANG, S.; HANZO, L., **Fifty years of MIMO detection: The road to large-scale MIMO**, IEEE Commun. Surv. Tutor.., vol. 17, no. 4, pp. 1941–1988, 2015.

[3] NGO, H. Q.; ASHIKHMIN, A.; YANG, H.; LARSSON, E. G. ; MARZETTA, T. L., **Cell-free massive MIMO versus small cells**, IEEE Trans. Wireless Commun., vol. 16, no. 3, pp. 1834–1850, 2017.

[4] WANG, X.; POOR, H. V., **Iterative (turbo) soft interference cancellation and decoding for coded CDMA**, IEEE Trans. on commun., vol. 47, no. 7, pp. 1046–1061, 1999.

[5] XIAO, B.; XIAO, K.; ZHANG, S.; CHEN, Z.; XIA, B. ; LIU, H., **Iterative detection and decoding for SCMA systems with LDPC codes**, In: 2015 INT. CONF. ON WIRELESS COMMUN. & SIGNAL PROCESS. (WCSP), pp. 1–5. IEEE, 2015.

[6] MATACHE, A.; JONES, C. ; WESEL, R., **Reduced complexity MIMO detectors for LDPC coded systems**, In: IEEE MILCOM 2004. MILITARY COMMUN. CONF., 2004., vol. 2, pp. 1073–1079. IEEE, 2004.

[7] DE LAMARE, R. C.; SAMPAIO-NETO, R., **Minimum mean-squared error iterative successive parallel arbitrated decision feedback detectors for DS-CDMA systems**, IEEE Trans. on Commun., vol. 56, no. 5, pp. 778–789, 2008.

[8] JING, S.; YANG, C.; YANG, J.; YOU, X. ; ZHANG, C., **Joint detection and decoding of polar-coded SCMA systems**, In: 2017 9TH INT. CONF. ON WIRELESS COMMUN. AND SIGNAL PROCESS. (WCSP), pp. 1–6. IEEE, 2017.

[9] LI, P.; DE LAMARE, R. C. ; FA, R., **Multiple feedback successive interference cancellation detection for multiuser MIMO systems**, IEEE Trans. Wireless Commun., vol. 10, no. 8, pp. 2434–2439, 2011.

[10] DE LAMARE, R. C., **Adaptive and iterative multi-branch MMSE decision feedback detection algorithms for multi-antenna systems**, IEEE Trans. Wireless Commun., vol. 12, no. 10, pp. 5294–5308, 2013.

[11] UCHOA, A. G.; DE LAMARE, R. C.; HEALY, C. ; LI, P., **Iterative detection and decoding algorithms for block-fading channels using LDPC codes**, In: 2014 IEEE WIRELESS COMMUN. AND NETW. CONF. (WCNC), pp. 803–808. IEEE, 2014.

[12] SHAO, Z.; DE LAMARE, R. C. ; LANDAU, L. T., **Iterative detection and decoding for large-scale multiple-antenna systems with 1-bit ADCs**, IEEE Wireless Commun.Lett., vol. 7, no. 3, pp. 476–479, 2017.

[13] SSETTUMBA, T.; DI RENNA, R. B.; LANDAU, L. T. ; DE LAMARE, R. C., **Iterative detection and decoding for cell-free massive MIMO using LDPC codes**, In: PROC. XL BRAZILIAN SYMP. ON TELECOMMUN. AND SIGNAL PROCESS.(SBRT), pp. 1–5, 2022.

[14] D'ANDREA, C.; LARSSON, E. G., **Improving cell-free massive MIMO by local per-bit soft detection**, IEEE Commun. Lett., vol. 25, no. 7, pp. 2400–2404, 2021.

[15] SHAKYA, I. L.; ALI, F. H., **Joint access point selection and interference cancellation for cell-free massive MIMO**, IEEE Commun. Letters, vol. 25, no. 4, pp. 1313–1317, 2020.

[16] SHAKYA, I.; ALI, F. H. ; STIPIDIS, E., **High user capacity collaborative code-division multiple access**, IET commun., vol. 5, no. 3, pp. 307–319, 2011.

[17] SHENTAL, O.; VENKATESAN, S.; ASHIKHMIN, A. ; VALENZUELA, R. A., **Massive BLAST: An architecture for realizing ultra-high data rates for large-scale MIMO**, IEEE Wireless Commun.Lett., vol. 7, no. 3, pp. 404–407, 2017.

[18] WOLNIANSKY, P.; FOSCHINI, G.; GOLDEN, G. ; VALENZUELA, R., **V-BLAST: an architecture for realizing very high data rates over the rich-scattering wireless channel**, In: 1998 URSI INT. SYMP. ON SIGNALS, SYST., AND ELECTRONICS. CONF. PROC. (CAT. NO.98EX167), pp. 295–300, 1998.

[19] MARZETTA, T. L., **Massive MIMO: an introduction**, Bell Labs Technical Journal, vol. 20, pp. 11–22, 2015.

[20] LARSSON, E. G.; EDFORS, O.; TUFVESSON, F. ; MARZETTA, T. L., **Massive MIMO for next generation wireless systems**, IEEE commun. mag., vol. 52, no. 2, pp. 186–195, 2014.

[21] BJÖRNSON, E.; SANGUINETTI, L.; WYMEERSCH, H.; HOYDIS, J. ; MARZETTA, T. L., **Massive MIMO is a reality—what is next?: Five promising research directions for antenna arrays**, Digital Signal Process., vol. 94, pp. 3–20, 2019.

[22] MARZETTA, T. L.; LARSSON, E. G. ; YANG, H., *Fundamentals of massive MIMO*, Cambridge University Press, 2016.

[23] ABE, T.; MATSUMOTO, T., **Space-time turbo equalization in frequency-selective MIMO channels**, IEEE Trans. on Veh. Technol., vol. 52, no. 3, pp. 469–475, 2003.

[24] JOHAM, M.; UTSCHICK, W. ; NOSSEK, J. A., **Linear transmit processing in MIMO communications systems**, IEEE Trans. Signal Process., vol. 53, no. 8, pp. 2700–2712, 2005.

[25] VERDU, S.; OTHERS, *Multiuser detection*, Cambridge university press, 1998.

[26] KAILATH, T.; VIKALO, H. ; HASSIBI, B., **MIMO receive algorithms**, Space-Time Wireless Syst.: From Array Process. to MIMO Commun., vol. 3, pp. 2, 2005.

[27] CHAE, C.-B.; TANG, T.; HEATH, R. W. ; CHO, S., **MIMO relaying with linear processing for multiuser transmission in fixed relay networks**, IEEE Trans. Signal Process., vol. 56, no. 2, pp. 727–738, 2008.

[28] DE LAMARE, R. C.; SAMPAIO-NETO, R., **Adaptive reduced-rank processing based on joint and iterative interpolation, decimation, and filtering**, IEEE Trans. on Signal Proc., vol. 57, no. 7, pp. 2503–2514, 2009.

[29] MUHARAR, R.; YUNIDA, Y. ; NASARUDDIN, N., **On the performance of multi-way massive MIMO relay with linear processing**, IEEE Access, 2024.

[30] WANG, Z.; ZHANG, J.; DU, H.; NIYATO, D.; CUI, S.; AI, B.; DEBBAH, M.; LETAIEF, K. B. ; POOR, H. V., **A tutorial on extremely large-scale mimo for 6G: Fundamentals, signal processing, and applications**, IEEE Commun. Surveys & Tutorials, 2024.

[31] FLETCHER, R., *Practical methods of optimization*, John Wiley & Sons, 2013.

[32] CHO, Y. S.; KIM, J.; YANG, W. Y. ; KANG, C. G., *MIMO-OFDM wireless communications with MATLAB*, John Wiley & Sons, 2010.

[33] STAMOULIS, A.; DIGGAVI, S. N. ; AL-DHAHIR, N., **Intercarrier interference in MIMO OFDM**, IEEE Trans. Signal Process., vol. 50, no. 10, pp. 2451–2464, 2002.

[34] GUO, D.; RASMUSSEN, L. K.; SUN, S. ; LIM, T. J., **A matrix-algebraic approach to linear parallel interference cancellation in CDMA**, IEEE Trans. on Commun., vol. 48, no. 1, pp. 152–161, 2000.

[35] BROWN, D. R.; MOTANI, M.; VEERAVALLI, V. V.; POOR, H. V. ; JOHNSON, C. R., **On the performance of linear parallel interference cancellation**, IEEE Trans. on Inf. Theory, vol. 47, no. 5, pp. 1957–1970, 2001.

[36] HAGENAUER, J.; OFFER, E. ; PAPKE, L., **Iterative decoding of binary block and convolutional codes**, IEEE Trans. on Inf. Theory, vol. 42, no. 2, pp. 429–445, 1996.

[37] SHEN, Y.; ZHOU, W.; HUANG, Y.; ZHANG, Z.; YOU, X. ; ZHANG, C., **Fast iterative soft-output list decoding of polar codes**, IEEE Trans. Signal Process., vol. 70, pp. 1361–1376, 2022.

[38] SUKUMAR, C. P.; SHEN, C.-A. ; ELTAWIL, A. M., **Joint detection and decoding for MIMO systems using convolutional codes: Algorithm and VLSI architecture**, IEEE Trans. on Circuits and Syst. I: Regular Papers, vol. 59, no. 9, pp. 1919–1931, 2012.

[39] DIOUF, M.; DIOP, I.; DIOUM, I.; TALL, K. ; FARSSI, S. M., **Iterative detection for MIMO systems associated with polar codes**, In: 2018 INT. CONF. ON WIRELESS COMMUN., SIGNAL PROCESS. AND NETWORKING (WISPNET), pp. 1–7. IEEE, 2018.

[40] CHEN, Y.-T.; SUN, W.-C.; CHENG, C.-C.; TSAI, T.-L.; UENG, Y.-L. ; YANG, C.-H., **An integrated message-passing detector and decoder for polar-coded massive MU-MIMO systems**, IEEE Trans. on Circuits and Syst.I: Regular Papers, vol. 66, no. 3, pp. 1205–1218, 2018.

[41] DE LAMARE, R. C.; SAMPAIO-NETO, R., **Signal detection and parameter estimation in massive MIMO systems**, 2015.

[42] MABROUK, A.; ZAYANI, R., **Joint P-FZF combining and NLD cancellation for uplink cell-free massive MIMO-OFDM**, In: 2024 IEEE WIRELESS COMMUN. AND NETW. CONF. (WCNC), pp. 1–6. IEEE, 2024.

[43] TESTI, E.; TRALLI, V. ; PAOLINI, E., **Access point cooperation strategies for coded random access in cell-free massive MIMO**, IEEE IoT J., 2024.

[44] ZHANG, Y.; PENG, Y.; TANG, X.; XIAO, L. ; JIANG, T., **Large-scale fading decoding aided user-centric cell-free massive MIMO: Uplink error probability analysis and detector design**, IEEE Trans. Wireless Commun., 2024.

[45] BJÖRNSON, E.; SANGUINETTI, L., **Scalable cell-free massive MIMO systems**, IEEE Trans. on Commun., vol. 68, no. 7, pp. 4247–4261, 2020.

[46] SSETTUMBA, T.; SHAO, Z.; LANDAU, L. T.; FACINA, M. S.; DA SILVA, P. B. ; DE LAMARE, R. C., **Centralized and decentralized IDD schemes for cell-free massive MIMO systems: AP selection and LLR refinement**, IEEE Access, 2024.

[47] LEE, H.; LEE, I., **New approach for coded layered space-time OFDM systems**, In: IEEE INT. CONF. ON COMMUN., 2005. ICC 2005. 2005, vol. 1, pp. 608–612. IEEE, 2005.

[48] SSETTUMBA, T.; DI RENNA, R. B.; LANDAU, L. T. ; DE LAMARE, R. C., **List-based detector and access points selection in cell-free massive MIMO using LDPC codes**, In: 2022 INT. SYMP. ON WIRELESS COMMUN. SYST. (ISWCS), pp. 1–6. IEEE, 2022.

[49] SSETTUMBA, T.; SHAO, Z.; LANDAU, L. T.; FACINA, M. S.; DA SILVA, P. B. ; DE LAMARE, R. C., **LLR refinement strategies for iterative detection and decoding schemes in cell-free massive MIMO networks**, In: 2023 57TH ASILOMAR CONF. ON SIGNALS, SYST., AND COMPUT., pp. 358–362. IEEE, 2023.

[50] HAMA, Y.; OCHIAI, H., **A low-complexity matched filter detector with parallel interference cancellation for massive MIMO systems**, In: 2016 IEEE 12TH INT. CONF. ON WIRELESS AND MOBILE COMPUT., NETW. AND COMMUN.(WIMOB), pp. 1–6. IEEE, 2016.

[51] DOUILLARD, C.; JÉZÉQUEL, M.; BERROU, C.; ELECTRONIQUE, D.; PICART, A.; DIDIER, P. ; GLAVIEUX, A., **Iterative correction of**

intersymbol interference: turbo-equalization, European Trans. on Telecommun., vol. 6, no. 5, pp. 507–511, 1995.

[52] DI RENNA, R. B.; DE LAMARE, R. C., **Adaptive LLR-based APs selection for grant-free random access in cell-free massive MIMO**, In: 2022 IEEE GLOBECOM WORKSHOPS (GC WKSHPS), pp. 196–201. IEEE, 2022.

[53] LI, Y.; LIN, Q.; LIU, Y.-F.; AI, B. ; WU, Y.-C., **Asynchronous activity detection for cell-free massive MIMO: From centralized to distributed algorithms**, IEEE Trans. Wireless Commun., vol. 22, no. 4, pp. 2477–2492, 2022.

[54] MASHDOUR, S.; DE LAMARE, R. C. ; LIMA, J. P., **Enhanced subset greedy multiuser scheduling in clustered cell-free massive MIMO systems**, IEEE Commun. Lett., vol. 27, no. 2, pp. 610–614, 2022.

[55] BUZZI, S.; D'ANDREA, C.; ZAPPONE, A. ; D'ELIA, C., **User-centric 5G cellular networks: Resource allocation and comparison with the cell-free massive MIMO approach**, IEEE Trans. Wireless Commun., vol. 19, no. 2, pp. 1250–1264, 2019.

[56] SHAIK, Z. H.; LARSSON, E. G., **Decentralized algorithms for out-of-system interference suppression in distributed MIMO**, IEEE Wireless Commun. Lett., 2024.

[57] SKLAR, B., *Digital communications: fundamentals and applications*, Pearson, 2021.

A
Computational Complexity of the proposed detectors

Table A.1: Computational Complexity per Detector

Detector	**Multiplications**
Local-MMSE	$2N^2LK + 2K^2NL + 8KNL + 4KL2^{M_c} + 2M_cKL2^{M_c} + KL$
Centralized-MMSE	$2N^2L^2K + 8KNL + 2K^2NL + 4K2^{M_c} + 2M_cK2^{M_c} + K$
Local-SIC	$4N^2LK + 2K^2NL + 8KNL + 9KL2^{M_c} + 4M_cKL2^{M_c} + KL$
Centralized-SIC	$2(NLK)^2 + 2(NL)^2K + K^2NL + 5NLK + K + 9K2^{M_c} + 4M_cK2^{M_c}$
Local-List	$4N^2LK + 5K^2NL + 12KNL + 9KL2^{M_c} + 4M_cKL2^{M_c} + 2KL$
Centralized-List	$2(NLK)^2 + 2(NL)^2K + 3K^2NL + 9NLK + K + 9K2^{M_c} + 4M_cK2^{M_c}$
Local-PIC	$4N^2LK + 3K^2NL + 8KNL + 9KL2^{M_c} + 4M_cKL2^{M_c} + KL$
Centralized-PIC	$2(NLK)^2 + 2(NL)^2K + K^2NL + 6NLK + K + 9K2^{M_c} + 4M_cK2^{M_c}$

Table A.2: Number of complex signaling to send from APs to CPU via fronthaul links in each coherence block or for each realization of UE statistics [1].

Cell Free Implementation	**Each Coherence block**	**Statistical Parameters**
Centralized/Level 4	τ_cNL	$KLN^2/2$
Distributed Level-2	$(\tau_c - \tau_p)\,KL$	–

B
Derivation of the Proposed Centralized Detector

We start our analysis by expressing the conditional expectation on the RHS of (3-10) as

$$F = \mathbb{E}\left\{ ||\tilde{s}_k - s_k||^2 \mid \hat{\mathbf{G}} \right\} = \mathbb{E}\left\{ (\tilde{s}_k - s_k)(\tilde{s}_k - s_k)^* \mid \hat{\mathbf{G}} \right\}. \tag{B-1}$$

Substituting (3-9) into (B-1) yields

$$\begin{aligned} F &= \mathbf{w}_k^H \mathbf{D}_k \mathbb{E}\left\{ \left(\mathbf{y} - \hat{\mathbf{G}}_{\mathrm{i}} \bar{\mathbf{s}}_{\mathrm{i}} \right) \left(\mathbf{y}^H - \bar{\mathbf{s}}_{\mathrm{i}}^H \hat{\mathbf{G}}_{\mathrm{i}}^H \right) \right\} \mathbf{D}_k^H \mathbf{w}_k \\ &- \mathbf{w}_k^H \mathbf{D}_k \mathbb{E}\left\{ \left(\mathbf{y} - \hat{\mathbf{G}}_{\mathrm{i}} \bar{\mathbf{s}}_{\mathrm{i}} \right) s_k^* \right\} - \mathbb{E}\left\{ s_k \left(\mathbf{y}^H - \bar{\mathbf{s}_{\mathrm{i}}^H} \hat{\mathbf{G}}_{\mathrm{i}}^H \right) \right\} \\ &\times \mathbf{D}_k^H \mathbf{w}_k + \mathbb{E}\left\{ s_k s_k^* \right\}. \end{aligned} \tag{B-2}$$

Further simplification of (B-2) can be done by letting $\mathbf{y}_R = \mathbf{y} - \hat{\mathbf{G}}_{\mathrm{i}} \bar{\mathbf{s}}_{\mathrm{i}}$. Thus, (B-2) can be re-written as

$$\begin{aligned} F &= \mathbf{w}_k^H \mathbf{D}_k \mathbb{E}\left\{ \mathbf{y}_R \mathbf{y}_R^H \right\} \mathbf{D}_k^H \mathbf{w}_k - \mathbf{w}_k^H \mathbf{D}_k \mathbb{E}\left\{ \mathbf{y}_R s_k^* \right\} \\ &- \mathbb{E}\left\{ s_k \mathbf{y}_R^H \right\} \mathbf{D}_k^H \mathbf{w}_k + \mathbb{E}\left\{ s_k s_k^* \right\}. \end{aligned} \tag{B-3}$$

Differentiating (B-3) with respect to w.r.t $\mathbf{w}_k^H$ we obtain

$$\frac{\partial F}{\partial \mathbf{w}_{\mathbf{k}}^{\mathbf{H}}} = \mathbf{D}_k \mathbb{E}\left\{ \mathbf{y}_R \mathbf{y}_R^H \right\} \mathbf{D}_k^H \mathbf{w}_k - \mathbf{D}_k \mathbb{E}\left\{ \mathbf{y}_R s_k^* \right\}. \tag{B-4}$$

The optimal MMSE filter is obtained by equating (B-4) to $\mathbf{0}$. Thus, the optimal MMSE filter $\mathbf{w}_k$ is given by

$$\mathbf{D}_k \mathbb{E}\left\{ \mathbf{y}_R \mathbf{y}_R^H \right\} \mathbf{D}_k^H \mathbf{w}_k - \mathbf{D}_k \mathbb{E}\left\{ \mathbf{y}_R s_k^* \right\} = 0. \tag{B-5}$$

The reader can confirm that (B-5) is the same as (3-11). By making $\mathbf{w}_k$ the subject of (B-5), we obtain (3-12). The terms $\mathbb{E}\{\mathbf{y}_R s_k^*\}$ and $\mathbb{E}\{\mathbf{y}_R \mathbf{y}_R^H\}$ are given by (3-13) and (3-14), where $\mathbb{E}\left\{ s_m s_m^* \right\} = |s_m|^2 + \sigma_m^2$, $\mathbb{E}\left\{ \tilde{\mathbf{g}}_m \tilde{\mathbf{g}}_m^H \right\} = \mathbf{C}_m$, $\mathbb{E}\left\{ \mathbf{n}\mathbf{n}^H \right\} = \sigma^2 \mathbf{I}_{NL}$, $\mathbb{E}\left\{ s_k s_k^H \right\} = \rho_k$, obtained after assuming statistical independence between each term in the RHS of (3-8) and using the orthogonality principle [57]. By substituting (3-13) and (3-14) into (3-12), we arrive at the

centralized MMSE filter given by (3-15).

C
Derivation of the Proposed Decentralized Detector

The derivation of the proposed local MMSE filter is similar to that of Appendix B. The expectation on the R.H.S of (3-39) can be expressed as

$$\begin{aligned} F_2 &= \mathbb{E}\left\{ ||\tilde{s}_{kl} - s_k||^2 \mid \hat{\mathbf{G}}_l \right\} \\ &= \mathbb{E}\left\{ (\tilde{s}_{kl} - s_k)(\tilde{s}_{kl} - s_k)^* \mid \hat{\mathbf{G}}_l \right\}. \end{aligned} \tag{C-1}$$

By substituting (3-38) into (C-1) we obtain

$$F_2 = \mathbb{E}\left\{ \left(\mathbf{w}_{kl}^H \mathbf{D}_{kl} \mathbf{y}_{Rl} - s_k \right) \left(\mathbf{w}_{kl}^H \mathbf{D}_{kl} \mathbf{y}_{Rl} - s_k \right)^* \right\}. \tag{C-2}$$

The term $\mathbf{y}_{Rl}$ is the residue signal obtained after soft-IC and substituting for y_l in the term in brackets of (3-38), we get

$$\mathbf{y}_{Rl} = \hat{\mathbf{g}}_{kl} s_k + \hat{\mathbf{G}}_{\mathrm{i}l} \left(\mathbf{s}_{\mathrm{i}} - \bar{\mathbf{s}}_{\mathrm{i}} \right) + \sum_{m=1}^{K} \tilde{\mathbf{g}}_{ml} s_m + \mathbf{n}_l. \tag{C-3}$$

After some mathematical and algebraic manipulations, (C-2) can be re-written as

$$\begin{aligned} F_2 = {} & \mathbf{w}_{kl}^H \mathbf{D}_{kl} \mathbb{E}\left\{ \mathbf{y}_{Rl} \mathbf{y}_{Rl}^H \right\} \mathbf{D}_{kl}^H \mathbf{w}_{kl} - \mathbf{w}_{kl}^H \mathbf{D}_{kl} \mathbb{E}\left\{ \mathbf{y}_{Rl} s_k^* \right\} \\ & - \mathbb{E}\left\{ s_k \mathbf{y}_{Rl}^H \right\} \mathbf{D}_{kl}^H \mathbf{w}_{kl} + \mathbb{E}\left\{ s_k s_k^* \right\} \end{aligned} \tag{C-4}$$

We take the first derivative of (C-4) w.r.t $\mathbf{w}_{kl}^H$ to arrive at

$$\frac{\partial F_2}{\partial \mathbf{w}_{kl}^H} = \mathbf{D}_{kl} \mathbb{E}\left\{ \mathbf{y}_{Rl} \mathbf{y}_{Rl}^H \right\} \mathbf{D}_{kl}^H \mathbf{w}_{kl} - \mathbf{D}_{kl} \mathbb{E}\left\{ \mathbf{y}_{Rl} s_k^* \right\}. \tag{C-5}$$

After equating the resulting expression in (C-5) to 0, we obtain

$$\mathbf{D}_{kl} \mathbb{E}\left\{ \mathbf{y}_{Rl} \mathbf{y}_{Rl}^H \right\} \mathbf{D}_{kl}^H \mathbf{w}_{kl} - \mathbf{D}_{kl} \mathbb{E}\left\{ \mathbf{y}_{Rl} s_k^* \right\} = 0. \tag{C-6}$$

The optimal local MMSE filter $\mathbf{w}_{kl}$ can be obtained from (C-6). The terms $\mathbb{E}\left\{ \mathbf{y}_{Rl} \mathbf{y}_{Rl}^H \right\}$ and $\mathbb{E}\left\{ \mathbf{y}_{Rl} s_k^* \right\}$ can be obtained from (3-26) and (3-27), respectively, where the terms $\mathbb{E}\left\{ \tilde{\mathbf{g}}_{ml} \tilde{\mathbf{g}}_{ml}^H \right\} = \mathbf{C}_{ml}$ and $\mathbb{E}\left\{ \mathbf{n}_l \mathbf{n}_l^H \right\} = \sigma^2 \mathbf{I}_N$, by taking

assumptions similar to those in Subsection A.

D
Derivation of the Soft Demapper Parameters for Centralized Processing

We start the proof by making some assumptions on the output of the MMSE filter to be a Gaussian approximation. The optimal soft bit metric which takes into account the channel estimation error and APs-Sel can be derived as below. Let k denote the desired UE which minimizes the mean square error (MSE). Then, (3-9) can be expressed as

$$\tilde{s}_k = \mathbf{w}_k^H \mathbf{D}_k \mathbf{y} - \mathbf{w}_k^H \mathbf{D}_k \hat{\mathbf{G}}_i \bar{\mathbf{s}}_{\mathrm{i}}. \tag{D-1}$$

By substituting (3-8) into (D-1) we obtain

$$\begin{aligned}\tilde{s}_k = \mathbf{w}_k^H \mathbf{D}_k \hat{\mathbf{g}}_k s_k + \mathbf{w}_k^H \mathbf{D}_k \hat{\mathbf{G}}_{\mathrm{i}} \left(\mathbf{s}_{\mathrm{i}} - \bar{\mathbf{s}}_{\mathrm{i}}\right) + \mathbf{w}_k^H \mathbf{D}_k \sum_{m=1}^{K} \tilde{\mathbf{g}}_m s_m \\ + \mathbf{w}_k^H \mathbf{D}_k \mathbf{n}.\end{aligned} \tag{D-2}$$

By comparing (D-2) with (3-46), it can be observed that

$$\omega_k = \mathbf{w}_k^H \tilde{\mathbf{D}}_k \hat{\mathbf{g}}_k, \tag{D-3}$$

and the interference-plus-noise term is given by

$$z_k = \mathbf{w}_k^H \mathbf{D}_k \hat{\mathbf{G}}_{\mathrm{i}} \left(\mathbf{s}_{\mathrm{i}} - \bar{\mathbf{s}}_{\mathrm{i}}\right) + \mathbf{w}_k^H \mathbf{D}_k \sum_{m=1}^{K} \tilde{\mathbf{g}}_m s_m + \mathbf{w}_k^H \mathbf{D}_k \mathbf{n}. \tag{D-4}$$

By assuming that z_k is a Gaussian random variable [36–40, 51] and assuming statistical independence of each term of (D-4), the variance $\kappa^2 = \mathbb{E}\left\{\mid u_k - \omega_k s_k \mid^2\right\} = \mathbb{E}\left\{z_k z_k^*\right\}$ of z_k is given by

$$\kappa^2 = \mathbf{w}_k^H \mathbf{D}_k \left(\hat{\mathbf{G}}_{\mathrm{i}} \Delta_{\mathrm{i}} \hat{\mathbf{G}}_{\mathrm{i}}^H + \sum_{m=1}^{K} \rho_m \mathbf{C}_m + \sigma^2 \mathbf{I}_{NL}\right) \mathbf{D}_k^H \mathbf{w}_k. \tag{D-5}$$

By substituting (D-3) and (D-5) into (4-52), the soft beliefs for the centralized processor can be obtained in each subsequent iteration.

E
Derivation of the Soft Demapper Parameter for Decentralized Processing

We also start by assuming that the output of the MMSE-SIC filter is a Gaussian random variable. We then derive the local optimal soft bit metric which takes the APs-Sel matrix, and channel estimation error as follows. Let k denote the desired UE which minimizes the mean square error (MSE). Then, (3-9) can be expressed as

$$\tilde{s}_k = \mathbf{w}_{kl}^H \mathbf{D}_{kl} \mathbf{y}_l - \mathbf{w}_{kl}^H \mathbf{D}_{kl} \hat{\mathbf{G}}_{il} \bar{\mathbf{s}}_{\mathrm{i}}. \tag{E-1}$$

By substituting (3-21) into (E-1) we obtain

$$\begin{aligned} \tilde{s}_k = \mathbf{w}_{kl}^H \mathbf{D}_{kl} \hat{\mathbf{g}}_{kl} s_k + \mathbf{w}_{kl}^H \mathbf{D}_{kl} \hat{\mathbf{G}}_{\mathrm{il}} \left(\mathbf{s}_{\mathrm{i}} - \bar{\mathbf{s}}_{\mathrm{i}} \right) + \mathbf{w}_{kl}^H \mathbf{D}_{kl} \sum_{m=1}^{K} \tilde{\mathbf{g}}_{ml} s_m \\ + \mathbf{w}_{kl}^H \mathbf{D}_{kl} \mathbf{n}_l. \end{aligned} \tag{E-2}$$

By comparing (E-2) with (3-46), it can be observed that

$$\omega_{kl} = \mathbf{w}_{kl}^H \tilde{\mathbf{D}}_{kl} \hat{\mathbf{g}}_{kl}, \tag{E-3}$$

and the interference-plus-noise term is given by

$$z_{kl} = \mathbf{w}_{kl}^H \mathbf{D}_{kl} \hat{\mathbf{G}}_{\mathrm{il}} \left(\mathbf{s}_{\mathrm{i}} - \bar{\mathbf{s}}_{\mathrm{i}} \right) + \mathbf{w}_{kl}^H \mathbf{D}_{kl} \sum_{m=1}^{K} \tilde{\mathbf{g}}_{ml} s_m + \mathbf{w}_{kl}^H \mathbf{D}_{kl} \mathbf{n}_l. \tag{E-4}$$

By assuming that z_{kl} is a Gaussian random variable [23, 35] and assuming statistical independence of each term of (E-4), the variance $\kappa_l^2 = \mathbb{E}\left\{ \mid u_{kl} - \omega_{kl} s_k \mid^2 \right\} = \mathbb{E}\left\{ z_{kl} z_{kl}^* \right\}$ of z_{kl} is given by

$$\kappa_l^2 = \mathbf{w}_{kl}^H \mathbf{D}_{kl} \left(\hat{\mathbf{G}}_{\mathrm{il}} \Delta_{\mathrm{il}} \hat{\mathbf{G}}_{\mathrm{il}}^H + \sum_{m=1}^{K} \rho_m \mathbf{C}_{ml} + \sigma^2 \mathbf{I}_N \right) \mathbf{D}_{kl}^H \mathbf{w}_{kl}. \tag{E-5}$$

By substituting (E-3) and (E-5) into (4-52), the soft beliefs for the lcoal processors can be obtained in each subsequent iteration at each AP.